PB80-179286

Development Study of a Novel Continuous-flow Impactor

TRW Systems and Energy
Redondo Beach, CA

Prepared for

Industrial Environmental Research Lab.
Research Triangle Park, NC

Jan 80

U.S. Department of Commerce
National Technical Information Service
NTIS.

PB80-179286

United States
Environmental Protection
Agency

Industrial Environmental Research
Laboratory
Research Triangle Park NC 27711

EPA-600/7-80-014
January 1980

EPA

Development Study of a Novel Continuous-flow Impactor

Interagency Energy/Environment R&D Program Report

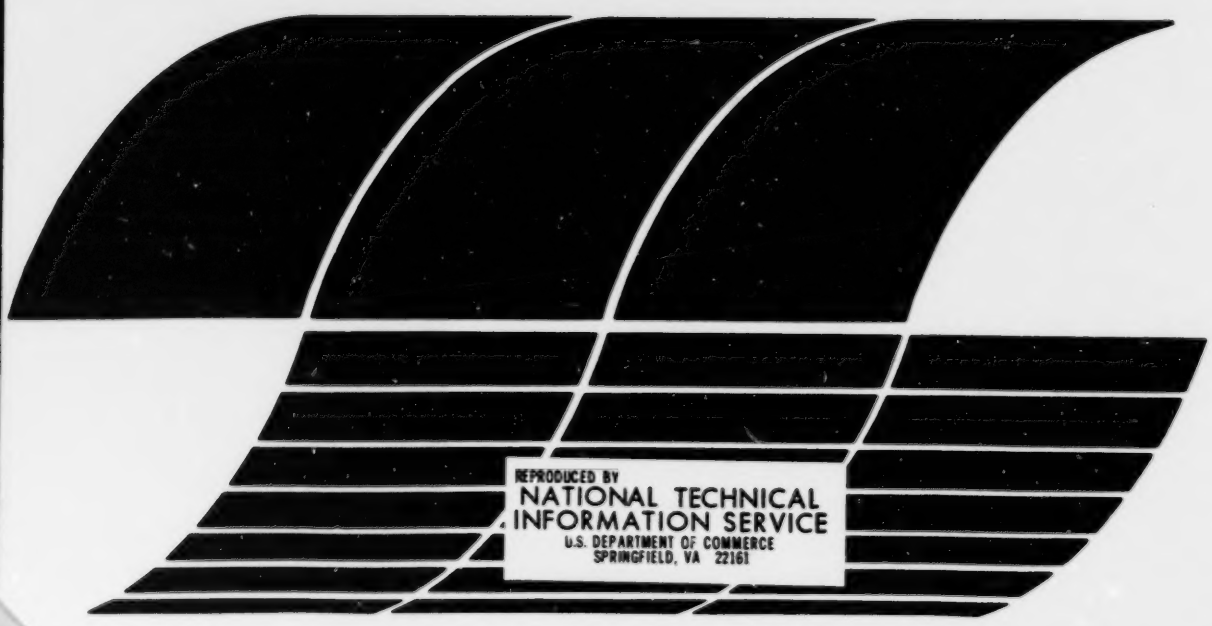

REPRODUCED BY
NATIONAL TECHNICAL
INFORMATION SERVICE
U.S. DEPARTMENT OF COMMERCE
SPRINGFIELD, VA 22161

RESEARCH REPORTING SERIES

Research reports of the Office of Research and Development, U.S. Environmental Protection Agency, have been grouped into nine series. These nine broad categories were established to facilitate further development and application of environmental technology. Elimination of traditional grouping was consciously planned to foster technology transfer and a maximum interface in related fields. The nine series are:

1. Environmental Health Effects Research
2. Environmental Protection Technology
3. Ecological Research
4. Environmental Monitoring
5. Socioeconomic Environmental Studies
6. Scientific and Technical Assessment Reports (STAR)
7. Interagency Energy-Environment Research and Development
8. "Special" Reports
9. Miscellaneous Reports

This report has been assigned to the INTERAGENCY ENERGY-ENVIRONMENT RESEARCH AND DEVELOPMENT series. Reports in this series result from the effort funded under the 17-agency Federal Energy/Environment Research and Development Program. These studies relate to EPA's mission to protect the public health and welfare from adverse effects of pollutants associated with energy systems. The goal of the Program is to assure the rapid development of domestic energy supplies in an environmentally-compatible manner by providing the necessary environmental data and control technology. Investigations include analyses of the transport of energy-related pollutants and their health and ecological effects; assessments of, and development of, control technologies for energy systems; and integrated assessments of a wide range of energy-related environmental issues.

EPA REVIEW NOTICE

This report has been reviewed by the participating Federal Agencies, and approved for publication. Approval does not signify that the contents necessarily reflect the views and policies of the Government, nor does mention of trade names or commercial products constitute endorsement or recommendation for use.

This document is available to the public through the National Technical Information Service, Springfield, Virginia 22161.

TECHNICAL REPORT DATA
(Please read Instructions on the reverse before completing)

1. REPORT NO.	2.	3. RECIPIENT'S ACCESSION NO.
EPA-600/7-80-014		PB80 179286

4. TITLE AND SUBTITLE	5. REPORT DATE
Development Study of a Novel Continuous-flow Impactor	January 1980
	6. PERFORMING ORGANIZATION CODE
7. AUTHOR(S)	8. PERFORMING ORGANIZATION REPORT NO.
E. F. Brooks, N. Gat, M. E. Taylor, T. E. Chamberlain, R. J. Golik, and R. Watson	
9. PERFORMING ORGANIZATION NAME AND ADDRESS	10. PROGRAM ELEMENT NO.
TRW Systems and Energy One Space Park Redondo Beach, California 90278	EHE624
	11. CONTRACT/GRANT NO.
	68-02-2165, Task 12
12. SPONSORING AGENCY NAME AND ADDRESS	13. TYPE OF REPORT AND PERIOD COVERED
EPA, Office of Research and Development Industrial Environmental Research Laboratory Research Triangle Park, NC 27711	Task Final; 7/76 - 11/78
	14. SPONSORING AGENCY CODE
	EPA/600/13

15. SUPPLEMENTARY NOTES IERL-RTP project officer is D. Bruce Harris, Mail Drop 62, 919/541-2557.

16. ABSTRACT The report gives results of a development study involving feasibility verification of a novel particle impactor in which the impaction surface is the interface between two opposing jets. Particles (which would impact a solid surface in a standard impactor) cross the interface between the aerosol-laden gas and a previously particle-free gas, are entrained in the latter, and are conveyed out for analysis. Work consisted of an initial literature search and analysis to determine the likelihood of success, followed by design, fabrication, and testing of a laboratory unit. A good particle separation capability was demonstrated. Upon completion of the laboratory tests, a design effort showed the feasibility of a staged in situ particle monitoring subsystem to give semicontinuous (nominal 1 minute cycle time) output of particle size distribution, among other applications.

17. KEY WORDS AND DOCUMENT ANALYSIS

a. DESCRIPTORS	b. IDENTIFIERS/OPEN ENDED TERMS	c. COSATI Field/Group
Pollution	Pollution Control	13B
Dust	Stationary Sources	11G
Aerosols	Particulate	07D
Impactors	Particle Impactors	13I
Monitors		14B
Particle Size Distribution		

18. DISTRIBUTION STATEMENT	19. SECURITY CLASS *(This Report)*	21. NO. OF PAGES
Release to Public	Unclassified	123
	20. SECURITY CLASS *(This page)*	22. PRICE
	Unclassified	

EPA Form 2220-1 (9-73)

EPA-600/7-80-014

January 1980

Development Study of a Novel Continuous-flow Impactor

by

E.F. Brooks, N. Gat, M.E. Taylor,
T.E. Chamberlain, R.J. Golik, and R. Watson

TRW Systems and Energy
One Space Park
Redondo Beach, California 90278

Contract No. 68-02-2165
Task No. 12
Program Element No. EHE624

EPA Project Officer: D. Bruce Harris

Industrial Environmental Research Laboratory
Office of Environmental Engineering and Technology
Research Triangle Park, NC 27711

Prepared for

U.S. ENVIRONMENTAL PROTECTION AGENCY
Office of Research and Development
Washington, DC 20460

ABSTRACT

The development study involved feasibility verification for a novel type of particle impactor in which the impaction surface is the interface between two opposing jets. Particles which would impact a solid surface in a standard impactor cross the interface between the aerosol laden gas and a previously particle free gas, are entrained in the latter and conveyed out for analysis. Work consisted of an initial literature search and analysis to determine the likelihood of success, followed by design, fabrication, and test of a laboratory unit. A good particle separation capability was demonstrated. Upon completion of the laboratory testing, a design effort showed the feasibility of a staged in situ particle monitoring subsystem to give semicontinuous (nominal one minute cycle time) output of particle size distribution, among other applications. This work was completed in May of 1979 under Task 12 of EPA Contract No. 68-02-2165.

CONTENTS

		Page
Abstract		ii
List of Figures		iii
List of Tables		viii
1	Conclusions	1
2	Recommendations	2
3	Introduction	3
4	Subtask 1 – Analysis and Literature Search	5
	4.1 Background	5
	4.2 Impinging Jet Stability	6
	4.3 Pre-Design Literature Search	11
5	Subtask 2 – Design and Fabrication of Test Unit	16
	5.1 Design Parameters Affecting Stability	16
	5.2 Variation of Stability Parameters	18
	5.3 Other Design Considerations	20
	5.4 Fabrication of Test Unit	23
6	Subtask 3 – Laboratory Testing	24
	6.1 Test Setup	24
	6.2 Test Conduct	30
	6.3 Test Results	35
	6.4 Interpretation of Test Results	48
7	Subtask 4 – Additional Particle Separation Testing	60
	7.1 Hardware Modifications	60
	7.2 Test Description	64
	7.3 Test Results	67

CONTENTS (Cont'd)

		Page
8	Subtask 5 — Instrument Utilization	74
	8.1 Staged Continuous Flow Impactor	74
	8.2 Additional Configurations	84
	8.3 Cost Estimates	86
9	Discussion of Results	90
10	References	92
11	Glossary	93
12	Appendices	95
	A. Stability Data	95
	B. Optical Monitoring of Continuous Flow Impactor Output Streams	106

FIGURES

Number		Page
1a.	Schematic of Standard Particle Impactor (From Reference 4)	6
1b.	Schematic of Impinging Jet Impactor	6
2a.	Illustration of Separation Streamline Distortion Instability	8
2b.	Illustration of Unequal Flow Instability	8
3a.	Subsonic Jet Flowfields	9
3b.	Impinging Jet Flowfields	9
4.	Schematic of Luna's Test Setup for Impinging Jet Stability Testing (From Reference 1)	10
5a.	Illustration of Large Particle Non-Collection Due to Large Orifice	12
5b.	Illustration of Large Particle Non-Collection Due to Small Orifice	12
5c.	Illustration of Local Flowfield Phenomena Which Permit Undesired Migration of Gases and Small Particles Across the Interface	13
6.	Anticipated Continuous Impactor Efficiency Performance Curve, Based on Known Hardware Limitations	15
7.	Continuous Flow Impactor Assembly Drawing	17
8.	Impactor Splitter Plate Designs	19
9.	Impactor Contoured Nozzle	21
10.	Impactor Conical Nozzle	22
11.	Test Setup Schematics	25
12.	Particle Sampling Detail	29
13.	Turbulence Profiles for Conical Nozzle	36
14.	Turbulence Profiles for Contoured Nozzle	37
15.	Flow Control Schematics	38

FIGURES (Cont'd)

Number		Page
16.	Data Trends for Particle Collection Efficiency Testing, all Configurations	41
17.	Particle Collection Efficiency as a Function of Particle Size, Configuration A	42
18.	Particle Collection Efficiency as a Function of Particle Size, Configuration B	43
19.	Particle Collection Efficiency as a Function of Particle Size, Configuration C	44
20.	Particle Collection Efficiency as a Function of Particle Size, Configuration D	45
21.	Particle Collection Efficiency as a Function of Particle Size, Configuration E	46
22.	Particle Collection Efficiency as a Function of Particle Size, Configuration F	47
23.	Schematic of Flowrate Variation Technique for Biased Inlet Flow Cases, Configurations D, E, and F	49
24.	Comparison of Continuous Impactor Data With Anderson First Stage	50
25.	Calculated Free Streamline Shape (From Reference 1)	53
26.	Theorized Efficiency Curves for Continuous Flow Impactor, Based on Accumulated Test Data	55
27a.	Effect of Sampling Tube When Sampling Aerosol Side	58
27b.	Effect of Sampling Tube When Sampling Clean Side	58
28.	Schematic of Revised Exhaust Flow Setup	61
29.	Impactor Outlet Detail-Configuration G	62
30.	Impactor Test Setup-Configuration G	63
31.	Sketch of Particle Counter Sampling Tube in Impactor Exhaust Line	65
32.	Particle Collection Efficiency as a Function of Particle Size for Size Range 4-16 Microns, Configuration G	68

FIGURES (Cont'd)

Number		Page
33.	Particle Collection Efficiency as a Function of Particle Size for Size Range .5-5 Microns, Configuration G	70
34.	Complete Fitted Separation Efficiency Curve for Configuration G, Showing Data Points in Overlap Region	71
35.	Comparison of Separation Curves for Configuration C, G, and the Anderson Impactor First Stage	72
36.	Flow System Schematic and Pressure Hierarchy for Staged Continuous Flow Impactor	75
37.	Staged Continuous Flow Impactor Installation	77
38.	Staged Continuous Flow Impactor Module	78
39.	Staged Continuous Flow Impactor Assembly - First Two Stages	80
40.	Schematic Diagram of Optical Concept	82
41.	Filter Holder Subassembly	88

TABLES

Number		Page
1.	Royco 225 Particle Size Discrimination Characteristics	28
2.	Operating Conditions for Particle Separation Tests	40
3.	Nominal Size Ranges for Staged Continuous Flow Impactor Applications	71
4.	Continuous Flow Impactor Production Cost Estimates	74

SECTION 1
CONCLUSIONS

- The concept of using two impinging jets for the purpose of inertial particle separation has been shown to be technically viable.

- In addition, preliminary design studies indicate that a staged impactor can easily be integrated into a sampling probe to perform in situ particulate size distribution measurements.

- Feasibility of a simple optical system compatible with the in situ sampling hardware has been shown analytically.

- The continuous flow impactor has a potentially greater accuracy capability than standard impactors since it inherently avoids the traditional problems of particle bounce and reentrainment.

- Potential applications for the continous flow impactor include control device evaluation, continuous monitoring of particulate emissions for regulatory purposes, and collection of particles in an inert atmosphere to quench chemical reactions.

- A basic understanding of the continuous flow impactor operational characteristics has been attained. This can serve as a background for development of a commercially viable instrument.

SECTION 2
RECOMMENDATIONS

- The demonstrated performance and potential usefulness of the continuous flow impactor argue strongly for development and testing of a field worthy prototype instrument. This development should be pursued.

SECTION 3
INTRODUCTION

The purpose of the work described in this report was to investigate the feasibility of an impactor design in which the impaction surface would be the interface between two opposing jets. Instead of hitting and sticking to a solid surface, the particles would cross over the interface and be entrained in a previously particle free gas. This second stream could then be analyzed for particle content, optical techniques being the most obvious. The proposed instrument would be used in stationary source sampling work. Among the most obvious attributes would be elimination of particle bounce and reentrainment problems associated with standard impactors. Its continuous operation capabilities, inherent in the design, would avoid the problems of stage overloading at locations such as control device inlets, as well as the present need for long sampling times due to low grain loadings at places like ESP outlets. The continuous operation feature would make the device a viable one for long term regulatory monitoring as well.

Work was divided into five subtasks:

1. Analysis and Literature Search — this was done to determine the likelihood of success prior to making a hardware commitment. A decision was made to proceed with hardware design mainly in the strength of thesis work performed by R. E. Luna, whose test setup employed two impinging jets.

2. Design and Fabrication of Test Unit — the laboratory test unit was primarily designed to promote stability of the jet/jet interface, and to allow for insertion of diagnostic instrumentation. Several physical variables were designed into the unit so that their effect on performance could be evaluated.

3. Initial Laboratory Testing - this consisted of stability testing and particle separation testing. An initial flow instability was eliminated through a simple, acceptable flow control addition.

Particle separation testing revealed an aerosol withdrawal problem which was handled in the next subtask.

4. Particle Separation Testing - this was an add-on subtask for the specific purpose of sharpening the separation efficiency, and dealt with changes in handling of the gas stream downstream of the virtual impaction region.

5. Instrument Utilization - preliminary design work has shown that a four stage device with a total of five output streams can be packaged in a probe capable of insertion through a standard four inch pipe nipple, thus allowing for in situ measurements. Calculations show that these input streams can be adequately monitored (also in situ) by simple optical units. Additional applications and first cut price estimates are also presented.

Results of the work performed are highly encouraging. Although some additional investigative testing will be required, there are no unresolved questions regarding concept feasibility. There is no real doubt that the instrument will work — the issue which will need to be resolved is how well the continuous flow impactor will work for a given system cost. Preliminary indications are that performance should be good — the device is simple in operation, contains no moving parts or delicate or exotic components. Flow control, which is the key to successful operation, will be accomplished in a production device through use of sonic orifices, which are very simple and reliable. Components most likely to need servicing (pump, light source, electronics) will be located ex situ to facilitate access, without degrading performance.

The initial R&D task has been successfully completed, its objectives accomplished. The next step should be development and field demonstration of a prototype field unit. Characteristics established during performance of the task indicate that the continuous flow impactor will be a very useful device for both short and long term stationary source testing, since it has capabilities not found in any other device currently in use.

SECTION 4
SUBTASK 1 - ANALYSIS AND LITERATURE SEARCH

The first task objective was to determine the feasibility of using impinging jets for particle size classification. This was accomplished through a review of the technical literature. The second part of the task involved another review to obtain impactor design parameters for the purpose of designing the laboratory test unit.

4.1 BACKGROUND

The concept which is the subject of this report is illustrated in Figure 1. A standard impactor configuration is shown in Figure 1a. It consists of a nozzle to direct a particle laden flow in a prescribed manner, and an impaction surface which the flow, and consequently some of the particles, strikes. Ideally, all of the particles which strike the surface are retained. The current task has been concerned with improving two characteristics of the standard impactor: limited time operation, and problems (particle bounce and reentrainment) associated with the impaction surface. Standard impactor operation is intermittent because the impaction surface must be physically removed and weighed to determine the mass of the collected particles. The improvement technique which has been selected is shown in Figure 1b. The gas/solid impaction interface has been replaced by a gas/gas interface so that particles of interest are transferred from the particle laden stream to a particle-free stream. This interface eliminates the traditional bounce and re-entrainment problems, but produces some new ones, described below. The primary advantages of the opposing jet technique are:

1. It produces particle size fractionated output streams which can be examined on a <u>continuous</u> basis to determine total particulate mass emissions and size distribution.
2. It can readily be used to simultaneously fractionate and collect particles in a chemically inert atmosphere.

There is a present and future need for devices with these capabilities, and it is this need which has been the reason for performing the task.

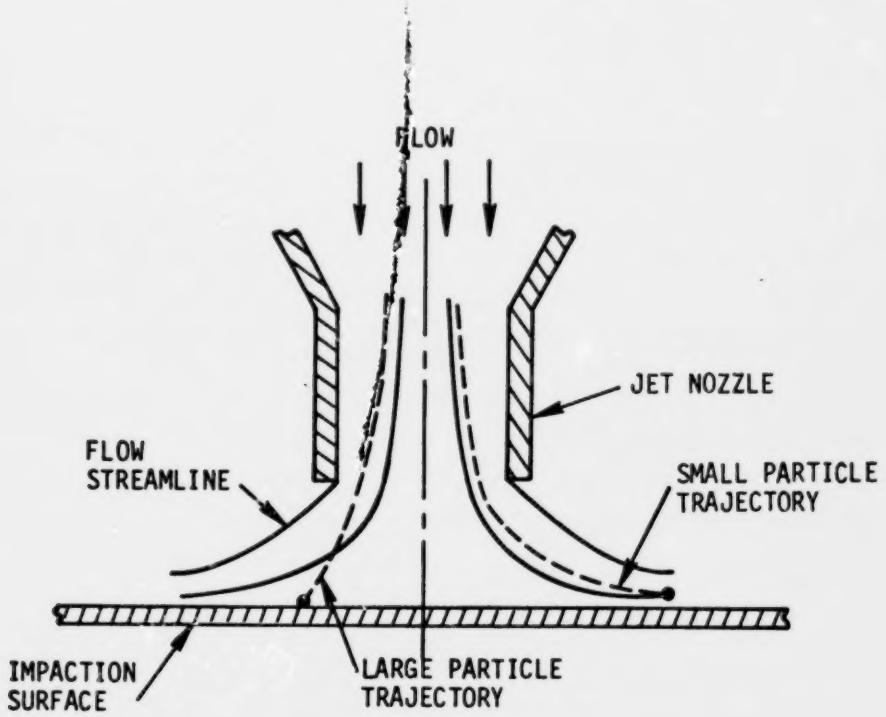

Figure 1a. Schematic of standard particle impactor (from Reference 4)

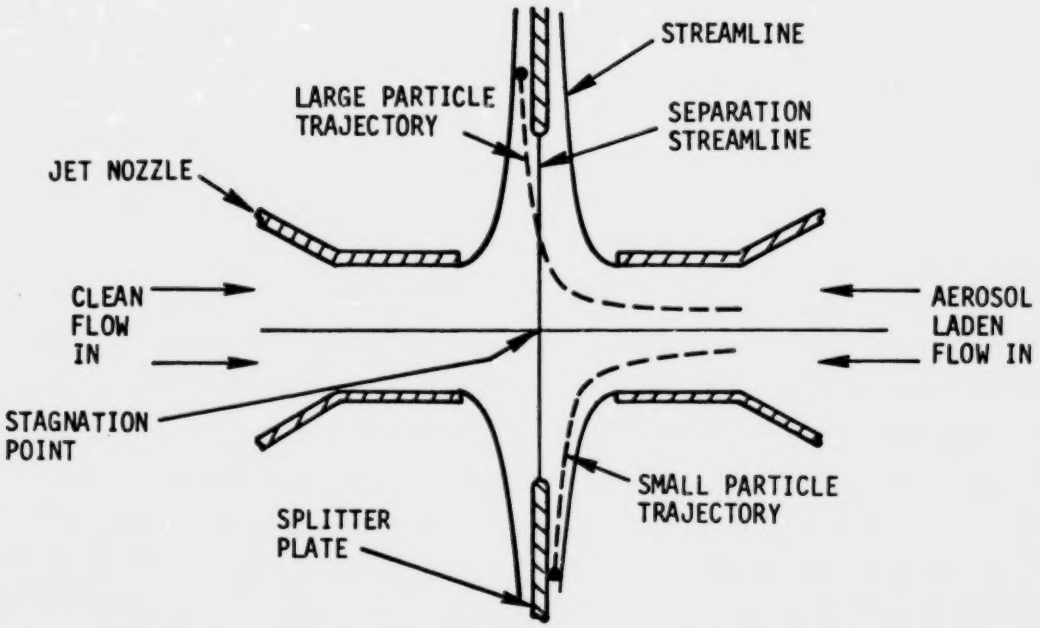

Figure 1b. Schematic of impinging jet impactor

4.2 IMPINGING JET STABILITY

The key to proper operation of an impinging jet impactor is stability of the gas/gas interface. The desired flowfield is illustrated in Figure 1b. Unacceptable flowfields resulting from instabilities are shown in Figure 2. Unstable operation would result in passage of significant amounts of gas from one or both nozzles through the plane of the desired interface. This would render the device incapable of separating particles in the desired manner. The first task objective was to determine whether the likelihood of stability was great enough to justify building and testing a laboratory model.

The structure of a jet of the type being considered is shown in Figure 3a, and the impinging jet flowfield is shown in Figure 3b. In standard impactor designs, the jet-to-plate spacing is such that part of the inviscid core remains by the time the flow hits the plate. The most useful literature information on the problem came from Reference 1, a PhD dissertation by R. E. Luna. His test setup is shown schematically in Figure 4. It consisted basically of two jets exhausting to room air, the jet flow rates being held constant through upstream pressure regulation and sonic orifices. He found that the flowfield and location of the interface were stable for jet spacings between 0.5 and 1.5 jet diameters, and that gross instabilities occurred for spacings greater than two diameters. For this application, a working definition of stability may be given as follows:

> The impactor flow is stable if, when disturbed, the interface returns to its original equilibrium position.

In addition to stability of the flow, flow steadiness is also an important feature. While stability is largely a property of the concept itself, steadiness is more related to the actual hardware configuration. As stated above, the impactor flow is stable if it returns to its equilibrium position after a disturbance. In addition, it will be steady if no disturbances occur. The most likely source of unsteadiness for this device

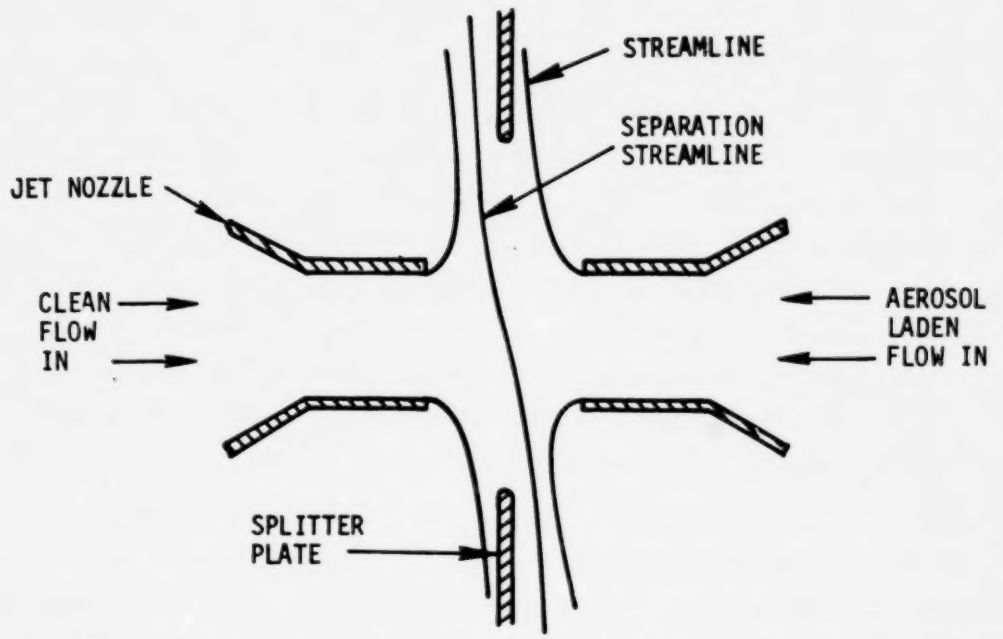

Location of separation streamline allows flow to cross through orifice

Figure 2a. Illustration of separation streamline dislocation instability

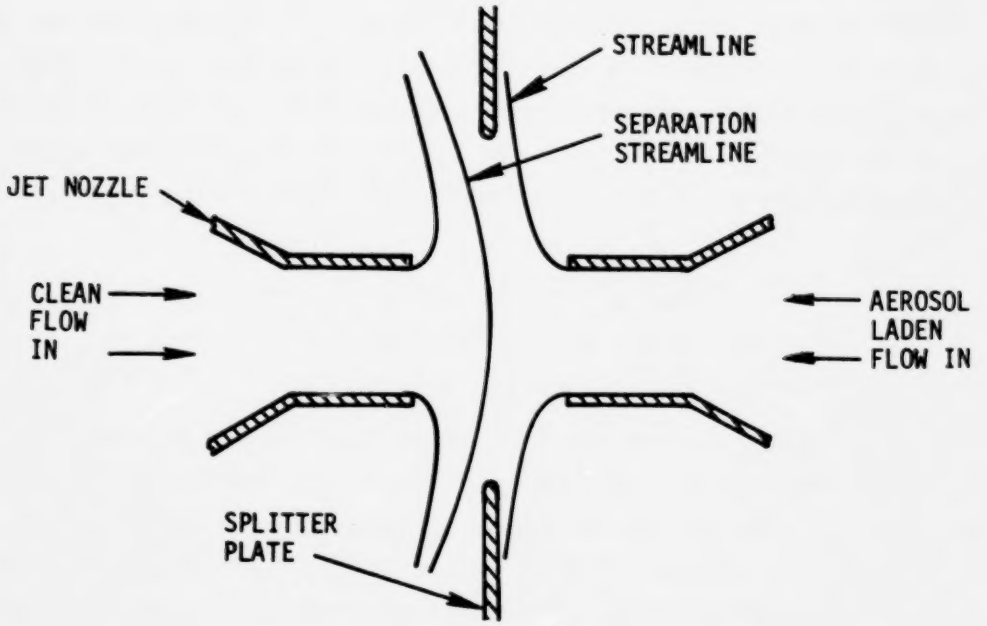

Higher flow rate through aerosol nozzle spills over to clean side

Figure 2b. Illustration of unequal flow instability

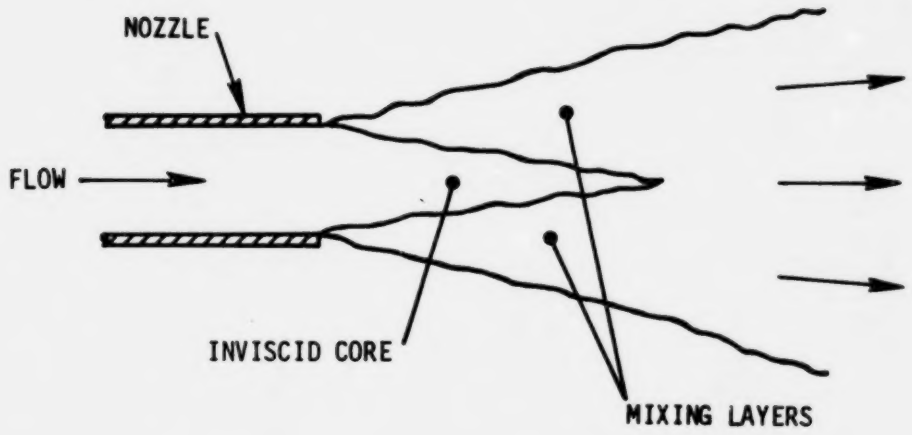

Figure 3a. Subsonic jet flowfields

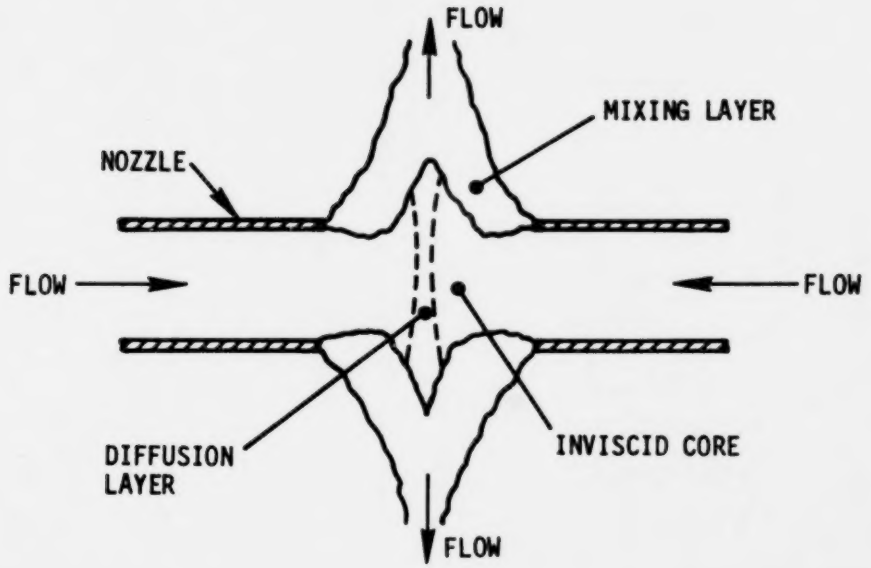

Figure 3b. Impinging jet flowfields

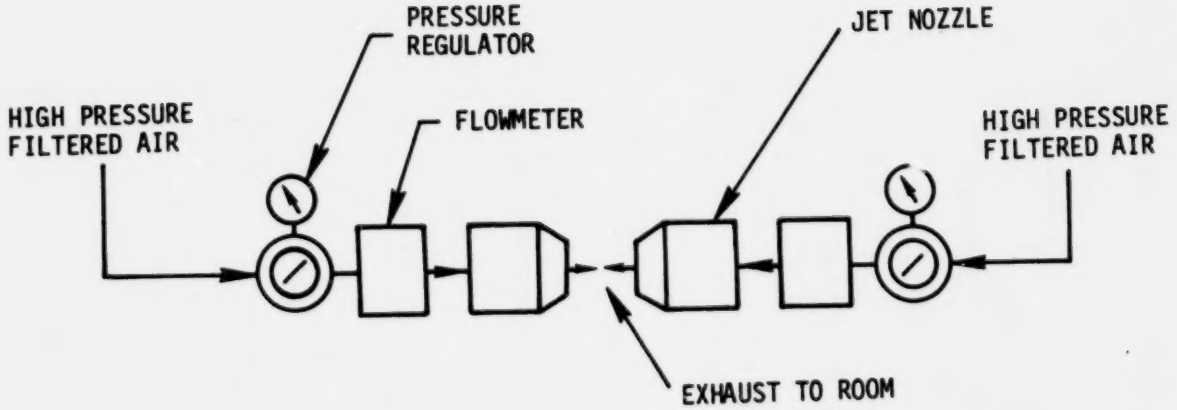

Key feature:

- The high pressure air source, regulator, and sonic orifice metering system guaranteed equal flow rates through the two nozzles
- Having both nozzles exhaust to the open room insured a steady external pressure field in the vicinity of the interface

Figure 4. Schematic of Luna's test setup for impinging jet stability testing (from Reference 1)

would be flow rate variations caused by changes in feed pressure, pump characteristics, etc. Even in a stable system, such variations would cause momentary changes in the shape and location of the interface, adversely affecting particle separation properties. In Luna's testing, acceptable steadiness was achieved by precise pressure regulation and metering of the flow to each jet, in addition to having the jets exhaust freely to (steady) room conditions.

Review of material in Reference 1 and of a similar study in Reference 2 led to the conclusion that flow stability could probably be achieved. A decision was made at this point to continue with hardware design, fabrication, and test.

4.3 PRE-DESIGN LITERATURE SEARCH

The literature review led to an early decision to work solely with round jets, rather than rectangular ones, for the following reasons:

- Impinging jet background data are available only for circular jets
- Theoretical calculations show sharper cutoffs for circular than for rectangular jets (Reference 3)
- Most commercially available impactors use circular jets (Reference 4)

The most important physical design parameters for a circular jet impactor are nozzle to plate spacing and nozzle geometry. For the impinging jet impactor, the following additional parameters must also be considered:

- Jet relative concentricity and angularity (relative jet alignment)
- Size of the interface orifice
- Shape of the interface orifice edge
- Relative flowrates of the two jets

The size of the interface orifice represents a particularly interesting engineering tradeoff, as illustrated in Figure 5. Figure 5a shows that if the orifice is large, a large particle crossing the interface near

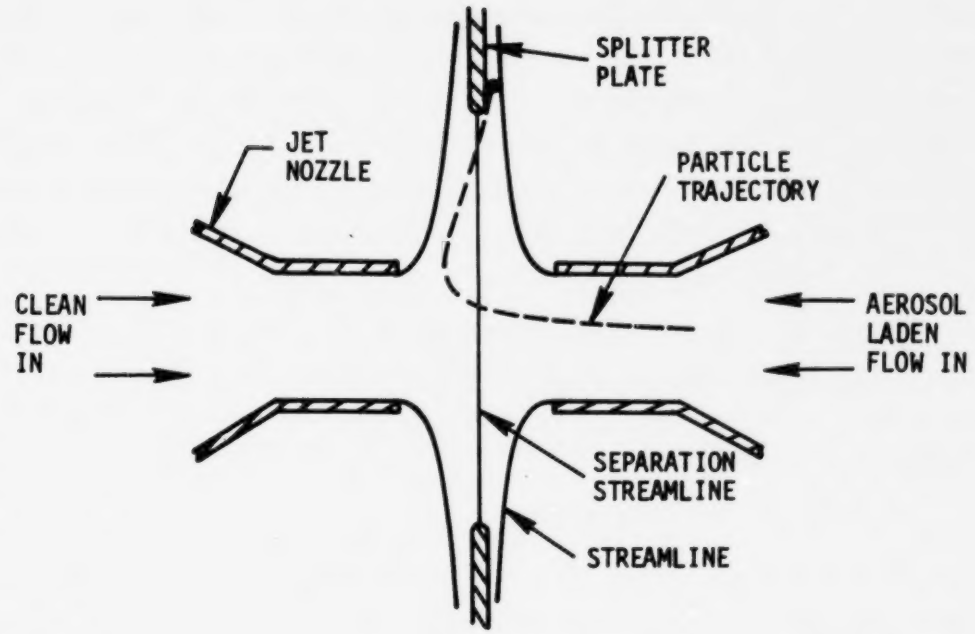

Figure 5a. Illustration of large particle non-collection due to large orifice

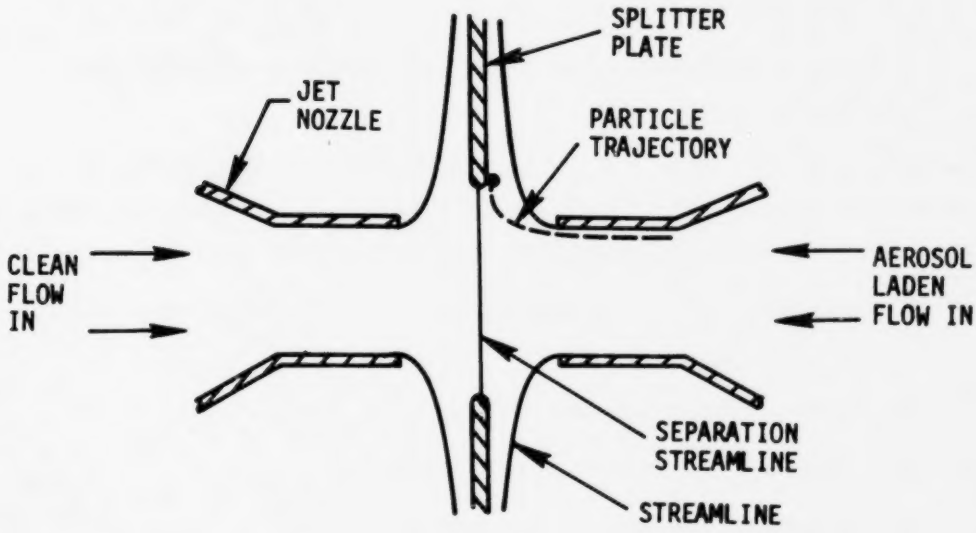

Figure 5b. Illustration of large particle non-collection due to small orifice

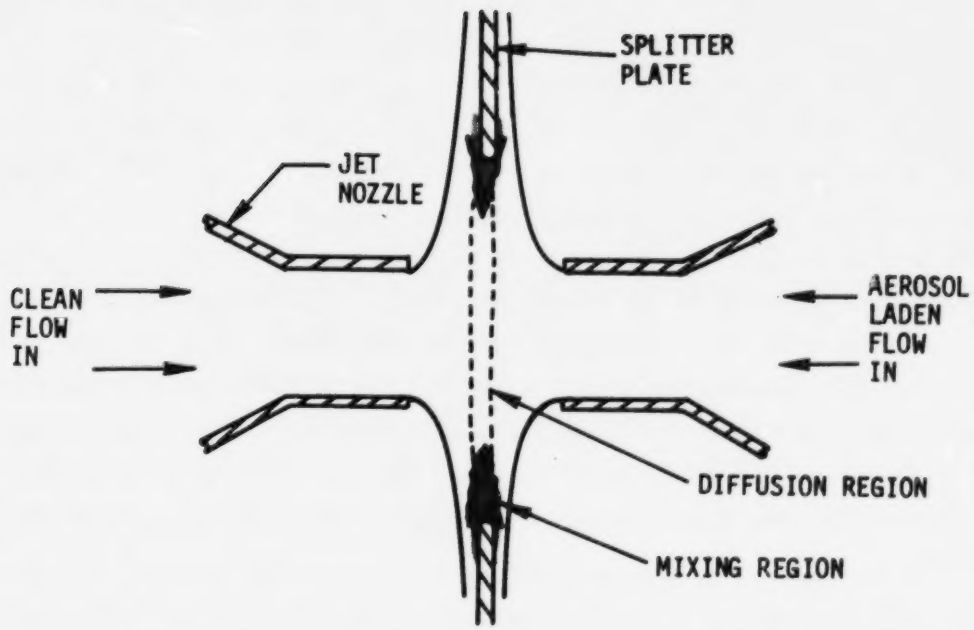

Figure 5c. Illustration of local flowfield phenomena which permit undesired migration of gases and small particles across the interface.

- Transfer of gas across the interface will occur by diffusion in the diffusion region. Transfer of particles in this region will occur by inertial means.
- The mixing region is the merging of the mixing layers in Figure 3B. Active turbulent mixing will occur here, resulting in transfer of both gases and small particles.
- Flow unsteadiness (not illustrated) will also cause momentary transfer of gas and particles across the interface by convection.

the axis of the jets may be swept back across the interface and not collected. Figure 5b shows that if the orifice is small, a large particle near the jet wall will not have an opportunity to be collected. Figure 5c, derived from Figure 3b, shows that at the interface, a mixing layer is set up between the two jets. As the mixing layer thickens along the interface, the mixing process carries small particles across the interface to the collection side. Thus some small particles will always be collected along with the larger particles. The larger the interface orifice, the more small particles will be collected. Thus for the impinging jet impactor we should expect to see an efficiency curve similar to that in Figure 6 — some small particles will always be collected, while some large particles will not be. Engineering tradeoffs would involve optimizing the efficiency curve for a particular application.

Identification of the primary physical variables for the device allowed us to proceed to the design and fabrication subtask discussed in the following section.

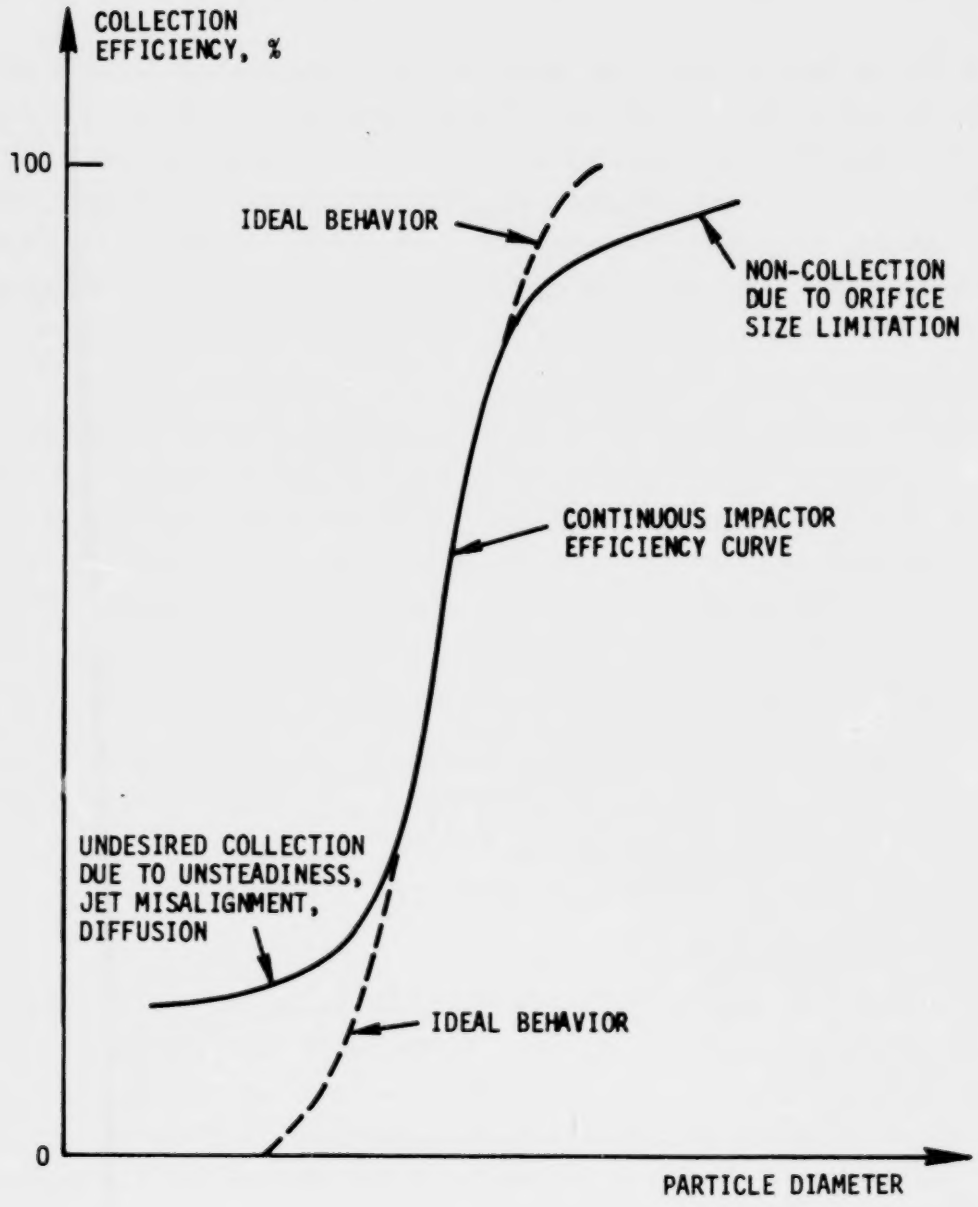

Figure 6. Anticipated continuous impactor efficiency performance curve, based on known hardware limitations

SECTION 5

SUBTASK 2 - DESIGN AND FABRICATION OF TEST UNIT

The philosophy behind the design of the prototype continuous flow impactor was to provide the capability to vary those parameters considered to be of possible importance to jet-jet interface stability, since the stability of impinging axisymmetric jets under stack sampling constraints had not been previously investigated. Flexibility in impactor configuration was, therefore, deemed necessary to identify configurations possessing stable flow which might be suitable for particle separation work.

The impactor, as shown in Figure 7, is seen to be basically a cylindrical housing, surrounded by two manifolds, with a ring shaped center plate to which different splitter plates may be attached. Cylindrical nozzle holders, to which various sized and shaped nozzles can be attached, are inserted into each end of the impactor and are positioned relative to the splitter plate by means of micrometer heads attached to the nozzle holders.

5.1 DESIGN PARAMETERS AFFECTING STABILITY

Parameters identified as being of probable importance to interface stability were associated with three aspects of the impactor configuration: nozzle - splitter plate separation, splitter plate orifice size and edge shape, and nozzle. Each of these aspects is discussed below.

5.1.1 Nozzle - Splitter Plate Separation

It was felt that nozzle - splitter plate separation might affect stability in two ways. First, there is the separation distance between the nozzle and the splitter plate, and between the two nozzles. Witze and Dwyer (Reference 2) showed that the steadiness (in the mean properties) of the flowfield produced by two impinging axisymmetric jets is dependent upon the distance between the nozzle exit planes. Luna (Reference 1) found similar results. Second, whether the nozzles are spaced at equal or unequal distances from the splitter plate might also affect stability.

5.1.2 Splitter Plate Orifice

The splitter plate orifice, it was thought, might affect stability in two ways, the first being the diameter of the orifice. This diameter

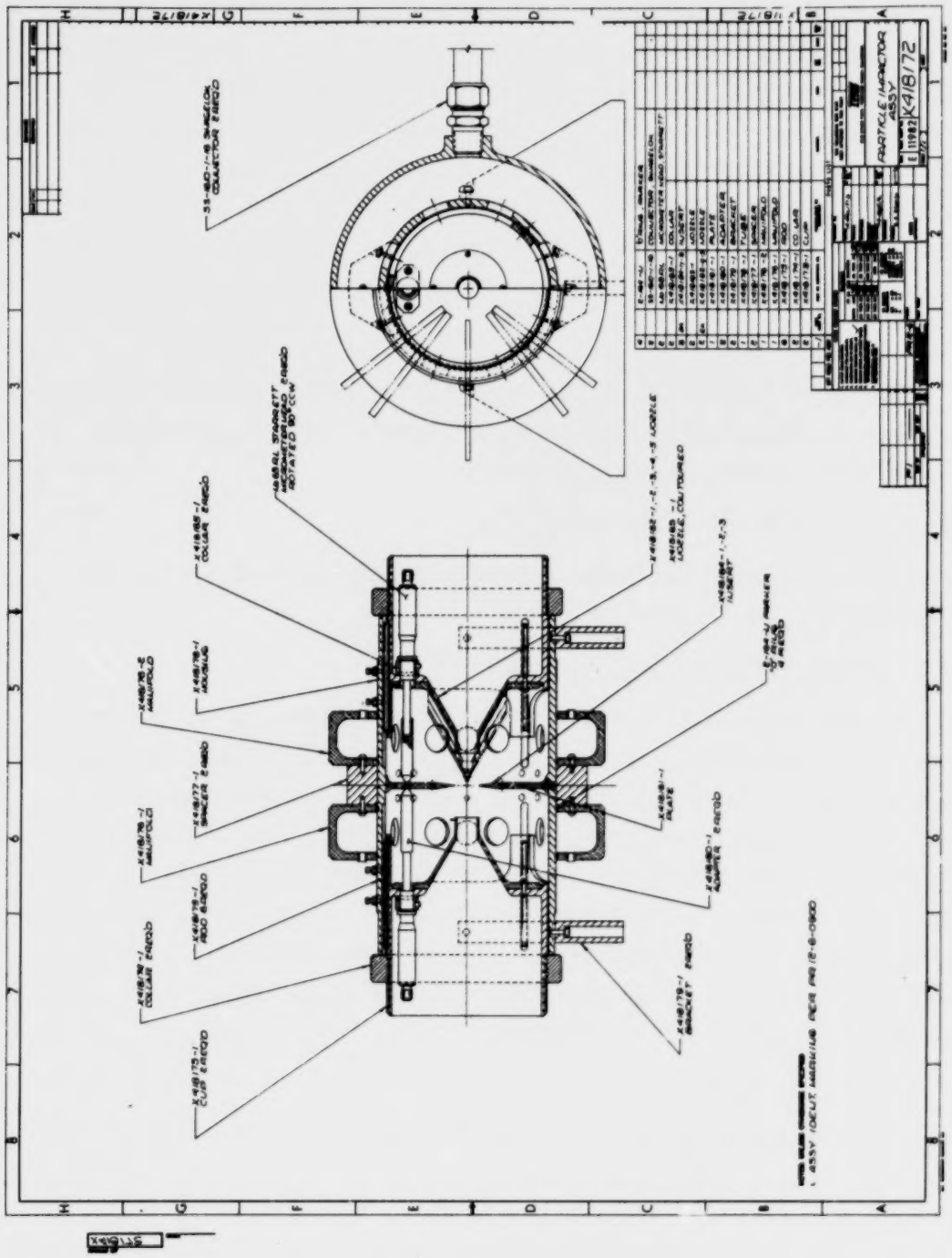

Figure 7. Continuous flow impactor assembly drawing

sets the size of the interface. A standard impactor, which is stable, may be considered to have an orifice diameter of zero. The bulk of the work in References 1 and 2 was done with no splitter plate, i.e., an infinite orifice. Our case lies somewhere in between. The second area of concern was the shape of the orifice edge. It was not known, at this stage of the study, whether the sharpness of the orifice edge would affect the ability of the interface to attach itself to the orifice edge, which determines whether or not there is flow across the orifice.

5.1.3 Nozzles

Aspects of nozzle design that were felt to have a possible effect on interface stability were nozzle diameter, which, in part, determines the flow Reynolds number, and nozzle shape.

5.2 VARIATION OF STABILITY PARAMETERS

Design features permitting variation of the parameters discussed in Section 5.2 are detailed below.

5.2.1 Nozzle-Splitter Plate Separation

The impactor was designed so that each nozzle-nozzle holder assembly could move independently with respect to the splitter plate. Micrometer heads attached to each assembly allow a nozzle to be positioned with respect to the splitter plate to within 0.001-inch. Therefore, any desired nozzle-splitter plate separation distance could be examined to determine its effect on interface stability. Since each nozzle-nozzle holder assembly moves independently of the other, the effect of both equal and unequal nozzle-splitter plate separation distances upon interface stability could be investigated.

5.2.2 Splitter Plate Orifice

The impactor center plate, shown in Figure 7, was designed so that various splitter plates, with orifices of different sizes and edge shapes, could be fitted to it. The splitter plate design is shown in Figure 8. Splitter plates were manufactured with orifice diameters of 1.0, 2.0, and 3.0 centimeters. For each orifice size, three different orifice edge shapes were used, yielding a total of nine different splitter plates available for stability testing.

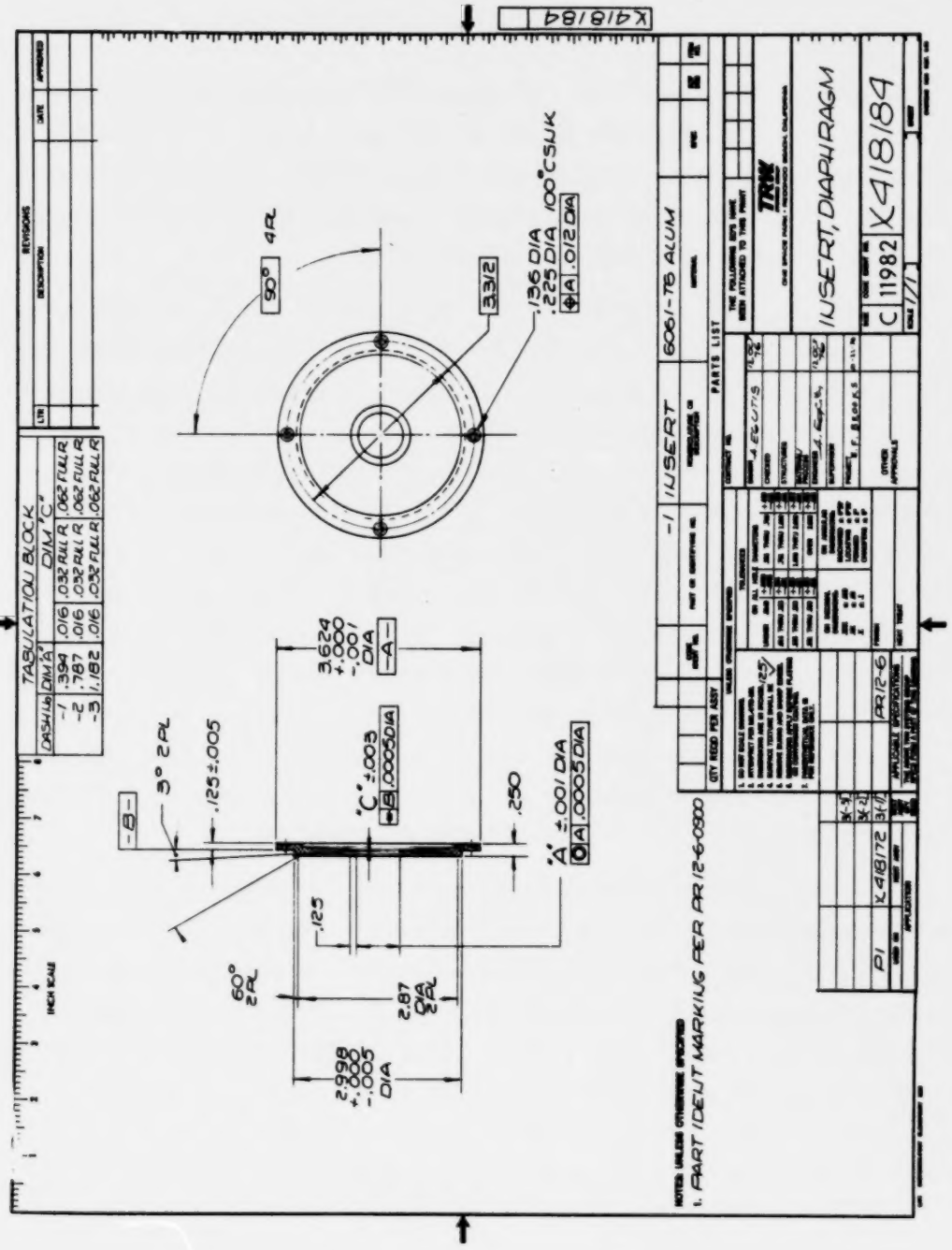

Figure 8. Impactor splitter plate designs

5.2.3 Nozzles

The effects of nozzle size and shape upon interface stability were examined by building different pairs of nozzles. Each nozzle assembly consisted of two parts, a nozzle and a nozzle holder, shown in Figures 7, 9, and 10. Only one set of nozzle holders was built, as each nozzle was designed to be compatible with the nozzle holders.

The nozzles were built in two different shapes, contoured and conical, as shown in Figures 9 and 10. Marple and Willeke (Reference 4) have shown that the more uniform the flow is at the nozzle exit, the sharper the cutoff will be in a standard impactor. This result should also be applicable to a continuous flow impactor. On the basis of this result, contoured nozzles, using the nozzle design of Smith and Wang (Reference 5) to achieve uniform flow at the nozzle exit, were built. A pair of conical nozzles was also built. It was hoped that a conical nozzle impactor would perform well enough, in comparison to a contoured nozzle impactor, to permit the use of the less expensive conical nozzles in any commercial application of the instrument. The conical nozzles had a cone angle of 60°, this being the same cone angle used in experiments by Ranz and Wong (Reference 6). A nozzle diameter of 1.0 cm for both contoured and conical nozzles was chosen for the initial studies of stability.

While it is believed that concentricity of the impactor nozzles with each other and with the splitter plate orifice is important to interface stability, it is felt that in a production model, tolerances normally encountered in machining would give adequate concentricity. Therefore, provisions to vary nozzle-nozzle and nozzle-splitter plate orifice concentricity were not included in the design of the impactor. Each nozzle-nozzle holder assembly rides on three precision shaftings resting in grooves in the impactor housing to assure concentricity of the nozzles and the splitter plate.

5.3 OTHER DESIGN CONSIDERATIONS

The impactor is connected to a vacuum pump through manifolds on each side of the splitter plate. There are eight equally sized and spaced circular inlets into each manifold from the impactor. The inlets and the cross-sectional area as seen by the flow inside the manifolds are large

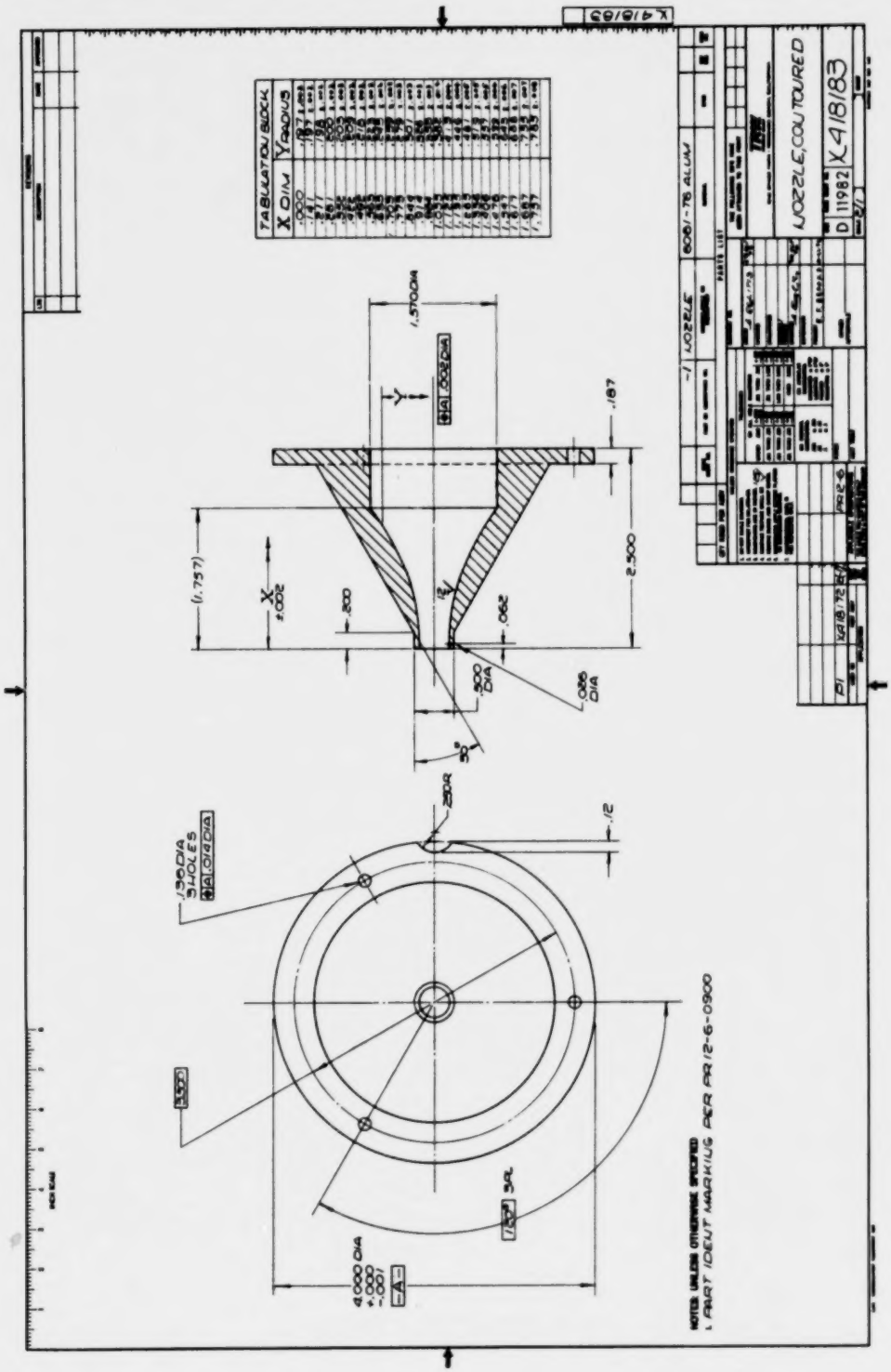

Figure 9. Impactor contoured nozzle

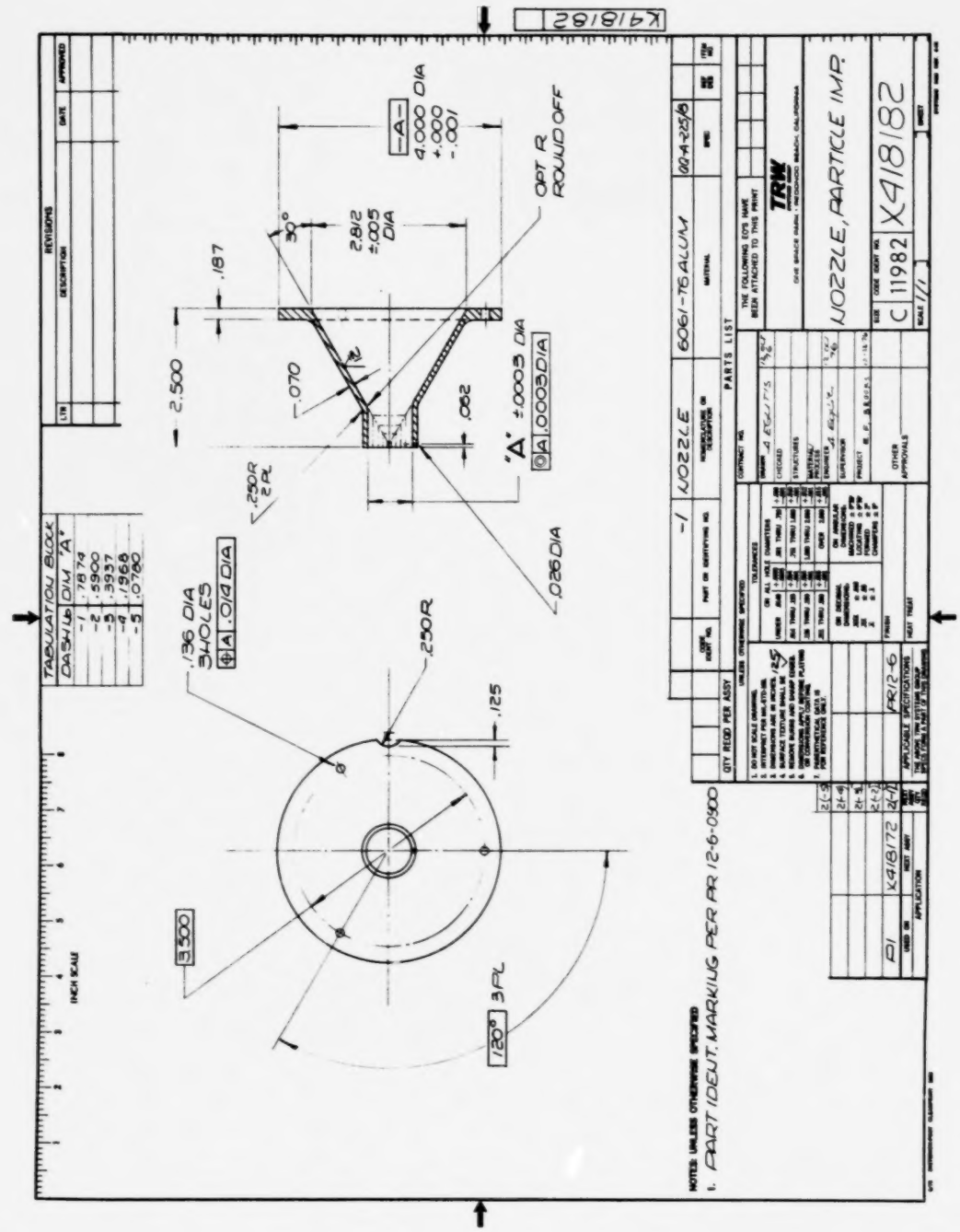

Figure 10. Impactor conical nozzle

compared to the nozzles, to prevent large pressure drops across the inlets and inside the manifolds. This assures symmetrical radial flow outward after impingement of the jets, rather than having more flow outwards toward the side of the manifold that is connected to the pump.

Access ports into the impactor, on either side of the splitter plate, were provided to allow hot wire anemometry measurements of interface stability and selective sampling of aerosols in the particle separation phase of testing.

5.4 FABRICATION OF TEST UNIT

All fabrication was performed in TRW machine shops. Aluminum was selected as the material for construction since the unit would only be operated at room conditions. No unusual problems were encountered during the fabrication effort.

Since there were significant doubts about the stability characteristics of the device during the early stages of the task, a large portion of the task budget was put into design and fabrication. Attention was concentrated on alignment and pressure distribution to maximize flow uniformity and eliminate disturbances and asymmetries as much as possible.

SECTION 6

SUBTASK 3 - INITIAL LABORATORY TESTING

6.1 TEST SETUP

Initial testing of the prototype continuous flow impactor was performed in the Engineering Sciences Laboratory nitrogen flow room. The basic test setup, common to both the stability and particle separation phases of testing, was as described below and shown in Figure 11.

Each of the impactor's two manifolds was connected by 1/4-inch stainless steel tubing to a rotameter flowmeter. The flowmeters could measure flow rates in the range from zero to approximately 0.65 l/s (1.5 cfm). Needle valves downstream of the flowmeters permitted adjustment of the flow rate through each manifold. Downstream of the needle valves, the two flows were merged into a 1/2-inch stainless steel line by means of a tee connector. The 1/2-inch line ran to a vacuum pump located in the room adjacent to the nitrogen flow room. The pump was located outside the test area to prevent the possibility of particle separation test data errors due to oil vapor droplets from the vacuum pump. The pump used in testing was a Welch Model 1403 Duo Seal Vacuum Pump, with a pumping capacity of 1.6 l/s (3.5 scfm).

Pressure taps were installed in the impactor housing tube to monitor the difference in impactor chamber static pressures on either side of the splitter plate, and installed in each nozzle, near the nozzle exit, to measure the pressure drop across each nozzle. The impactor housing pressure taps were connected to the ports of a MKS 77H-10 Pressure Head which was connected to a MKS Type 77 Baratron Pressure Meter. The pressure taps from each pair of nozzles were connected to one port of a MKS 77H-1 Pressure Head through a five-way switching valve. The second port was left open to ambient air and the pressure head was connected to a second MKS Type 77 Baratron Pressure Meter. This arrangement allowed the measurement of only one nozzle pressure drop at a time, but the use of the five-way valve permitted rapid changing of the connector between pressure head and nozzle pressure taps.

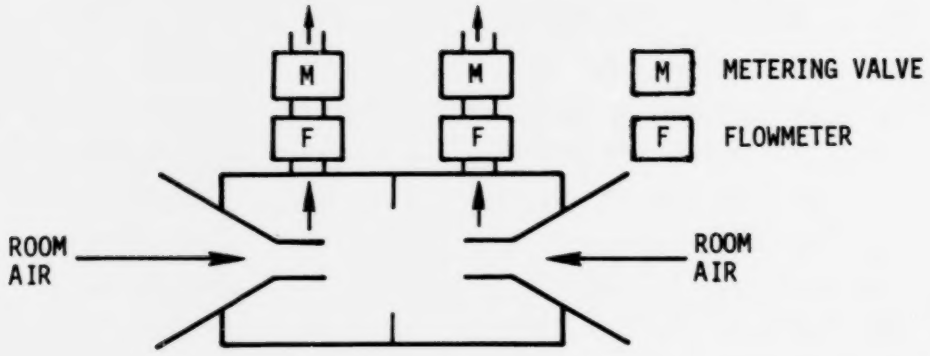

a. Stability test - initial

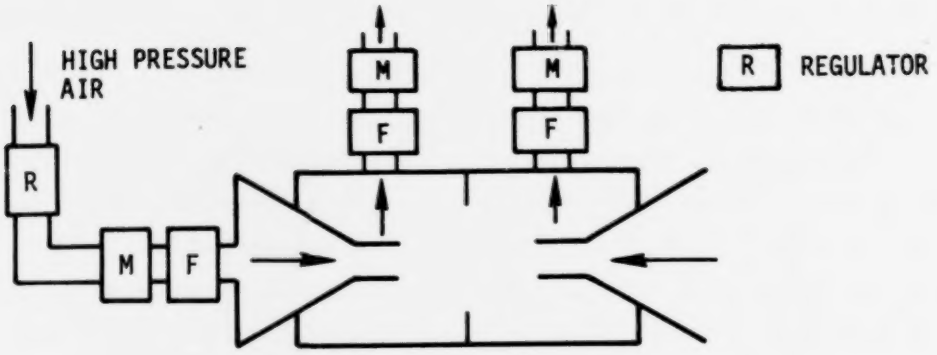

b. Stability test-modified

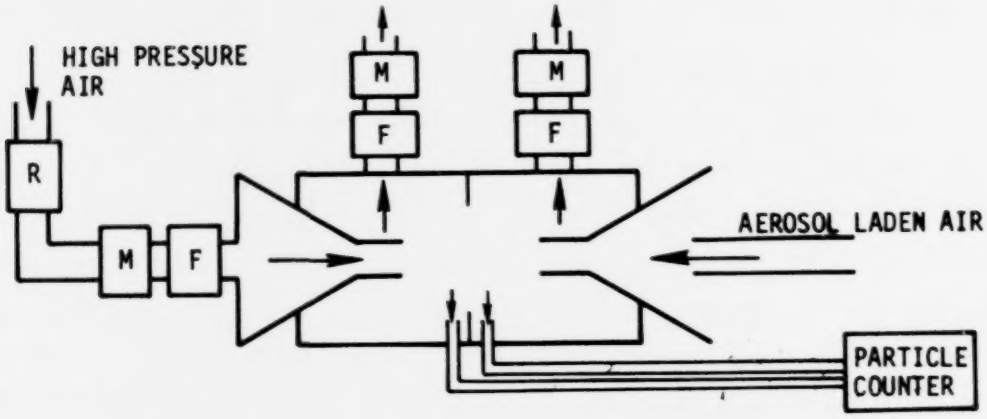

c. Particle separation test

Figure 11. Test setup schematics

6.1.1 Stability Test Setup

In addition to the basic test setup for the impactor, additional equipment was used in the stability phase of testing. A Thermo Systems Inc. (TSI) Model 1010 Constant Temperature Anemometer and a TSI Model 1220 hot film sensor probe were used to measure fluctuations in one jet with the splitter plate orifice blocked off. A Hewlett Packard Model 410C Multimeter was used to measure the RMS (root mean square) value of the signal fluctuations from the TSI probe, and a Tektronix oscilloscope was used to estimate the peak-to-peak value of the fluctuations in the signal. A Leeds and Northrup Model W Speedomax Strip Chart Recorder was used to record the pressure drops across the impactor nozzles and the static pressure difference in the impactor across the splitter plate.

During the stability phase of testing, it was decided that, in addition to controlling the flow downstream of each manifold, flow rate control was also needed upstream of one of the two nozzles. A plate was made to fit into the inlet of the nozzle-nozzle holder assembly, leakage being prevented by use of two O-rings set in grooves in the plate. The plate was fitted with a 1-1/2 inch pipe fitting which was reduced down to a 1/4-inch tube fitting. The plate was connected by 1/4-inch flexible tubing to a rotameter flowmeter. A needle valve was located upstream of the flowmeter. The valve was connected by 1/4-inch flexible tubing to a regulated nitrogen bottle or trailer. This upstream flow control was used in the remainder of the stability test phase, as shown in Figure 11b.

6.1.2 Particle Separation Test Setup

The setup for the particle separation phase of testing consisted of the basic setup described above and the following equipment, as shown schematically in Figure 11c.

Control of flow into one nozzle, using the end plate-flowmeter-needle valve combination described in Section 6.1.1, was used during the entire particle separation phase of testing. A regulated nitrogen bottle or trailer was used as the gas source. The nozzle with the upstream flow control provided the clean jet, i.e., the jet into which particles were not injected.

A Berglund Liu Model 3050 Monodisperse Aerosol Generator, built by Thermo Systems, Inc., was used as the source of monodisperse particles that were injected into the impactor. The aerosol generator was equipped with a B&K Model E-310B Sine/Square Wave Generator and a Harvard Apparatus Model 975 Compact Infusion Pump. The pump used B-D Plastipak Disposable plastic syringes as a source for the solutions used in the aerosol generator. The particles generated were introduced into the impactor by positioning the aerosol generator outlet hose at the inlet to the nozzle-nozzle holder assembly that had not been modified for upstream flow control.

The aerosol generator functions in the following manner. A solution of non-volatile solute in a volatile solvent is pumped by the infusion pump through a filter into the aerosol generator. The solution is forced through a small orifice, with a diameter of five, ten, or twenty microns, in the form of a liquid column. The orifice is in a disc that is vibrated by a piezoelectric crystal connected to the signal generator. The oscillation of the orifice causes the column of solution to break up into uniformly sized droplets. The droplets pass through a second, larger orifice. Gas also flows through this orifice, preventing the droplets from combining to form larger droplets. The droplets are then entrained in gas flowing upward through the aerosol generator's vertical drying column. This gas flow serves two purposes. First, it evaporates the solvent, leaving only the solute as a liquid or a solid particle, depending on whether the solute is a liquid or a solid. Second, it carries these solute particles through the outlet hose at the top of the drying column to the point of application of the particles. The gas source used during testing with the aerosol generator was a regulated nitrogen bottle or trailer. Knowing the solution feed rate into the aerosol generator, the frequency of oscillation of the orifice, and the concentation of the solution used, the size of the particles produced can be calculated accurately.

A Royco Model 225 Particle Counter Mainframe with Sensor, equipped with a Model 518 digital display plug-in readout meter to display particle counts, was used to count particles in samples drawn from either side of the impactor splitter plate. The samples were drawn out through 1/4-inch stainless steel tubes inserted through ports in the impactor housing. The sampling tubes were located on either side of the splitter plate at a

radial distance of two nozzle diameters from the impactor centerline and at a distance of approximately 3/4 of a nozzle diameter from the face of the splitter plate, as shown in Figure 12. The tubes were placed as close as possible to the interface area, without being so close as to affect the flowfield, in order to avoid sampling in an area where loss of particles to the wall could occur. The sampling tubes were connected, alternately, to the particle counter sensor by a minimum length of flexible tubing. The sensor was connected by flexible tubing to a pump located in the counter mainframe. This pump was used to draw the samples from the impactor.

The Royco Model 225 particle counter uses a near forward scattering optical system in its sensor to detect particles. It can detect particles with diameters of 0.5 microns or greater. The counter can handle particle concentrations of up to 3×10^3 per cubic centimeter, and can sample at two flow rates, 50 and 5 cm^3/sec. The counter mainframe is equipped with a built-in calibration circuit and meter to calibrate the counter whenever desired. The Model 518 readout module has a five channel memory into which the particle counts in five adjustable size ranges may be simulataneously stored. As used in the particle separation tests, the 518 module stored particle counts in the following size ranges:

Table 1. Royco 225 Particle Size Discrimination Characteristics

Module Channel	Size Range
1	All particles > 0.5 microns
2	All particles > 0.7 microns
3	All particles > 1.4 microns
4	All particles > 3.0 microns
5	All particles > 5.0 microns

The module can be set to store counts taken over one minute or ten minute periods, or the sample time duration can be controlled externally. The counter was calibrated by a Royco employee during the test phase and found to be in proper working order.

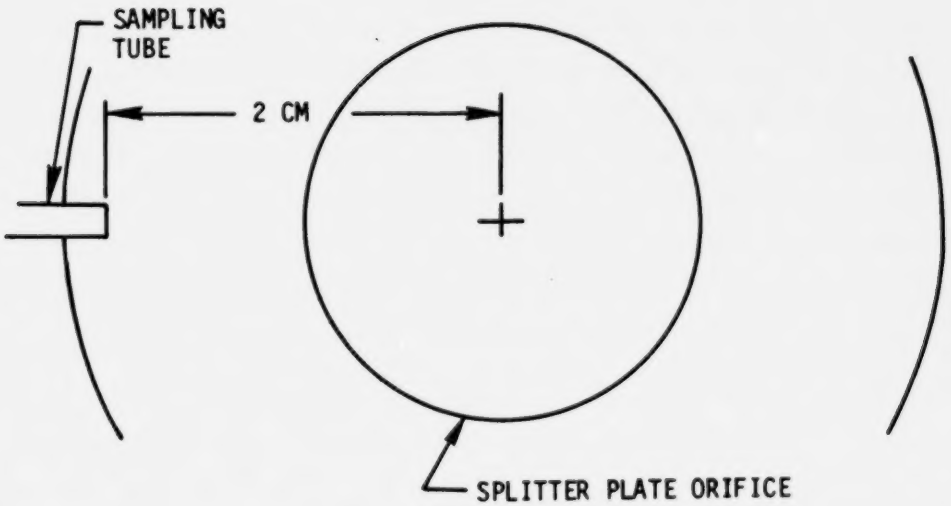

a. Overhead view

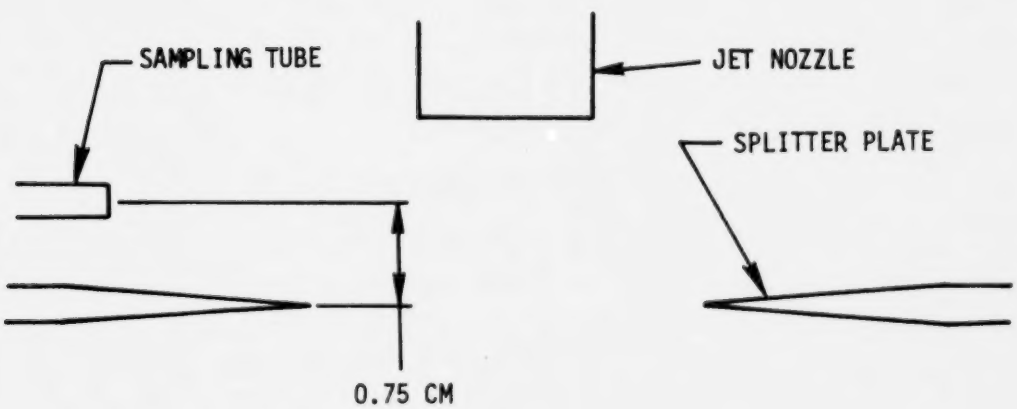

b. Side view

Figure 12. Particle sampling detail

6.2 TEST CONDUCT

6.2.1 Stability Testing

The first phase of testing dealt with investigation of the gas dynamic properties of the impactor. The intended diagnostics techniques were hot film anemometry and pressure measurement. The instability mode which was considered to be of greatest concern prior to testing was oscillation of the interface, which would allow some of the flow from each side to cross over to the other side. That mode turned out not to be the one which was actually observed during the test. The type of instability which did occur, and is described in detail in Section 6.3.1, resulted in major alterations of the originally proposed stability test sequence. The stability testing as it actually occurred is described below.

6.2.1.1 Standard Impactor Configuration Investigation

It was decided that data would be taken with a standard impactor configuration (Figure 1a) to serve as baseline data. The data obtained consisted of hot film anemometer velocity and turbulence traverses in the vicinity of the jet. A splitter plate with no hole was the impactor surface. The purpose was to provide quantitative information about the jet behavior which would be compared to data taken from the opposing jet configuration. Data were taken for both conical and contoured nozzles. Results are presented in Section 6.3.1.

6.2.1.2 Opposing Jet Configuration Investigations

Upon completion of the hot film testing described above, the opposing jet configuration was set up to repeat the hot film measurements. Nozzle differential pressure readings made it very evident that the desired and intended equal flow through each of the two nozzles was not being obtained. The test setup at this point was as shown in Figure 11a. The nozzle flowrates were observed to vary randomly over a range of ± 60% or more from the nominal desired flow, even though the flowrate through each outlet manifold stayed constant.

After enough pressure data were obtained to substantiate the nature of the instability, a meeting was held to discuss the problem and the configuration shown in Figure 11b was proposed. Stability was verified

for this configuration by means of pressure and flow measurements, as described in Section 6.3.1. At this point, a decision was made to proceed directly to particle separation testing, due to budget and schedule constraints, so no hot film work was performed on the opposing jet configuration.

6.2.2 Particle Separation Testing

6.2.2.1 Impactor Configurations Tested

Specifications for the impactor configurations tested in the particle separation phase of testing, such as nozzle-nozzle spacing and splitter plate orifice size, are given in Table 2 (p. 40). The variations made in configuration were suggested by the results of particle separation for previously tested configurations. Two comments, concerning nozzle-nozzle spacing and splitter plate orifice edge shape, should be made. The nozzle-nozzle spacing was fixed at 1.5 nozzle diameters, with equal spacing between each nozzle and the splitter plate, giving a nozzle-splitter plate spacing of 0.75 nozzle diameters. Unequal spacing was not tried because it was felt that this would be equivalent to having unequal flow rates through the impactor nozzles, which was tested. The nozzle-nozzle spacing used was chosen for two reasons. First, Marple and Willeke (Reference 4) have shown that for a standard impactor with a round jet, the 50% cutoff size drops rapidly for nozzle-to-plate spacings less than 0.5 nozzle diameters. This means that for small nozzle-to-plate spacings, almost all particles are collected instead of particle separation into different size classes being achieved. Therefore, the nozzle-nozzle spacing had to be greater than 1.0 nozzle diameters. Second, Luna (Reference 1) demonstrated that the flowfield produced by two impinging circular jets is unstable if the nozzle-nozzle spacing is greater than 2.0 nozzle diameters. So, as a compromise between these two limits, a nozzle-nozzle spacing of 1.5 nozzle diameters was used. This is the same spacing preferred by Luna. The splitter plate orifice edge shape was not varied due to a lack of time.

6.2.2.2 Aerosol Generator Operation

The size of the particles generated by the Berglund Liu Model 3050 aerosol generator depend on three factors: 1) solution volume flow rate, 2) frequency of oscillation of orifice, and 3) solution concentration. To accurately know the size of the particles produced, each of these factors must be known accurately.

The solution volume flow rate was determined by flowing distilled water from the infusion pump into a graduated cylinder and measuring the time in which a certain volume of water flowed. The pump was run at an intermediate pump speed setting. The relationship between flow rates for two different pump speed settings was known, so the flow rate at the recommended pump speed setting could then be determined. The infusion pump was calibrated with two different sized syringes, 20 cc and 10 cc, which were used with the 20 micron and 10 micron orifice plates, respectively.

The signal generator supplied with the aerosol generator was tested by the Metrology Department, which concluded that the generator met the manufacturer's specifications. The operating frequency range for the aerosol generator depends on the orifice size of the vibrating plate. The procedure used to determine the frequency range is described later in this section.

Solutions of Di Octyl Phthalate (DOP) in reagent grade isopropyl alcohol, prepared by the Chemistry Department, were used in the aerosol generator. The concentrations, by volume, of the solutions prepred were 1:1000, 1:500, 1:250, 1:125, and 2:125.

The 10 micron and 20 micron orifice plates were used in the aerosol generator. The solution flow rate is higher, but the operating frequency range is lower for the 20 micron orifice than the 10 micron orifice. The operating manual provided with the aerosol generator lists the proper infusion pump speed setting for each size orifice, with which one can then determine the solution flow rate for each size orifice, as described above, and the nominal operating frequency range for each size orifice. The actual frequency range is determined in the following manner. Solution is flowed through the orifice at the proper rate. The solution column is deflected by gas flowing through a nozzle at a rate of 700 cc per minute. Beginning at the lower end of the nominal frequency range, the signal generator frequency setting is increased until a nonuniformly sized particle stream is observed. The frequency at which this occurs, f_{max}, is the maximum frequency at which uniform droplets can be produced for the given orifice end solution flow rate. The minimum recommended frequency is 0.5 f_{max}, so the operating frequency range is 0.5 f_{max} to f_{max}. The manufacturer claims that the best performance is obtained at a frequency of 0.6 f_{max}.

The sizes of particles used in the particle separation phase of testing could be calculated once the solution volume flow rate, frequency range, and solution concentration were known. The particle size (diameter) range used in the testing was 2.44 to 11.56 microns.

The gas flow rate through the aerosol generator is controlled by two sets of rotameter flowmeters and needle valves built into the aerosol generator. During the particle separation phase of testing, this flow rate was always kept greater than the flow rate through the nozzle into which the particles were introduced. The resultant excess flow, which exited from the impactor through the nozzle holder inlet, was designed to prevent particles in the room air from being introduced into the impactor.

6.2.2.3 Particle Counter Operation

The Royco Model 225 particle counter, as noted in Section 6.1.2, can sample at two different flow rates, 50 and 5 cm^3/s, and for durations of one and ten minutes. During the particle separation testing, a sample flow rate of 50 cm^3/s and a sample duration of one minute were used. The shorter sample duration was used to avoid errors in the measured separation efficiency due to possible changes over a long period in the output from the aerosol generator caused by a slow drift in the pressure at which nitrogen was supplied to the aerosol generator.

6.2.2.4 Particle Separation Test Procedure

The procedure for the particle separation phase of testing is listed below:

(1) Set up the impactor in the configuration to be tested.

(2) Start vacuum pump, nitrogen flow through clean side of impactor (i.e., side into which particles are not injected), and set flow rates through impactor.

(3) Aerosol generator is started. Due to high initial liquid flow rate needed to start generator, must wait several minutes for liquid flow rate to decrease to proper rate before taking sample from impactor.

(4) Take sample from sample tube on one side of splitter plate.

(5) Record particle counts on all five readout meter channels (recording counts on all channels serves as a check on whether the aerosol generator is producing monodisperse particles).

(6) Connect particle counter to sample tube on other side of splitter plate.

(7) Take sample.

(8) Record particle counts on all readout meter channels.

(9) Repeat steps (4) through (8) two to four times.

(10) After every three to four pair of measurements, where steps (4) through (8) constitute a pair of measurements, check the particle counter calibration using its built-in calibration circuit and meter.

(11) Change particle size by changing frequency setting of signal generator.

(12) Repeat steps (4) through (10).

(13) Repeat steps (10) through (11) until measurements have been made at all desired frequency settings.

(14) Turn off infusion pump. Leave aerosol generator nitrogen flow on.

(15) Take particle count measurements on each side of the splitter plate. (This step is used to check whether the nitrogen used is clean.).

(16) Turn off aerosol generator nitrogen flow and signal generator.

(17) Turn off vacuum pump and impactor clean side nitrogen flow.

(18) Change aerosol generator vibrating orifice plate if desired.

(19) Flush aerosol generator with reagent grade isopropyl alcohol.

(20) Change solution in aerosol generator if desired.

(21) Repeat steps (2) through (20).

(22) Repeat step (21) until impactor configuration has been tested at all desired aerosol generator settings.

(23) Repeat steps (1) through (22) until all desired impactor configurations have been tested.

6.3 TEST RESULTS

6.3.1 Stability Testing

6.3.1.1 Standard Impactor Configuration Investigation

Turbulence profiles obtained using a hot film anemometer are presented in Figures 13 and 14 for the conical and contoured nozzles, respectively. The data trends show relatively low turbulence levels in the jet itself. As the nozzle to plate spacing increased, the measured turbulence level in the jet also increased due to the effect of mixing. Turbulence was seen to increase rapidly in the region where the flow was being turned (up to a distance of about 5 nozzle radii) and then it started to drop off after completion of the turn.

It was the original intent to repeat the measurements in the opposing jet configuration, but the stability problems described in the following paragraph required too much attention, and no addition hot film data were taken. The data in Figures 13 and 14 indicate the probable existence of rapidly increasing turbulence along the interface between the jets, suggesting that some turbulent mixing will occur along the interface which would cause small particle to be convected across the interface.

6.3.2.2 Opposing Jet Configuration Investigations

It is useful to consider flow through the impactor as consisting of four separate streams – two inlet streams and two outlet streams. Conservation of mass requires that the sum of the inlet flowrates be equal to the sum of the outlet flowrates. In the test setup used by Luna, shown in Figure 15a, each of the two inlet flowrates was actively and separately maintained constant, while the outlet flowrates simply merged into a single flow. This type of setup was excellent for investigating the basic stability of opposing jets, but is not applicable to the source sampling problem. In the present investigation, it was recognized that the aerosol laden stream must be altered as little as possible prior to impaction and analysis.

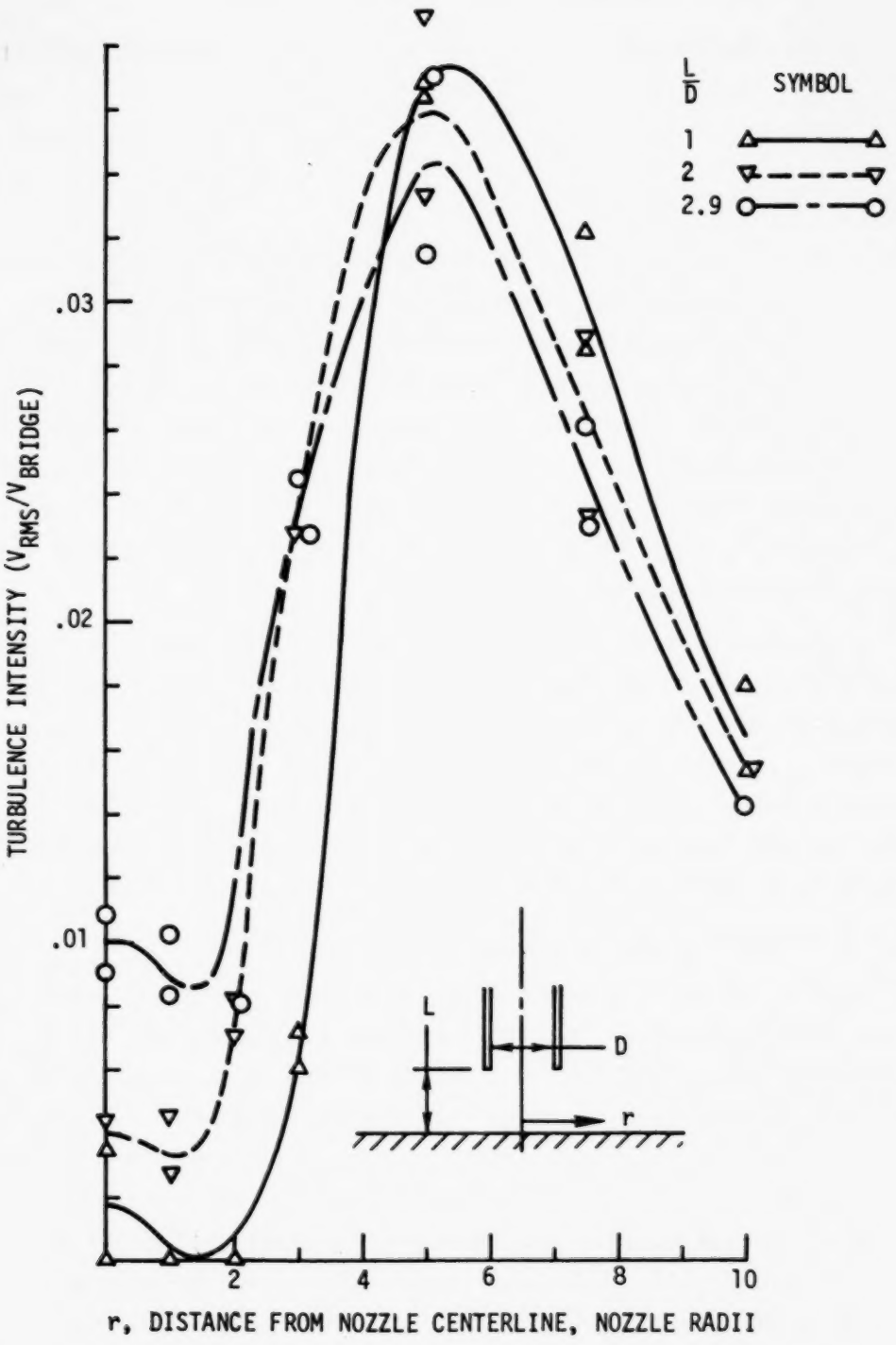

Figure 13. Turbulence profiles for conical nozzle

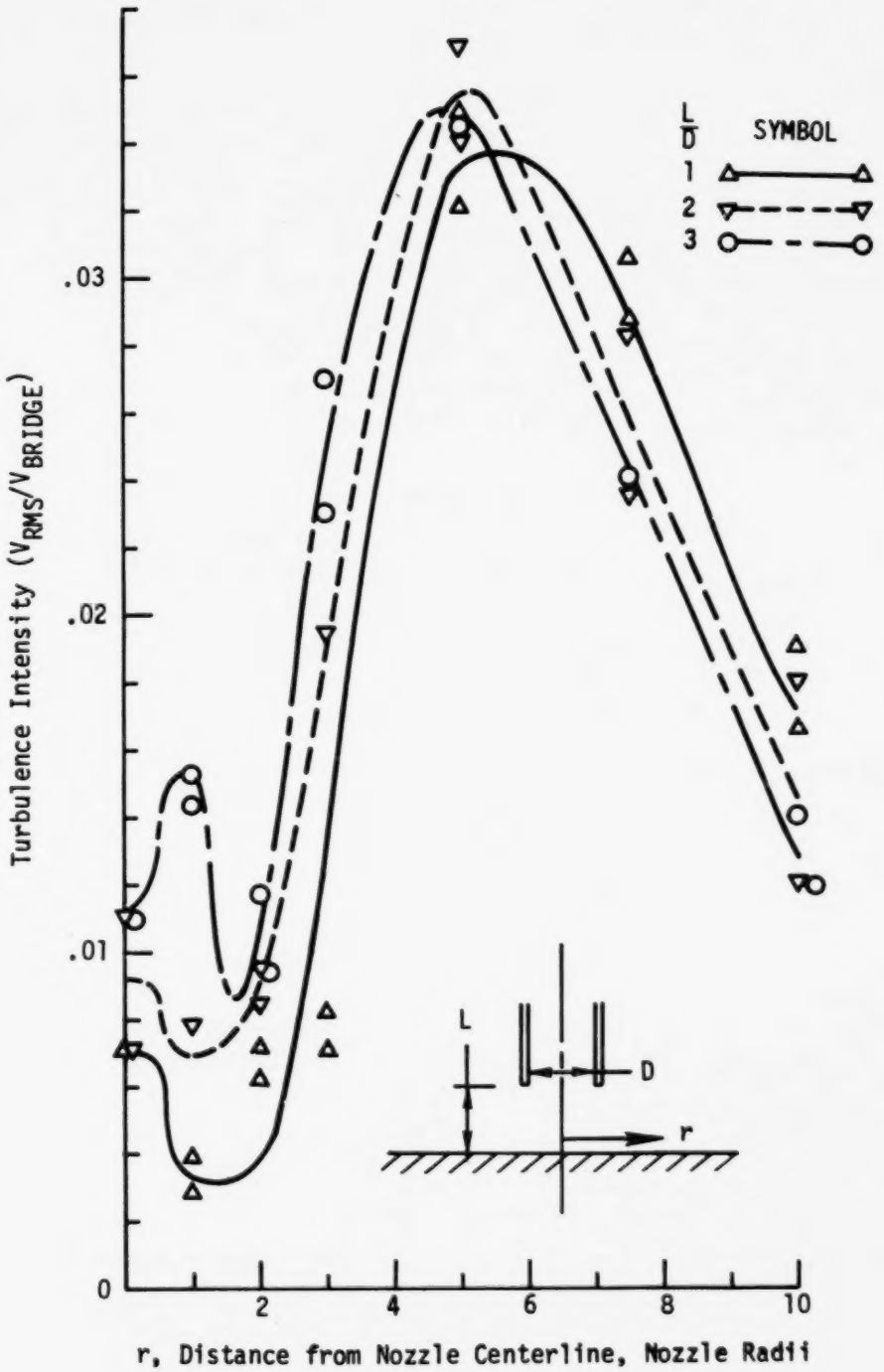

Figure 14. Turbulence profiles for contoured nozzle

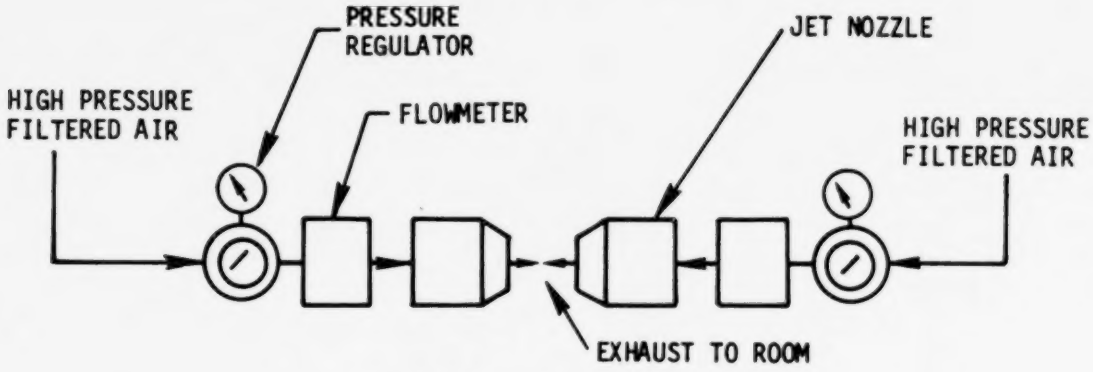

a. Luna's test configuration
(from Reference 1)

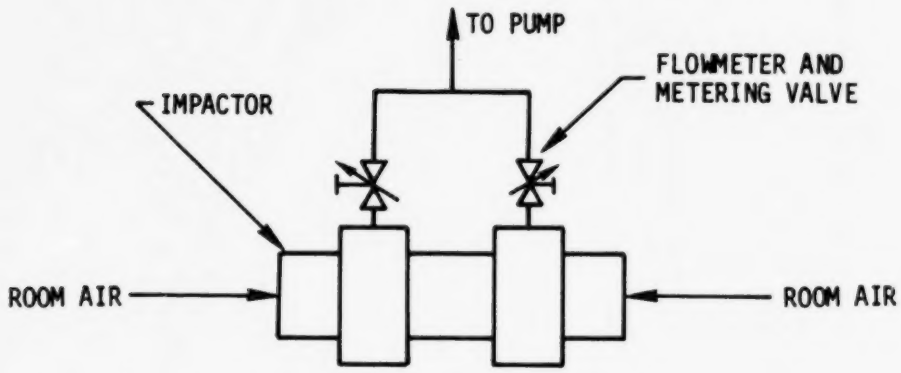

b. Stability - original

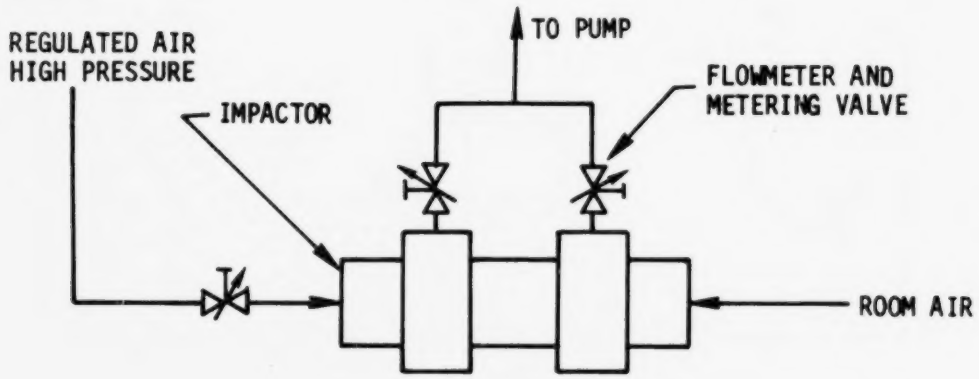

c. Stability - modified

Figure 15. Flow control schematics

In addition, the two output streams had to be kept separate for purposes of analysis. We therefore selected the configuration shown in Figure 15b for the laboratory setup. Flow control was performed only on the outlet streams each of which was maintained at a flowrate of 470 cm^3/s. No controls were initially established on the inlet streams other than to insure that the inlet geometries were identical. The wisdom of hindsight reveals that identical geometry was not sufficient to promote identical flows through the two inlets. It was observed during the early stability testing that while the sum of the inlet flowrates remained constant, the individual flowrates varied over as much as ±60% range in a random manner. This was a very gross instability, worse than the interface instability which was the original concern and which Luna investigated in detail.

The solution to the problem was to actively meter the "clean side" inlet flow in addition to the two outlet flows. This provided the necessary stabilizing constraint — metering of the outlet flows fixed the total flowrate, and metering of one of the inlet flows therefore passively regulated the other inlet flow. The final configuration is shown in Figure 15c. As is shown in Section VII, this approach is compatible with source sampling requirements.

Visual observation of pressures and flows for this configuration in Figure 15c confirmed flow stability. Pressure traces were obtained and are presented in Appendix A. The traces show pressure (and consequently flow) stability to the performance limits of the regulator used on the clean side inlet.

6.3.2 Particle Separation Testing

Results for this phase of the test work are presented as efficiency curves — separation efficiency as a function of particle size. Calibrations for six separate physical configuration/flow combinations were obtained. The variety of conditions has helped to provide an understanding of how this instrument functions, and to identify the critical design and operational parameters. Operating conditions are summarized in Table 2, and the efficiency curves are shown in Figures 16 through 22. Figure 16 is a summary plot of the data trends for each configuration, while the

Table 2. OPERATING CONDITIONS FOR PARTICLE SEPARATION TESTS

CONFIGURATION	FIGURE	FLOWRATES, CM^3/S				SPLITTER PLATE ORIFICE DIAMETER, CM	NOZZLE SHAPE
		CLEAN SIDE		AEROSOL SIDE			
		IN	OUT	IN	OUT		
A	17	470	470	470	470	3	Conical
B	18	470	470	470	470	3	Contoured
C	19	470	470	470	470	2	Contoured
D	20	420	470	520	470	3	Conical
E	21	420	470	520	470	2	Countoured
F	22	520	470	420	470	3	Conical

For all configurations, nozzle/nozzle spacing was 1.5 cm.

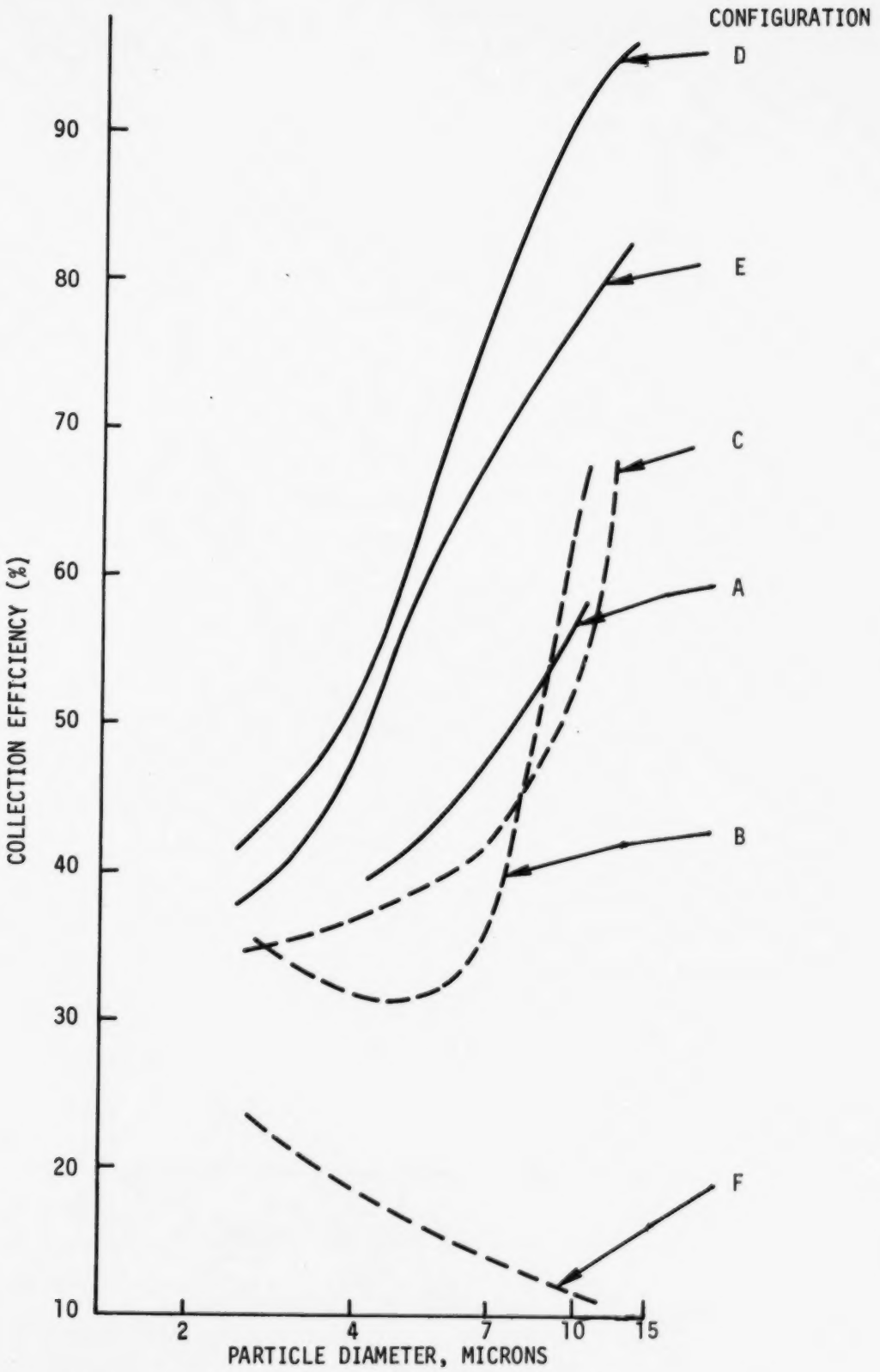

Figure 16. Data trends for particle collection efficiency testing, all configurations

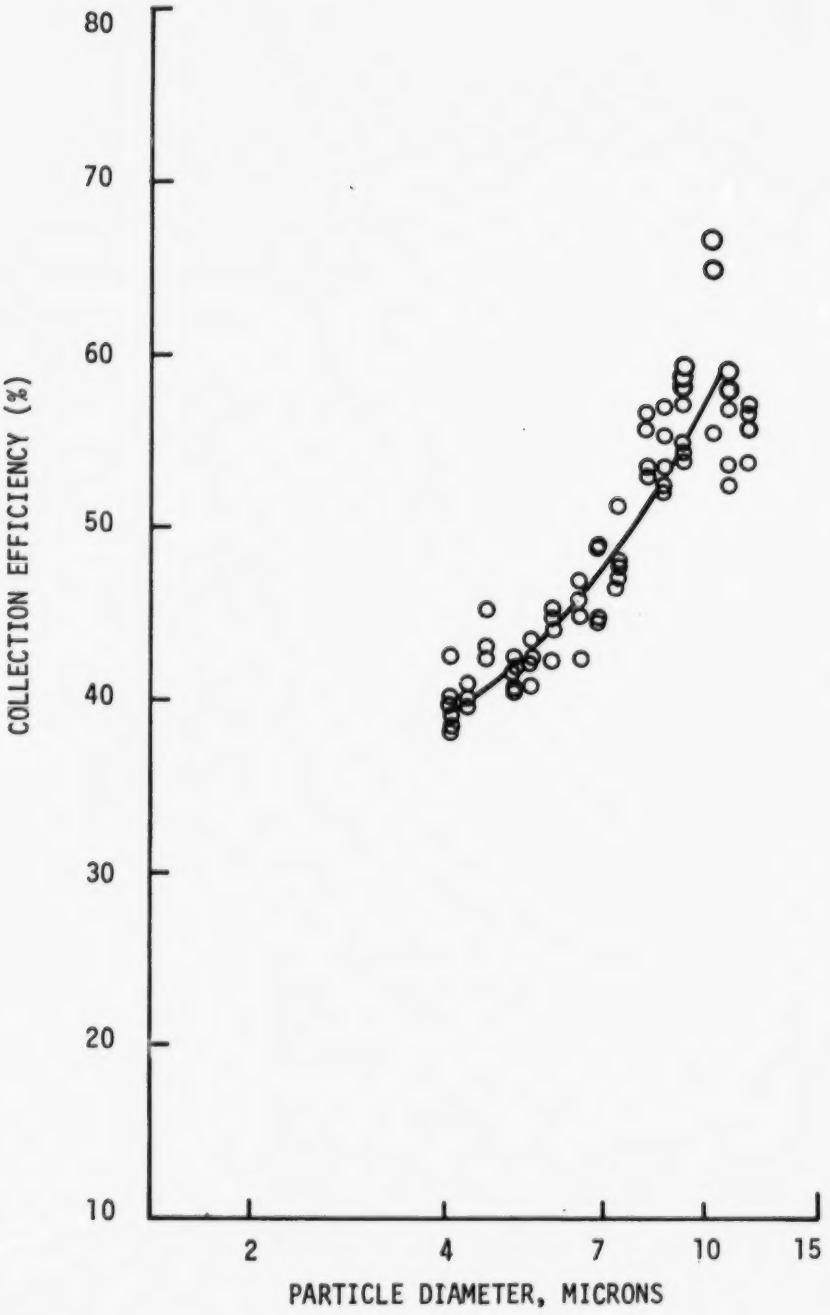

Figure 17. Particle collection efficiency as a function of particle size, Configuration A

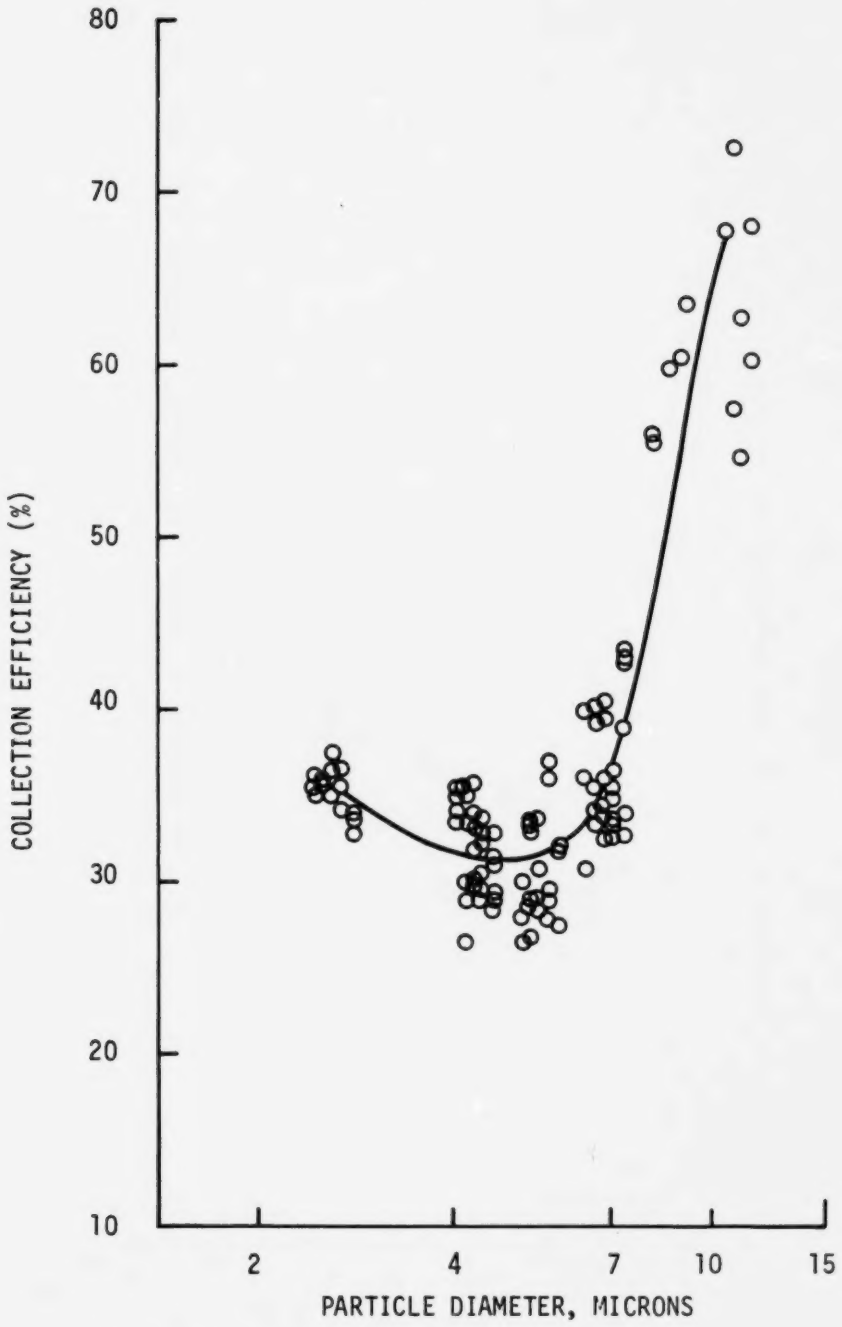

Figure 18. Particle collection efficiency as a function of particle size, Configuration B

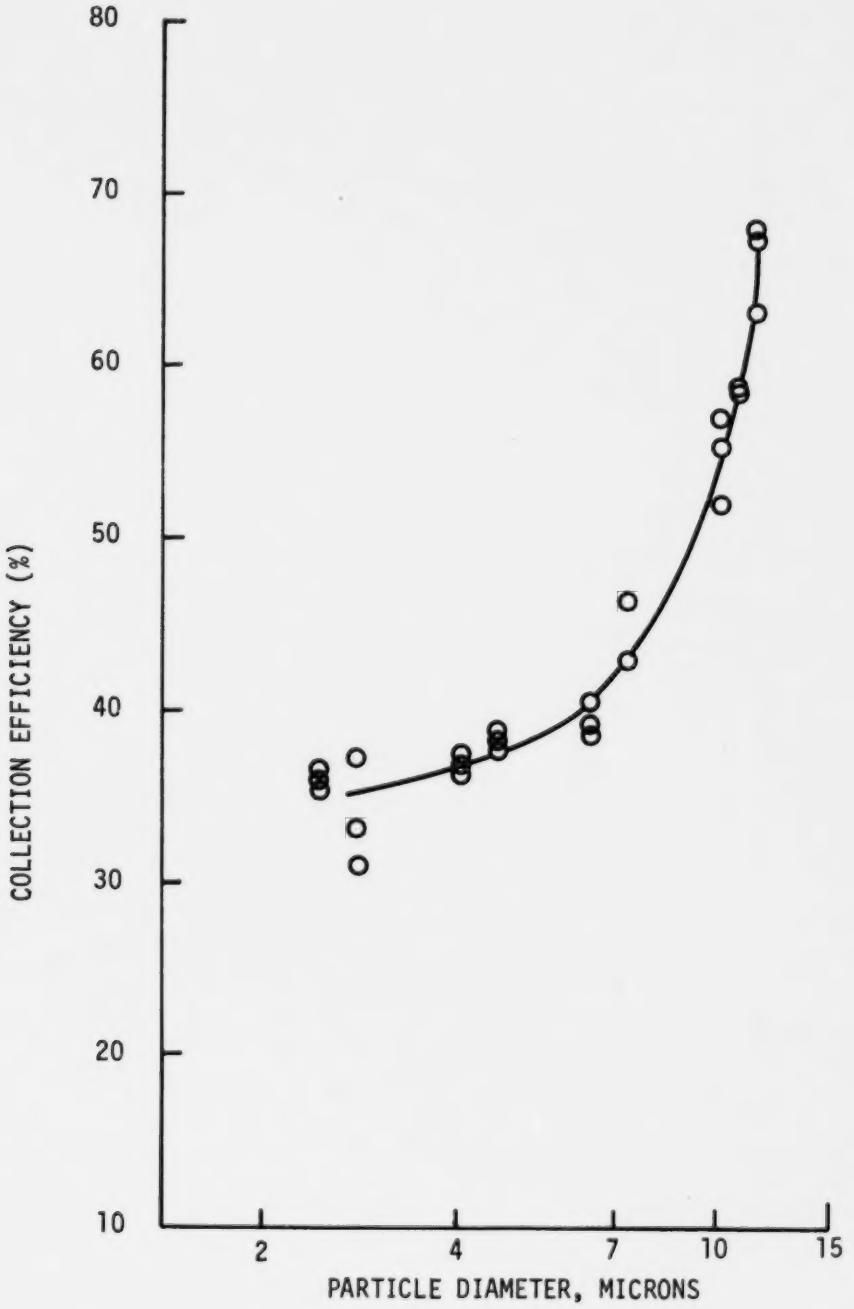

Figure 19. Particle collection efficiency as a function of particle size, Configuration C

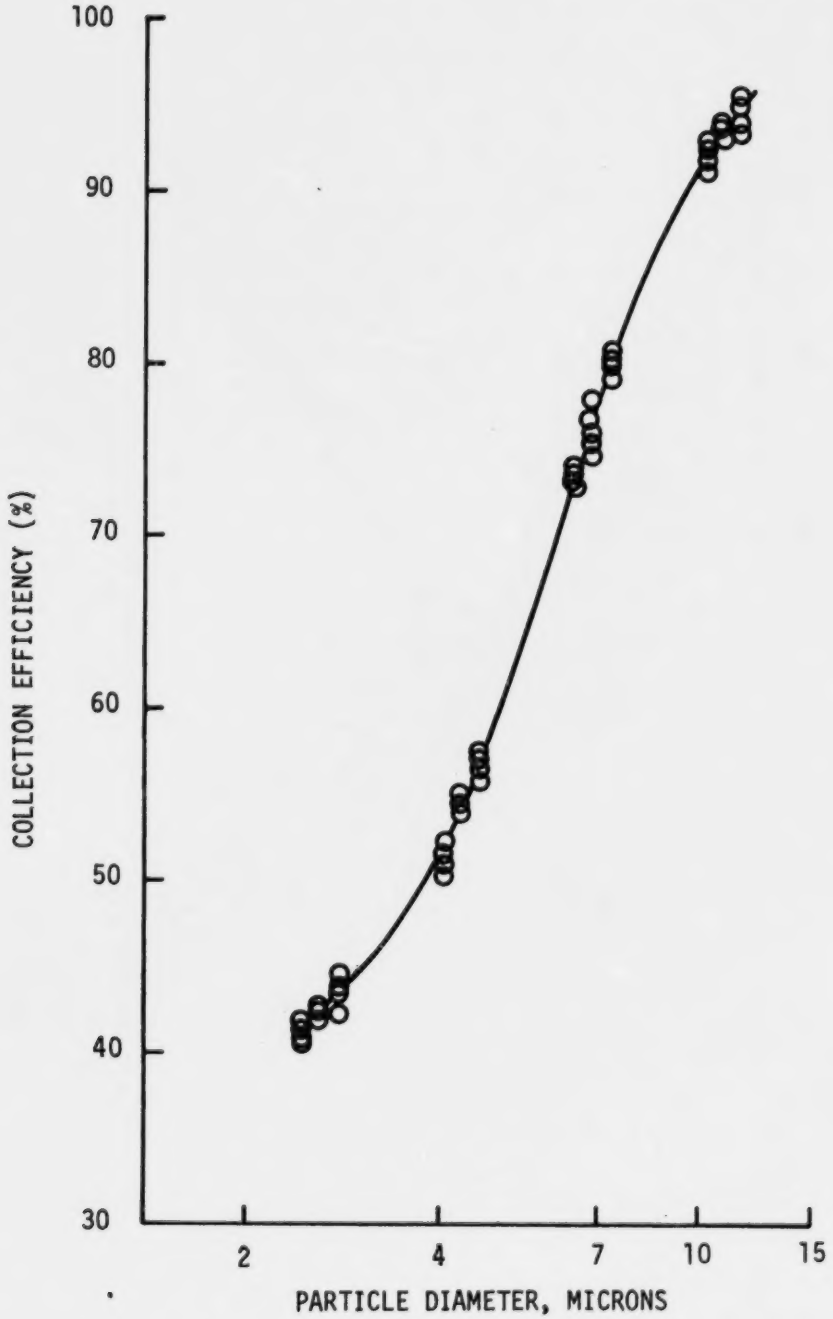

Figure 20. Particle collection efficiency as a function of particle size, Configuration D

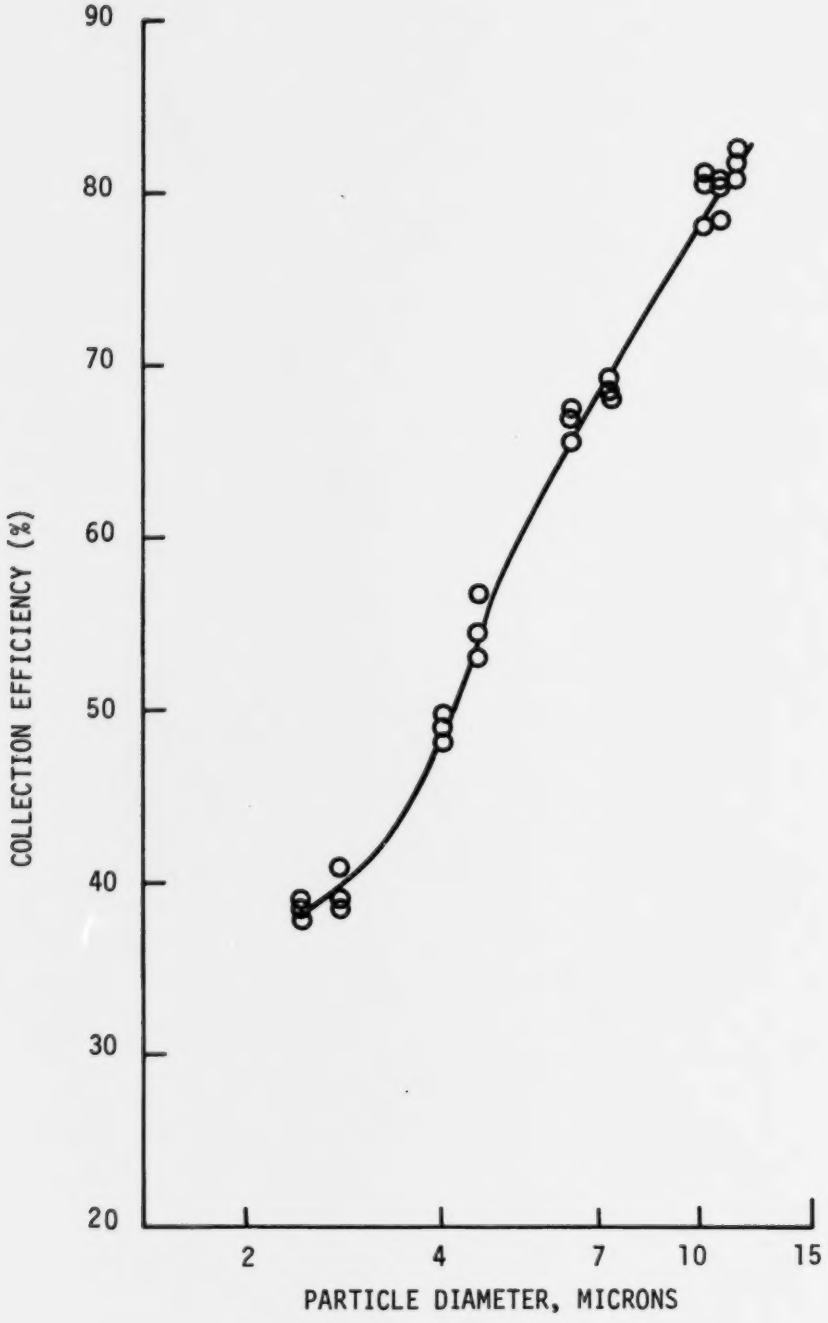

Figure 21. Particle collection efficiency as a function of particle size, Configuration E

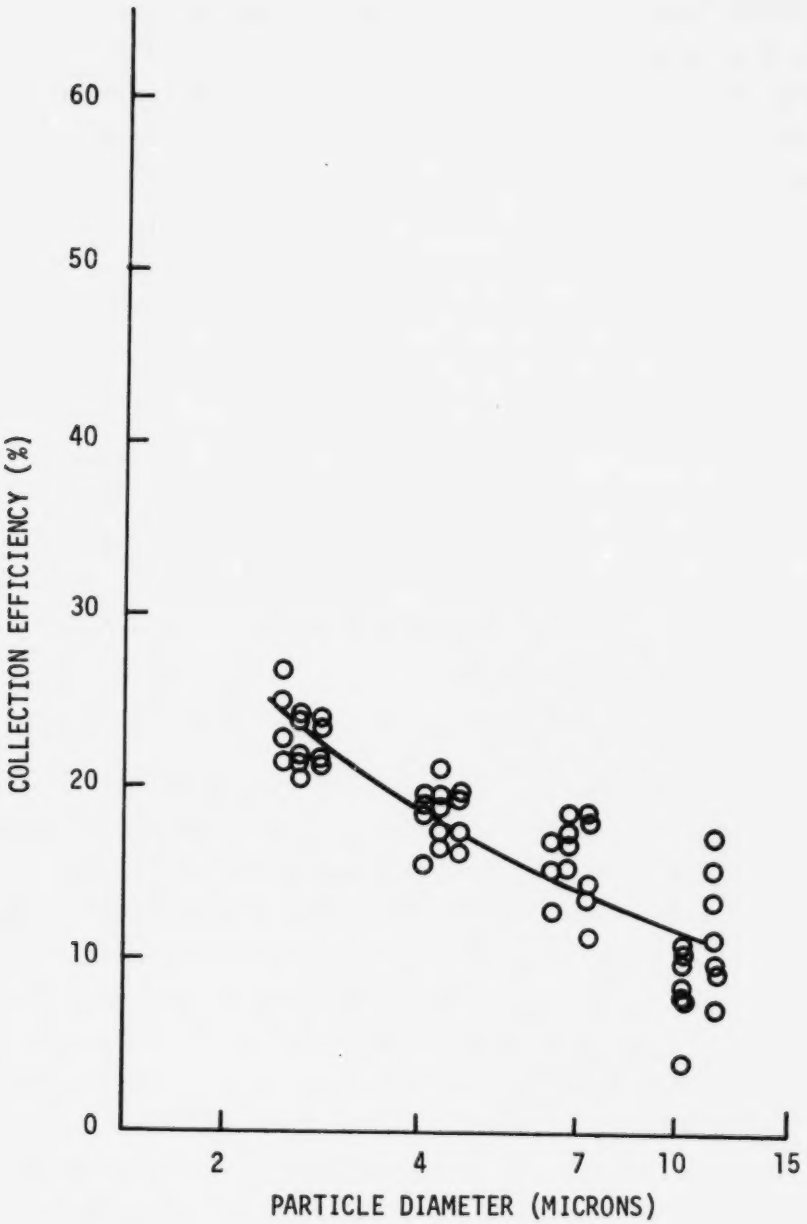

Figure 22. Particle collection efficiency as a function of particle size, Configuration F

remaining figures show the individual data points obtained. Although differing numbers of data points were obtained for the various configurations, in each case a large enough number of points was obtained with sufficiently narrow scatter to establish the data trends. Thus the occurrence of decreasing efficiency with increasing particle size, for example, which occurred for two of the configurations, is considered to be a real phenomenon and not due to measurement errors. As Table 2 shows, the parameters varied were nozzle shape, orifice size, and relative flowrate through the nozzles. The nature of the flowrate variation is shown schematically in Figure 23. For all configurations, exhaust flowrates were maintained equal, while the clean side nozzle flow was regulated to provide equal or unequal flows through the nozzles.

The efficiency curves for four of the configurations are compared with that of the first stage of an Anderson impactor (Reference 4) in Figure 24, and show comparable sharpness of cutoff for the portions of the curves above 40% efficiency. The problems associated with unwanted collection of small particles are discussed below.

6.4 INTERPRETATION OF TEST RESULTS

The possibility of the flowrate instability observed early in the test program was anticipated, but it was originally felt that good control of the inlet geometry would result in stable operation. When this proved not to be the case, appropriate time and effort had to be devoted to finding a solution to the problem. The solution of metering the clean side inlet flow was very successful, but the effort involved in achieving it precluded (from a budget and schedule standpoint) any further investigation of the flow properties in the region of the interface itself. Some information has been inferred about the interface region from the particle separation test data, discussed below. The stability testing showed a definite need to control three of the four flowrates involved, and it is felt that this can be done in a production item without introducing great hardware complexity. We can now proceed with interpretation of the particle separation data.

The first check performed on the data was to compare data with a theoretical calculation of the 50% efficiency point. The 50% efficiency

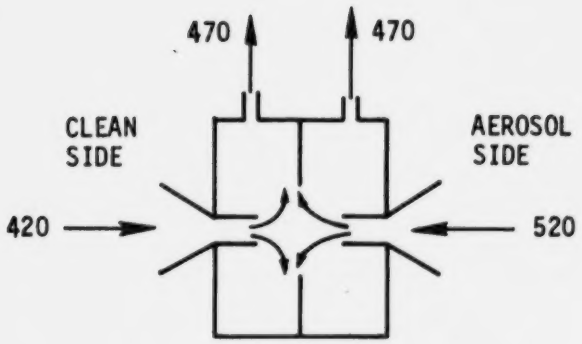

FLOWRATES FOR CONFIGURATIONS D AND E, CM^3/S

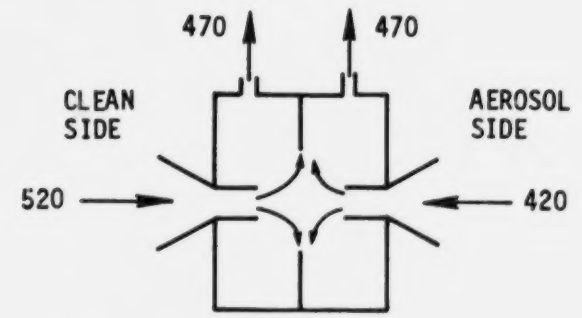

FLOWRATES FOR CONFIGURATION F, CM^3/S

Figure 23. Schematic of flowrate variation technique for biased inlet flow cases, Configurations D, E and F.

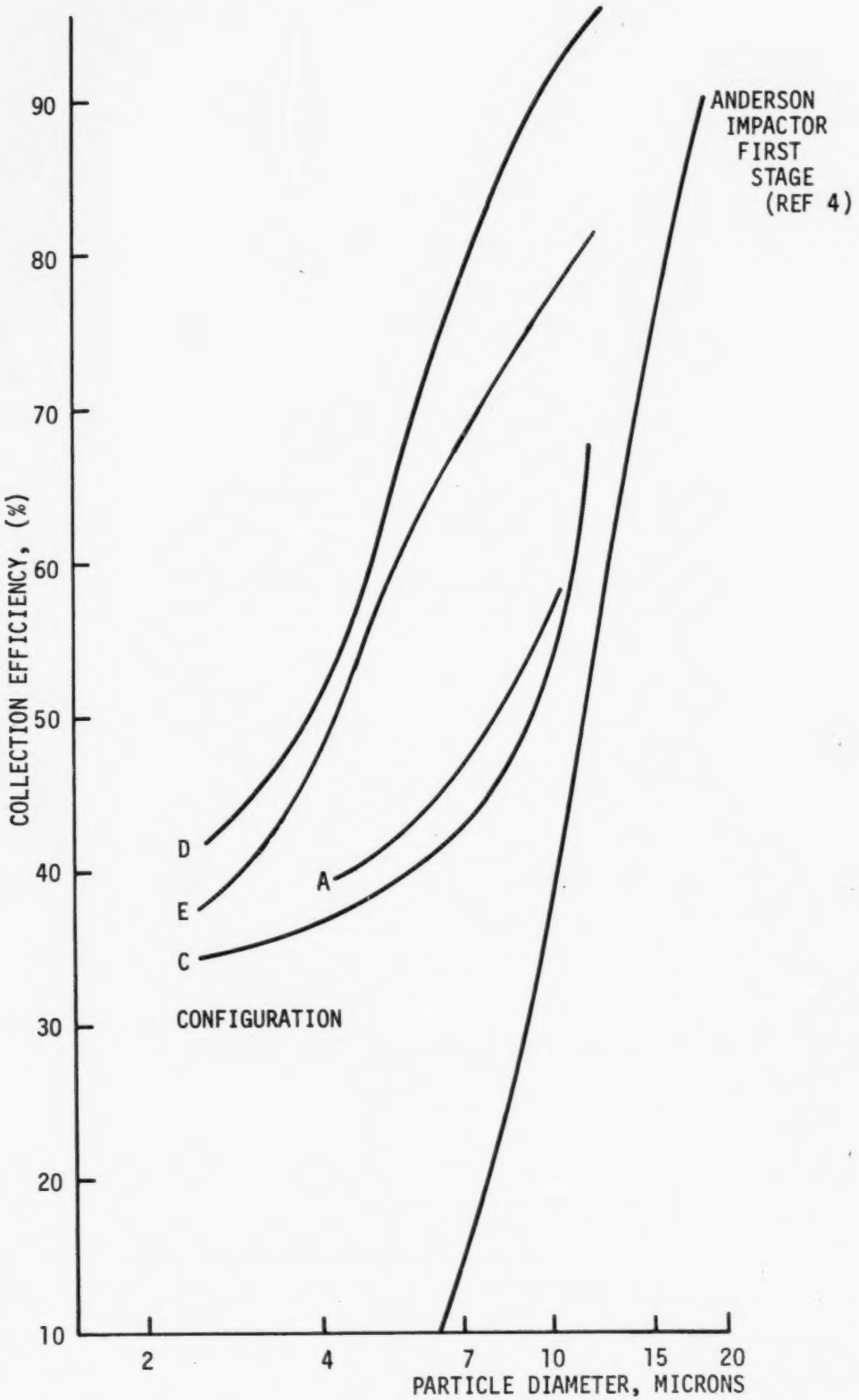

Figure 24. Comparison of continuous impactor data with Anderson first stage

particle diameter was calculated from Figure 12 of Reference 4, which showed that at 50% efficiency, we have

$$\sqrt{STK} = 0.474$$

By definition

$$STK = \frac{\rho_p C V_o D_p^2}{18\mu r_{jet}} = \text{Stokes number}$$

where

ρ_p = particle density, $\sim$ 1.1 g/cm^3 for DOP

C = Cunningham slip correction factor, $\sim$ 1.02 in the region of interest

V_o = mean jet (nozzle) velocity

D_p = particle diameter

μ = gas viscosity, 1.781×10^{-4} g/cm-s

r_{jet} = nozzle radius, 0.5 cm

For our case, we had a flowrate of 1 CFM, or 472 cm^3/s, which gives V_o = 601 cm/s. Thus we have

$$STK = \frac{(1.1)\ (1.02)\ (601)\ D_p^2}{(18)\ (1.781 \times 10^{-4})\ (.5)}$$

$$STK = 4.21 \times 10^5\ D_p^2$$

so that

$$D_{p_{50}} = \frac{0.474}{\sqrt{4.21 \times 10^5}} = 7.31 \times 10^{-4} \text{cm} = 7.31\mu$$

The observed 50% efficiency point for configurations A, B, and C, Figures 17-19, were 7.6, 8.4, and 9.3μ, respectively. Since the conical nozzle used in Configuration A most approximates the configuration used to obtain the background data for the calculated point, agreement between calculation and experiment was considered to be excellent, and confirmed that basic operation of the device was not significantly different from that of a

standard impactor. The unequal inlet flowrates in Configurations D-F were a sufficient deviation from the standard impactor that a comparison with standard cutoff calculations would not be meaningful.

Figure 24 is illustrative of problems during this early development phase of the task. Sharpness of cutoff above 50% efficiency is seen to be comparable to that of one of the most successful impactor designs, which is good. Unfortunately, the sharpness is seen not to continue into the low efficiency part of the curve — a significant percentage of small particles was collected in all cases. Such collection has definite implications as to what is occurring in the vicinity of the interface. Configurations D, E, and F in Table 2 were used for the specific purpose of investigating possible improvements to the top and bottom ends of the efficiency curve through deliberate flow biasing.

The results for configurations D and E (Figures 16 and 17) are easily understood. The higher flow rate through the aerosol nozzle (by convention, "aerosol nozzle" will refer to the nozzle through which the particle generator output flows, while "clean nozzle" will refer to the nozzle through which the initially particle free gas flows) dictated that some of the aerosol laden gas would exhaust on the clean side of the splitter plate. Since this gas would carry its entrained particles along with it, we would expect a leftward shift of the efficiency curve compared to the equal flowrate case. The major difference between configurations D and E was the larger orifice size for D, which, as Figure 5 suggests, resulted in higher efficiencies for a given particle size for configuration D.

The "leveling out" of collection efficiencies at around 30% for configurations A, B, and C and the unusual shape of the efficiency curve for configuration F were initially puzzling. The following scenario, based on the test data, was hypothesized upon conclusion of initial testing. The hypothesis was confirmed by subsequent tests, as described in Section VII.

It became clear that the key to the unusual portions of the efficiency curves is as illustrated in Figure 25. This figure, adapted from Reference 1, shows the calculated free streamline shape for the configuration tested. The nozzle I.D. was one centimeter, and the distance from

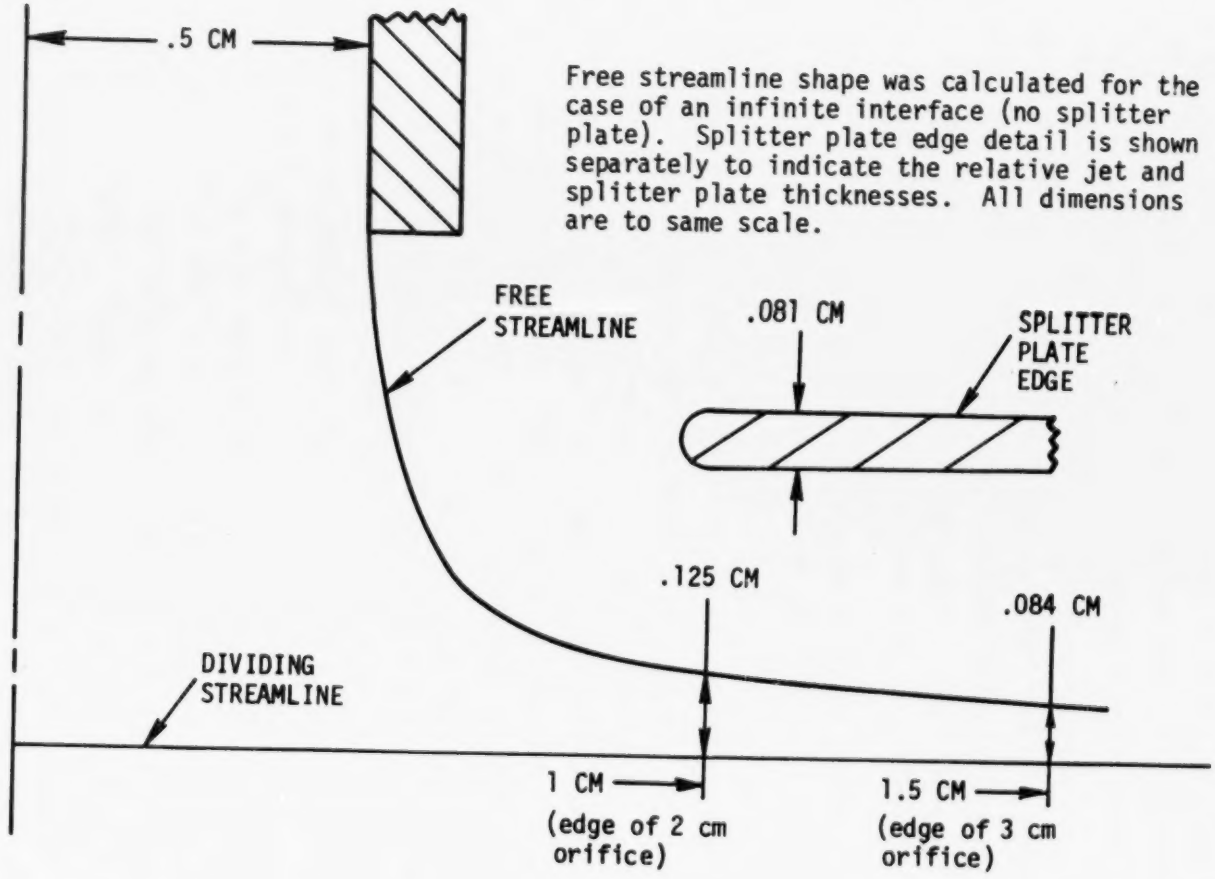
.5 CM
Free streamline shape was calculated for the case of an infinite interface (no splitter plate). Splitter plate edge detail is shown separately to indicate the relative jet and splitter plate thicknesses. All dimensions are to same scale.
FREE STREAMLINE
.081 CM
SPLITTER PLATE EDGE
.125 CM
.084 CM
DIVIDING STREAMLINE
1 CM
(edge of 2 cm orifice)
1.5 CM
(edge of 3 cm orifice)

Figure 25. Calculated free streamline shape (from Reference 1)

the jet exit to the interface was 0.75 cm. Figure 25 shows the predicted thickness of the jet along the interface. As noted in Table 2, two orifice diameters were used – 2 and 3 cm. At the edge of the orifice, the calculated flow heights were 0.125 cm and 0.084 cm, respectively, for the 2 cm and 3 cm orifices. The thickness of the splitter plate edge was 0.081 cm, which means that the local thickness of the flowing region was of the same order as the splitter plate thickness (i.e., quite thin). It is now clear that the unusual data trends were due to passage of this thin layer of gas across the interface. Such passage would be promoted for one or more of four major reasons: instability, unsteadiness, misalignment or sample tube placement, in addition to the minor sources of diffusion and mixing.

In the following discussion, keep in mind that the jet thickness near the edge of the splitter plate is only about one millimeter. A momentary pressure pulse on the aerosol side of the splitter plate could cause the thin jet to cross over to the other side of the plate, carrying entrained particles with it. This gives particles a second mechanism (the first being inertia) by which to cross from the aerosol side to the clean side. Large particles with sufficient inertia resist the turning drag force as the flow turns normal to the original direction, and pass across the interface to be collected on the clean side. The smallest particles will have insufficient inertia to resist the drag force and will go wherever the flow they are entrained in goes. If the flow crosses the interface, the small particles go with it. Now consider particles of an intermediate size. Many of these particles will not have sufficient inertia to cross the interface by their own momentum. They will then turn and flow along the thin layer next to the interface. If the jet now oscillates back and forth across the splitter plate, some of these intermediate particles will have enough inertia to continue in a nearly straight line and stay on the aerosol side, while others, particularly the smaller ones, will stay with the flow and cross over the interface. In this kind of situation, we would expect relatively high collection efficiencies for large particles, a collection efficiency for the smallest particles which would be dependent on the amount of gas transfer across the splitter plate, and a minimum collection efficiency at some in-between size. For a calibration over a wide range of particle sizes, then, we would expect an efficiency curve as depicted in Figure 26, which is a refinement of Figure 6. We would

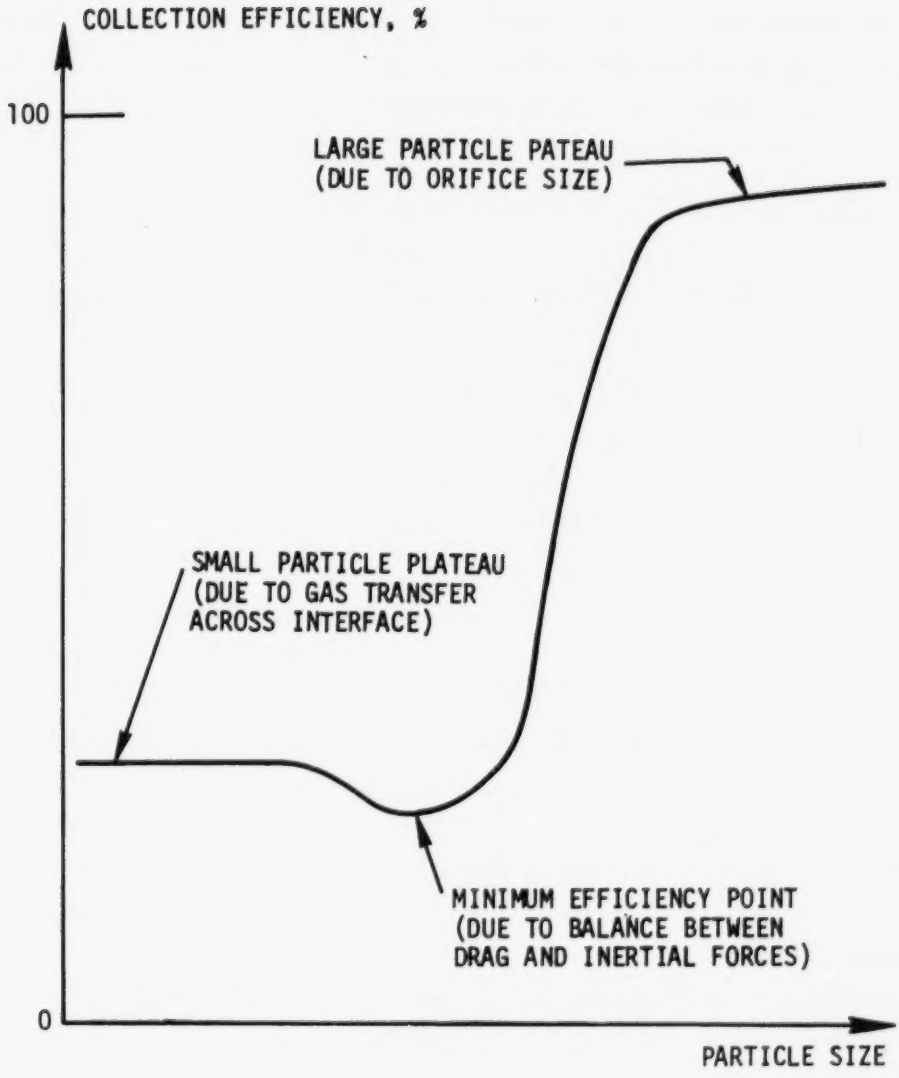

Figure 26. Theorized efficiency curve for continuous flow, impactor, based on accumulated test data

expect plateaus above zero and below 100% efficiency for the smallest and largest particles, respectively, and a minimum efficiency somewhere in between. Sections of this basic curve apply to the obtained efficiency curves for all configurations tested. Configurations A, B, and C would fit around the middle of the proposed curve. The aerosol flow biased configurations, D and E, are shifted to the left of A, B, and C by the bias, while the clean flow biased configuration, F, is shifted to the right of the basic configuration.

The conclusion was eventually reached, then, that the calibration curves for configurations A, B, and C would have the basic shape of the curve in Figure 26 if tested over a wide enough range of particle sizes.

The above is a theory of what happens if there is significant gas transfer across the interface. Now we need to consider what could cause such transfer. A misalignment of the nozzles would be expected to produce a flow pattern as shown in Figure 2a, resulting in the undesired transfer of gas. In our case, great care was taken in both initial design and during setup to avoid alignment problems. After each installation, the nozzle alignment was verified by inserting a close fitting steel pin through both nozzles to insure axial co-linearity. This leaves us with three identified remaining mechanisms: instability, unsteadiness, and the effect of the sampling tube. Although the problem was not pinpointed with certainty until later in the program, we felt that there was a strong argument for considering the sampling tube to be the culprit. A possible case may be made for unsteadiness since the rotameter floats downstream of the splitter plate were seen to vibrate constantly, as such floats are notorious in doing. In a subsonic stream such as occurred during the test, such fluctuations would feed back upstream and affect the flow in the vicinity of the interface. The feeling at that time was that unsteadiness observed during testing was not of sufficient magnitude to cause the gas transfer inferred from the separation data.

Oscillation of the interface was considered at the beginning of the task to be the most likely instability to occur, which is why nine different splitter plates were designed (Figure 10). We had hoped to

investigate the effect of various splitter plate edge configurations on stability. Unfortunately, other problems took precedence and we were not able to perform this investigation.

The shape of the jet and the location of and flowrate through the sampling tube now combine, unfortunately in retrospect, to give the correct explanation of the initially obtained particle separation data. Pertinent facts were:

- The sampling tube was located well away from the thin sheet flowing radially outward along the splitter plate
- The flowrate through the sampling tube was 10% of the jet flowrate
- Separation data were generated by drawing samples from each side of the splitter plate and comparing readings.

The reason for choosing the sampling location used (Figure 12) was to be near as possible to the interface in order to avoid sampling after significant wall losses may have occurred. The laboratory unit was designed primarily to promote, and to provide a capability to investigate, stability. Particle sampling considerations by necessity were then reduced in importance. Test data now strongly show that the sampling tubes should have been located further out radially and closer to the splitter plate.

Current feelings on the effect of the sampling tube are shown in Figure 27. Figure 25 shows the limiting streamline for operations without sample withdrawal to the particle counter. Figures 27a and 27b show the effect was to produce a pressure gradient normal to the splitter plate, which produced a local detachment of the jet on the side being sampled. This locally caused gas from the other side to be drawn across the interface and into the probe. Particle trajectories shown in Figure 27 indicate only the general curve shape shown in Figure 26 was obtained:

- Large particle – when sampling was done on the aerosol side, large particles which had crossed the interface would likely have enough inertia to avoid being turned around and drawn back over, so sampling on the aerosol side would not produce an error. However, the clean side gas would be diluted with

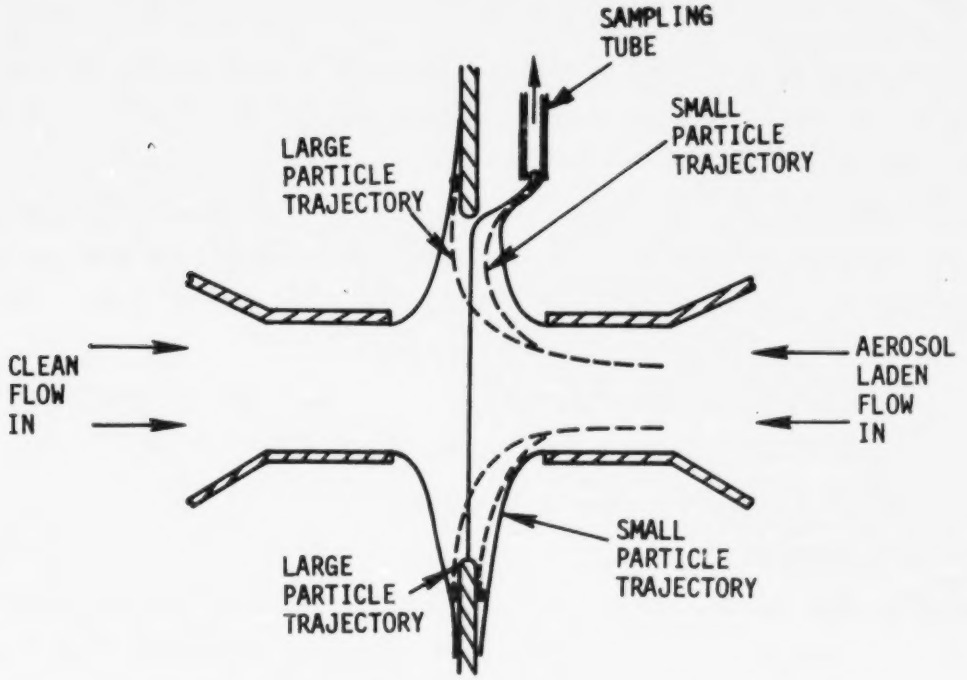

Figure 27a. Effect of sampling tube when sampling aerosol side.

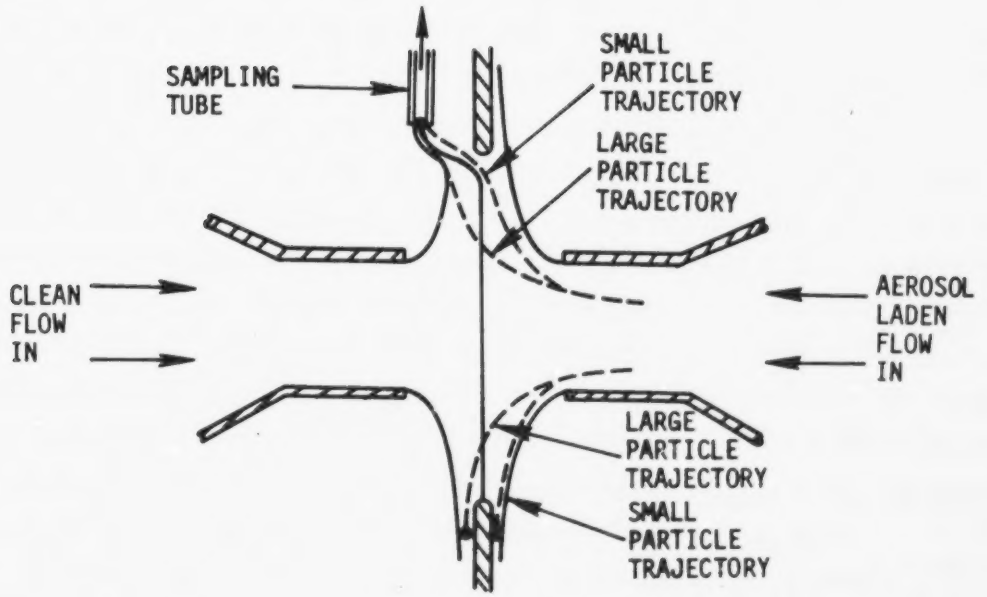

Figure 27b. Effect of sampling tube when sampling clean side.

gas from the aerosol side which is now relatively free of large particles, and the dilution would show up as a low efficiency for large particles

- Medium size particles – near the 50% cutoff point, the number density would be roughly the same on either side of the splitter plate, so the sampling error would be small. Passage of gas across the interface would, however, artificially lessen the sharpness of the separation curve.
- Small particles – small particles will stay entrained in the gas. During sampling on the aerosol side, dilution with the clean gas (relatively free of small particles) would artificially lower the small particle concentration. On the other side, diverting the aerosol gas across the interface would raise the small particle population. The combination of the two would show significant collection of small particles.

Nothing in Luna's work or in our observations of steadiness of the flows (see traces in Appendix A) suggested the presence of instabilities or unsteadiness capable of producing the high collection efficiencies for small particles which were observed, especially for configurations B and C. The sampling tube theory illustrated in Figure 27 seems highly plausible, both qualitatively and quantitatively. Present feeling is that proper sample withdrawal technique would result in much more normal efficiency curves.

The original task was sufficiently low on funds that additional laboratory testing to eliminate the anomaly was not possible immediately. Initial testing was completed in early 1977, and a final report draft was issued in April of 1977. Fortunately, a funding increase was obtained for more testing in 1978. This additional test work centered around the sample extraction problem, and was completed in October, 1978. The testing confirmed that the above postulated scenario was indeed correct, and greatly improved results were obtained, as described in the next section.

SECTION 7
SUBTASK 4 - ADDITIONAL PARTICLE SEPARATION TESTING

The specific objective of this subtask was to improve the shape of the collection efficiency curve. This was done successfully by changing the manner in which gas was withdrawn from the impactor, which minimized transfer of gas across the interface. The testing also made it clear that we have gone as far as we can with the development model impactor, and that further work can best be performed with improved hardware. The additional testing added substantially to our knowledge about this type of particle separation technique, and has made us confident that good field worthy systems can be produced at reasonable cost.

7.1 HARDWARE MODIFICATIONS

An inadequate means of withdrawing samples for the particle counter was cited as the primary reason for the relatively poor particle efficiency curves obtained during initial testing. The purpose of the hardware modifications performed during this subtask was both to improve performance and to withdraw gas in a manner compatible with preliminary designs for second generation hardware. Since the previously used technique involved creation of a non-symmetric flow field in the vicinity of the splitter plate orifice, the most important single consideration was to obtain a symmetric flow field.

The original withdrawal technique is shown in Figures 11c and 12. The revised system tested during this subtask is shown schematically in Figure 28. Seven of the eight manifold holes (Figure 7) on each side of the splitter plate were taped up to minimize gas recirculation. The remaining hole on each side was used as an entry hole for the new half inch diameter exhaust tubes, which were positioned opposite each other and pointing toward the splitter plate as shown in Figure 28. The tube to plate spacing was selected to provide a steadily increasing gas velocity from the plenum to the exhaust tube. These tubes were then connected to flexible plastic tubing by means of quick - connects, as shown in Figures 29 and 30, which then led to the particle counter and to the flowmeters used to

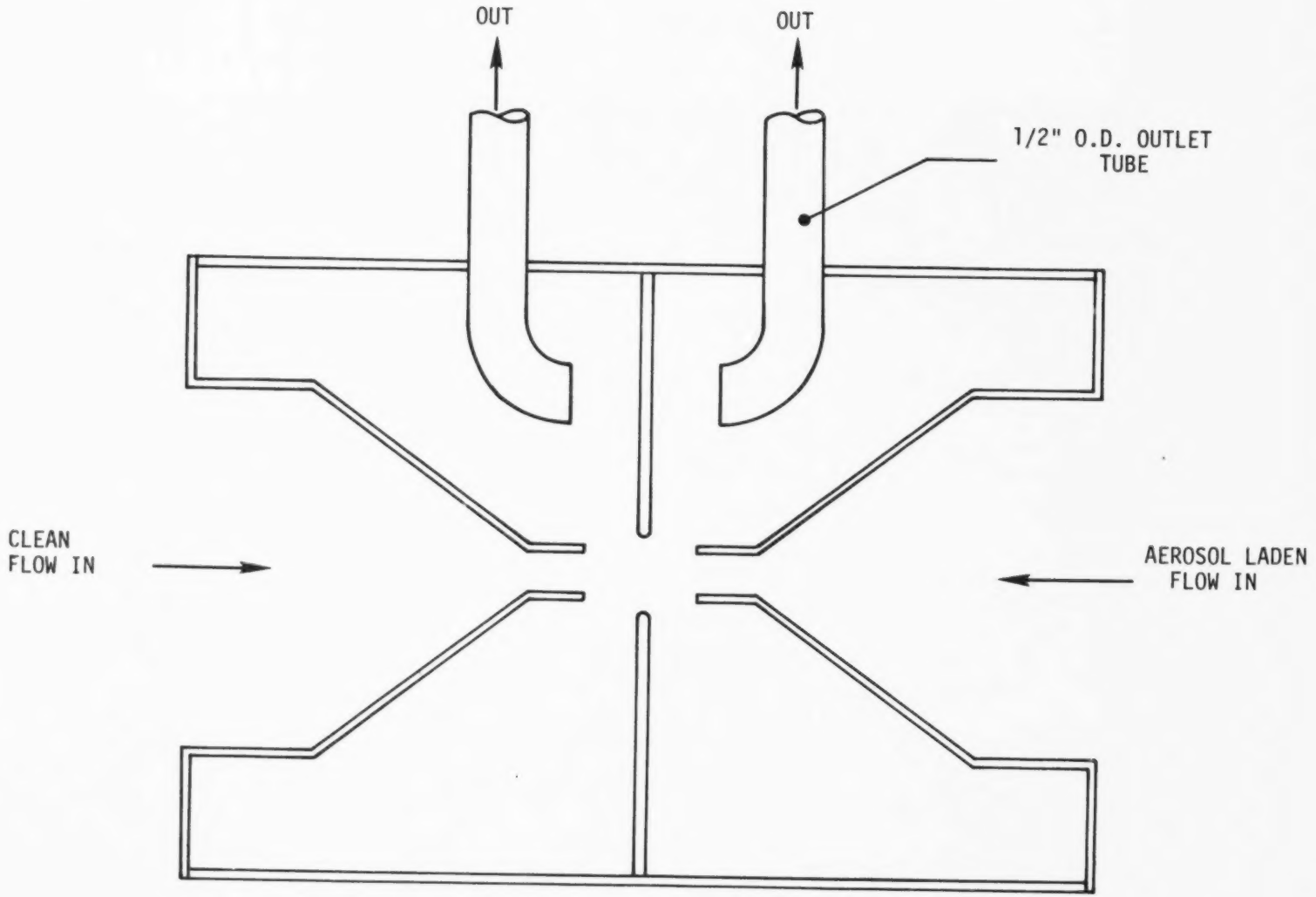

Figure 28. Schematic of revised exhaust flow setup

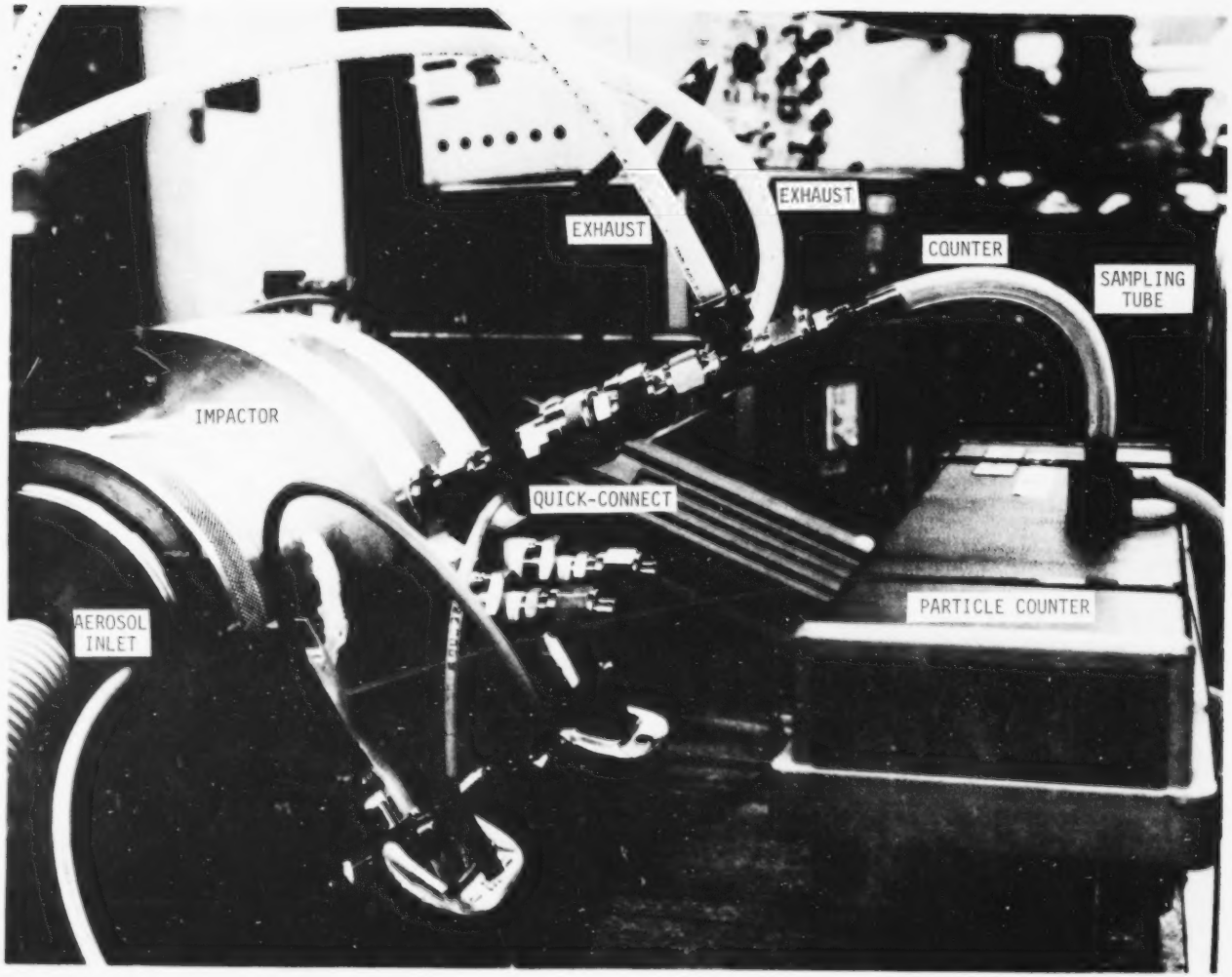

Figure 29. Impactor outlet detail - Configuration G

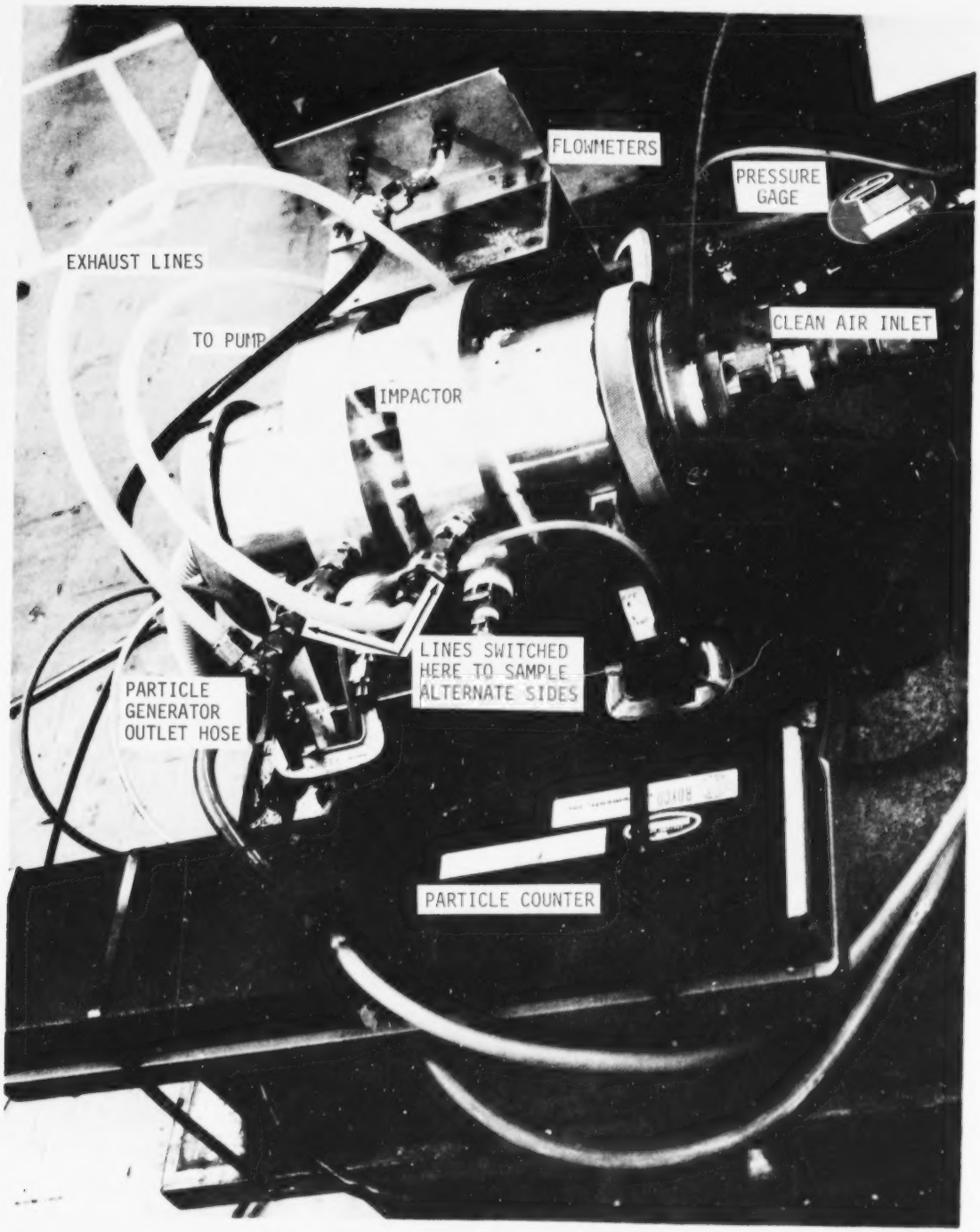

Figure 30. Impactor test setup - Configuration G

adjust the outlet flow. Recall that the relatively low sample flow rate for the Royco 225 counter (10% of the nominal flow through each nozzle) necessitated the splitting of the exhaust flow on the side being sampled.

The configuration shown in Figures 28-30 represents several improvements over the initial configuration. The most important one, of course, is that in the revised configuration, a symmetric exhaust gas pattern was achieved within the impactor, so that the flow pattern in the vicinity of the splitter plate orifice would no longer be disturbed. The flow to the particle counter was split off from the main flow by means of the isokinetic sampling nozzle shown in Figure 31. In the previous work, the exhaust flows had to be adjusted every time the sample location was changed form one side of the plate to the other. In the revised configuration, use of the quick-connects made this unnecessary. This resulted in less data scatter than was obtained in the initial work.

The modifications made, while not particularly costly or complex, had a very dramatic effect on impactor performance. The rest of the system remained as it was during the previous test work.

7.2 TEST DESCRIPTION

During the year and a half between completion of subtask 3 and the start of the test work for this subtask, the impactor itself was not idle - it made several trips between the east and west coasts. Somewhere along the way, the contoured nozzles and two of the three splitter plates were lost, stolen, or strayed, leaving us with the conical nozzles and the splitter plate with the 2 cm diameter orifice. We decided to run a full test with this configuration before making any decision to fabricate replacement hardware. As it turned out, additional fabrication was not required.

Since the original test setup had been completely torn down, it was necessary to re-acquire support equipment (valves, flowmeters, pump, particle counter, etc.) and floor space to set up for the additional testing. The only particular problem encountered was in getting the Vibrating Orifice aerosol generator to function properly. The difficulty was traced to scratches below the orifice place, which kept the O-ring

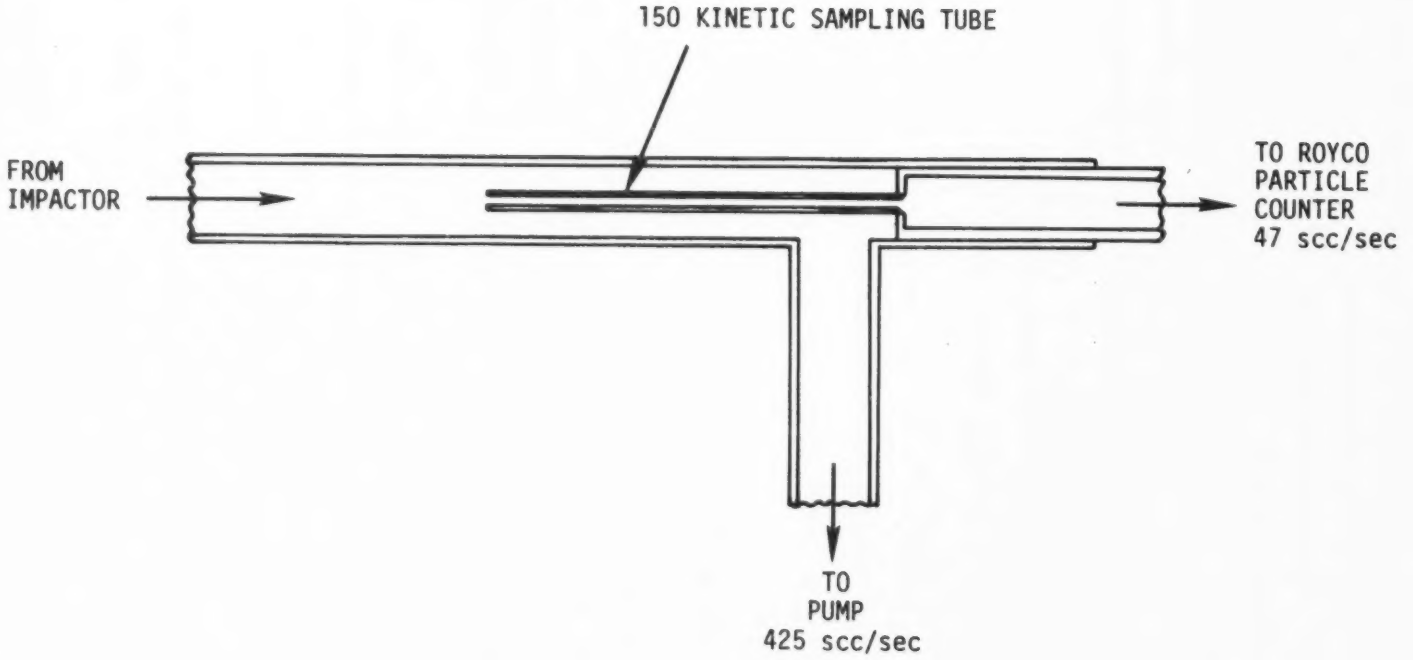

Figure 31. Sketch of particle counter sampling tube in impactor exhaust line

from sealing properly, and other gremlins in the system. Leakage was solved by polishing the sealing surfaces, and the gremlins were banished by benevolent gnomes supplied by the factory. Once the setup was complete, with all equipment working properly, the test work was completed in a short time.

In the context of the previous work, the test configuration may be referred to as configuration G, and had the following conditions:

Configuration : G

Orifice Diameter: 2 cm

Nozzle Shape : Conical

Flowrates : 470 cm^3/s, all flow streams

Nozzle/nozzle spacing: 1.5 cm

A collection efficiency curve was produced with the use of two aerosol sources - the TSI Vibrating Orifice Generator for the range 4-15.5 μ, and room air (combined with the sizing capability of the counter) in the range .5 - 5 μ. As was the case with the previous work, the aerosol generator used DOP (in alcohol) for the aerosol. Basic procedure was as follows (see Section 6.2.2.4 for detailed procedure):

- Start the clean side flow and adjust for proper flow rate
- Start the aerosol generator and particle counter
- After the generator has stabilized (∿ 10 minutes), adjust clean side inlet flow and outlet flows to achieve proper balance
- Take particle count data on each side of the splitter plate
- Change generator operating conditions as required for next particle size
- For room air testing, turn off aerosol generator and disconnect generator outlet hose. Balance the flows and take particle counter readings

7.3 TEST RESULTS

7.3.1 Aerosol Generator Testing

The collection efficiency curve from the testing with the aerosol generator is shown in Figure 32. Data scatter is considerably less than that for the similar configurations A, B, and C (Figures 17-19), and the separation is much improved. We were unable to go higher than 15.5 microns in particle size due to internal losses - not enough particles made it all the way through to the counter to obtain a large enough sample. We were limited at the low end to 4 μ because the smallest orifice for the generator adamantly refused to function properly. The high end limitation was a fundamental problem of the hardware configuration itself - the large plenums on either side of the splitter plate, which were designed specifically to promote jet stability and allow access for diagnostic probes, also provided a large volume which permitted dropout of the large particles. A more appropriate physical configuration will be required to investigate separation efficiency for the largest particles.

7.3.2 Room Air Testing

It was important to extend the separation curve to particle sizes below 4 μ in order to get information about gas transfer across the orifice. After investigating several ways of producing small particles, we decided the simplest, but still acceptable in terms of accuracy, would be to use the polydisperse distribution in ordinary unfiltered room air. The separation efficiency as a function of size could then be determined by means of the diagnostic sizing capability of the Royco particle counter, which, in the window mode, displays the following size ranges:

Channel	Size Range, μ
1	.5 - .7
2	.7 - 1.4
3	1.4 - 3
4	3 - 5
5	> 5

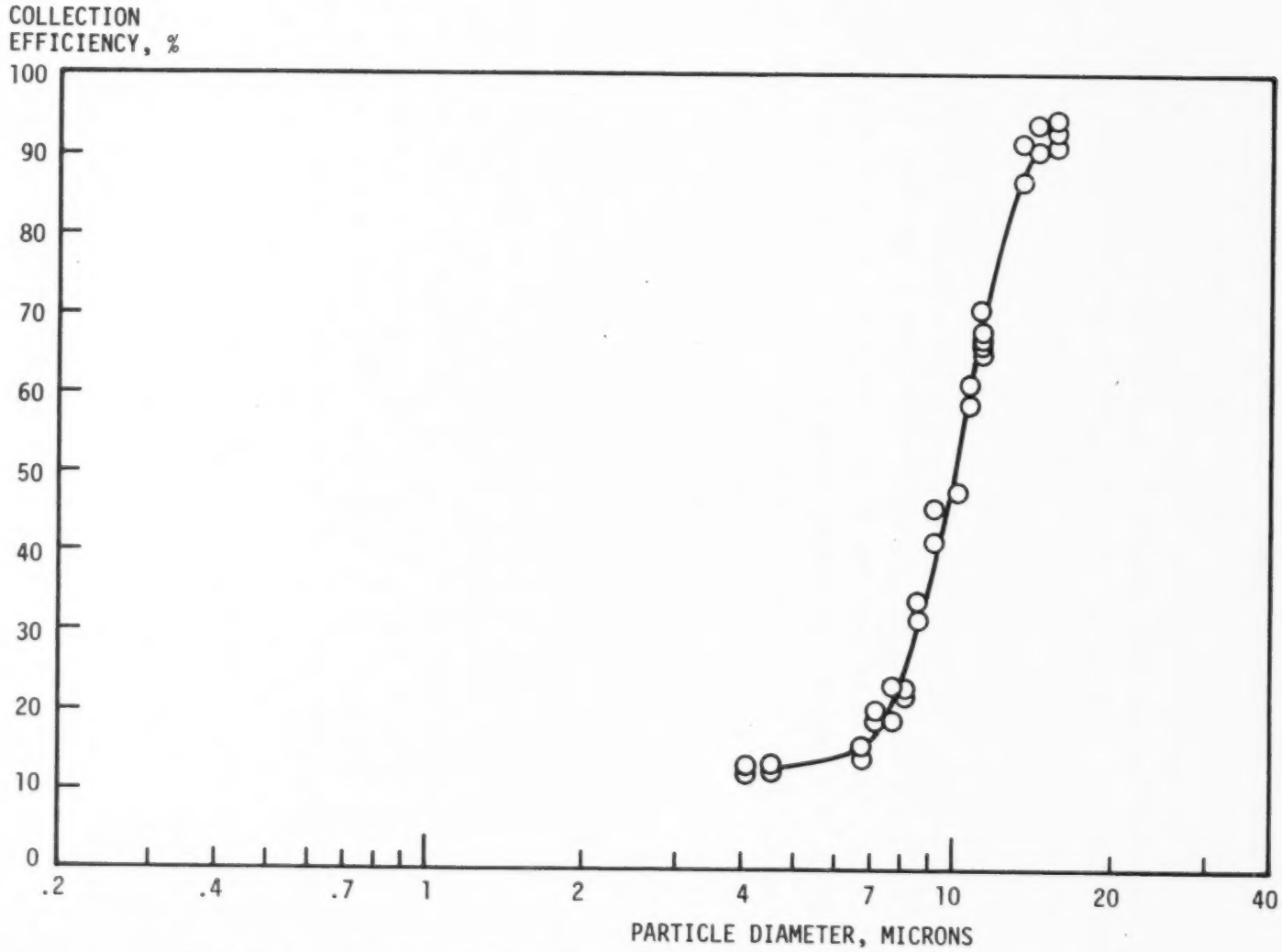

Figure 32. Particle collection efficiency as a function of particle size for size range 4-16 microns, Configuration G

Thus the first four channels allowed us to examine four bands of particle sizes. Results are presented in Figure 33, where the horizontal lines represent the net collection efficiency for particles in the designated size range. The wider spread for channels 3 and, especially, 4, is almost certainly statistical in nature rather than being representative of the actual collection. The "clean side" counts for channel 4 were typically in the range of 10 - 30, compared to 5000 and 1000 for channels 1 and 2, respectively. For each channel shown, a simple average of the individual values may be considered as representative.

7.3.3 Comparison With Other Data

The full set of calibration data for configuration G is shown in Figure 34. Note that there is good agreement in the overlap region for the room air and aerosol generator data. Recall from section 6.4 that the calculated 50% cut point for a standard impactor under our operating conditions is 7.31 μ. The 50% cut point for configuration G, from Figure 34, was 9.9 μ. The difference is due to the relatively small orifice diameter (twice the nozzle diameter), as previously explained. Configuration C, which had the same orifice diameter, had a 50% cut point of 9.3 μ, which is reasonably close to that for configuration G.

A comparison of configurations C, G, and the first stage of the Anderson viable sampler is shown in Figure 35. The dramatic improvement in performance between configurations C and G is quite evident, and, since only the gas exhaust configuration was changed, the performance increase clearly confirms the correctness of the hypothesis about the initially poor performance of the continuous impactor. The configuration G data also shows the presence of another as yet unresolved problem. The configuration G curve is sharper than that for the Anderson impactor down to an efficiency of about 20%, and it levels out at about 10%. This is strongly indicative of a net transfer of about 10% of the "aerosol side" gas stream to the "clean side" of the splitter plate. This problem was previously masked by the large gas transfer in the vicinity of the sampling tube. The gas transfer in configuration G is a direct result of unsteadiness of flow through the rotameters used as metering devices during the test. A continuous oscillation of the rotameter floats was visually observable.

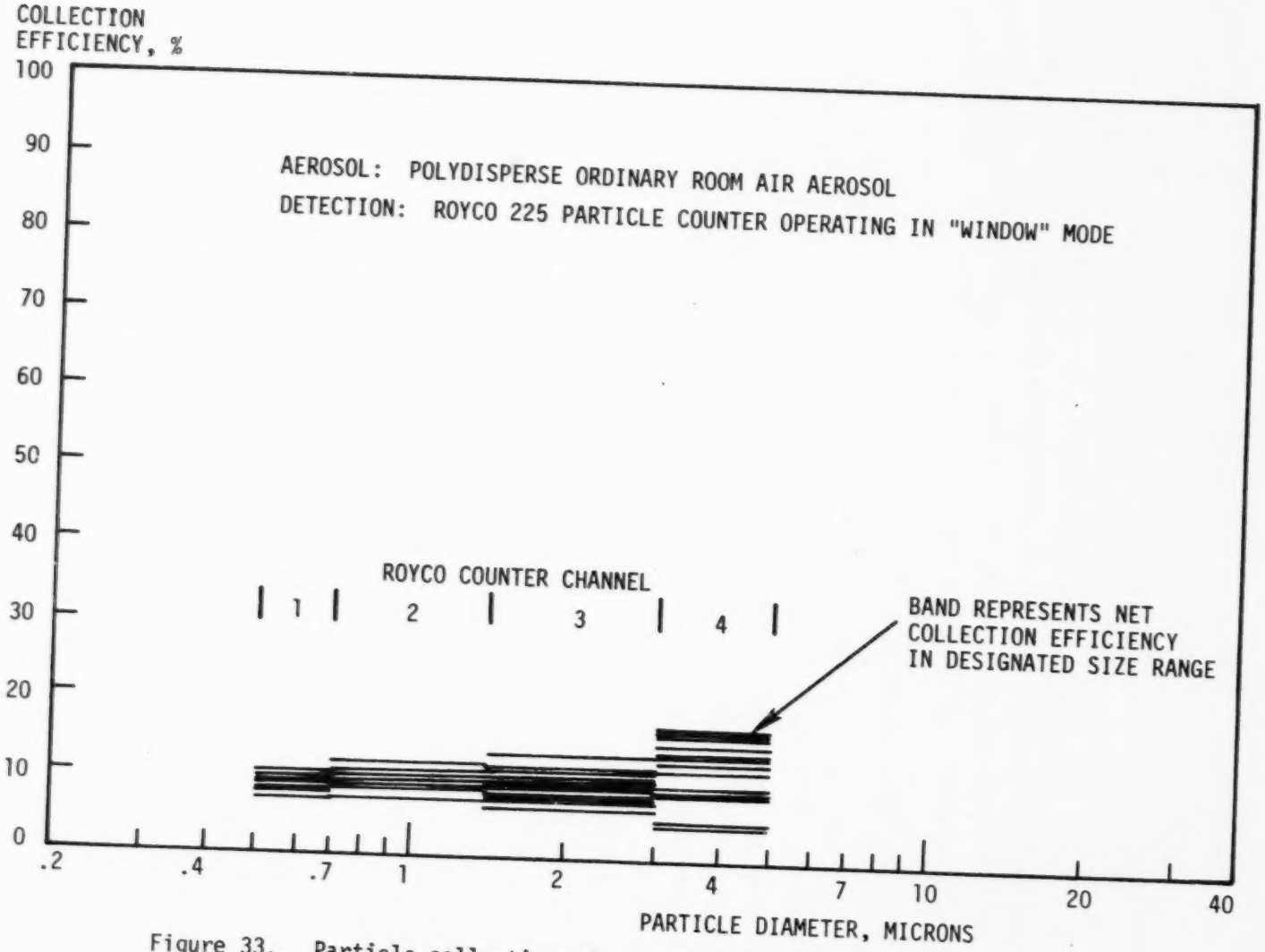

Figure 33. Particle collection efficiency as a function of particle size for size range .5-5 microns, Configuration G

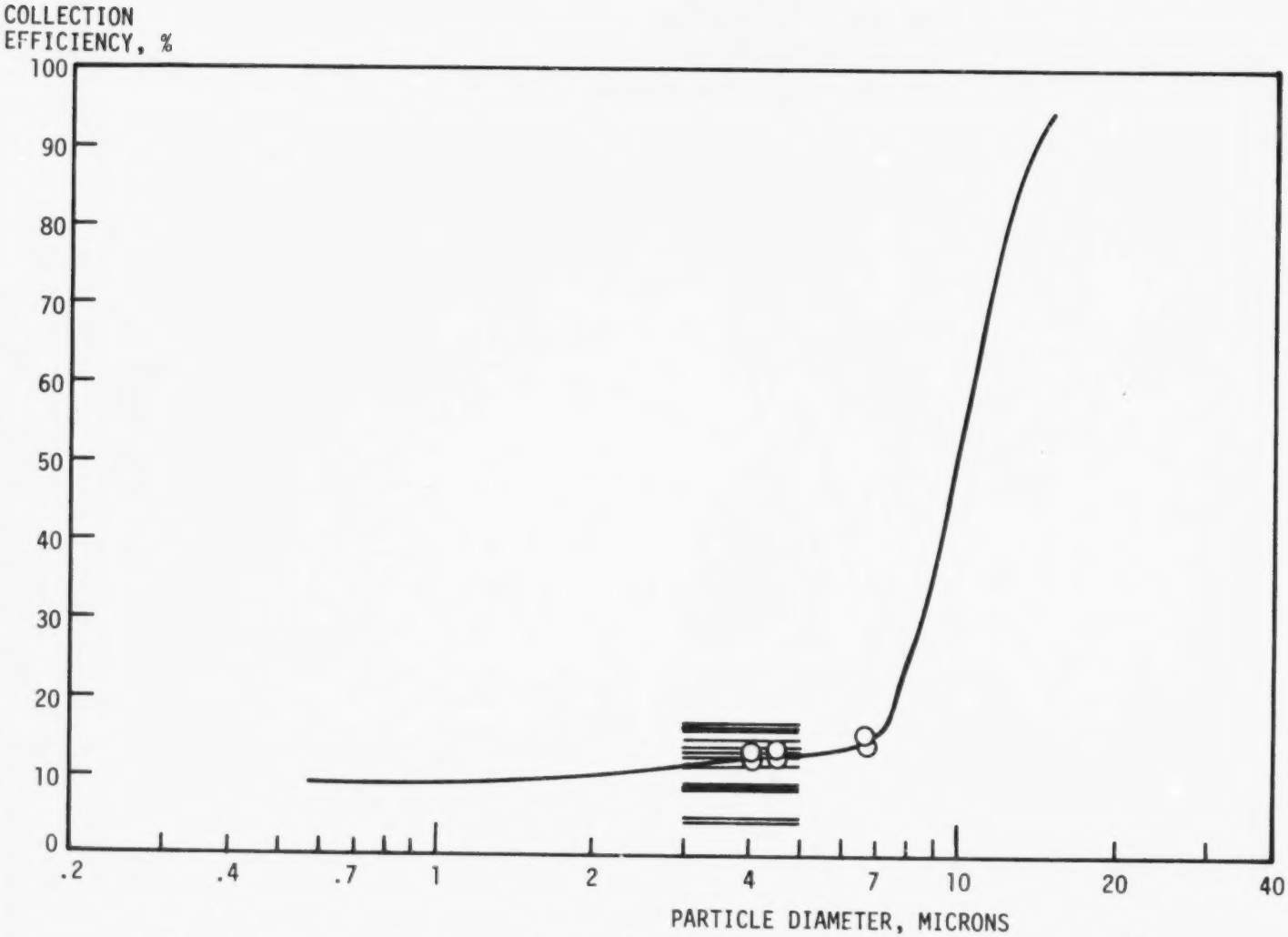

Figure 34. Complete fitted separation efficicncy curve for Configuration G, showing data points in overlap region

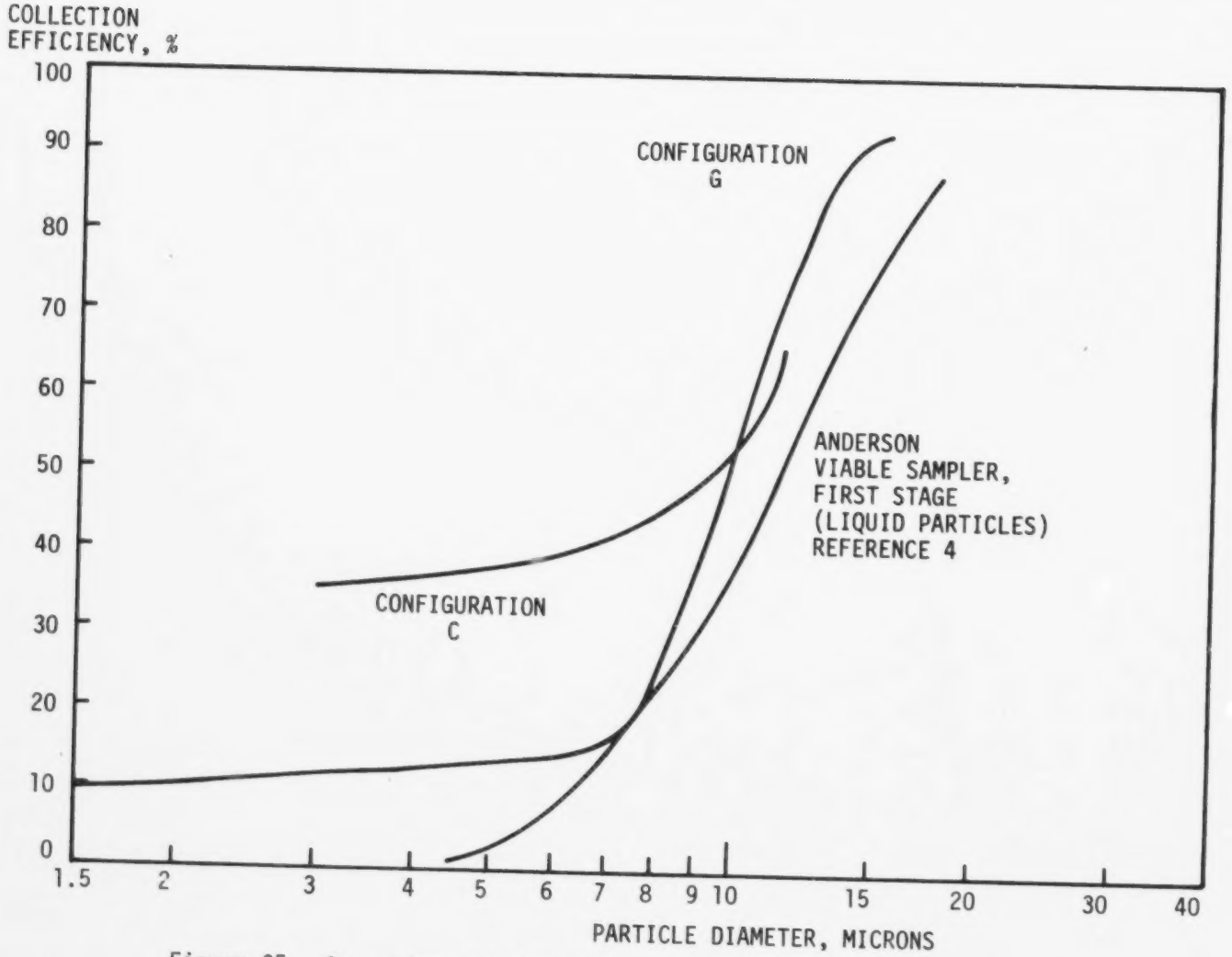

Figure 35. Comparison of separation curves for Configurations C, G, and the Anderson Impactor first stage

The rotameters were selected for use primarily for purposes of convenience. It is now clear that future work will require better flow control elements, and this is reflected in the recommended design in Section VIII.

7.3.4 Summary

The specific purpose of this task was to correct a deficiency in the previous test setup, and hopefully obtain better separation efficiency. The deficiency was felt to be the way in which aerosol samples were removed from the impactor and delivered to the particle counter. Test work during this subtask showed that the diagnosis was correct. When we switched to a fully symmetrical exhaust technique, a very dramatic improvement in performance occurred. The only substantial remaining problem is a higher than desired small particle carryover, and we presently feel that this is due to instabilities in the feed and exhaust systems which have been due primarily to the use of rotameters and their control values as measurement and control devices. Sonic orifices and pressure regulators will be preferred for future work, as described in the following section.

This subtask accomplished several important things. First, it constituted a reasonable and successful conclusion to proof of principle testing. Keep in mind that the laboratory model impactor design was primarily intended for investigation of gas dynamic phenomena and promotion of a stable jet/jet interface - particle separation characteristics were quite secondary. In that context, then, the achieved separation efficiency can be considered to be quite good. Further work should focus on redesign of the impactor for field applications, including minimization of small particle carryover and internal losses, and fabrication and test of a staged version of the device. The laboratory model device tested in this task has served its purpose well, but will not be appropriate for future work.

SECTION 8
SUBTASK 5 - INSTRUMENT UTILIZATION

The laboratory test unit was designed specifically for basic investigatory testing. There was no intention for the unit to have any resemblance to a field usable device, other than the basic operating principle. After the concept was successfully demonstrated, as discussed in the previous section, a brief study was made to investigate possible packaging and monitoring techniques applicable to a field usable unit. There are several distinct configurations of the continuous flow impactor which could be of value in source testing. The discussion below will concentrate on one of them — a staged impactor with five size fractionated output streams, with an optical monitor on each stream. Other configurations are then considered as modifications to this basic one. In each case, preliminary design is for in situ operation.

8.1 STAGED CONTINUOUS FLOW IMPACTOR

8.1.1 Flow Related Components

Fluid mechanically, the proposed staged impactor will operate in the same manner as the laboratory unit — outlet flows and the clean side inlet flows will be actively metered, resulting in passive metering of the aerosol laden flow. The flow schematic of a four stage device having a total of five size fractionated output streams is shown in Figure 36, and includes the pressure hierarchy for the system. The aerosol laden flow (flue gas) enters the "aerosol side" of each stage, where it is met by an equal clean flow. Sonic orifices to meter the inlet and outlet flows are the simplest and surest way to control the flows. A similar system was used with great success to produce highly stable flows in the wind tunnel built by TRW to calibrate the Viking Meteorology Instrument System wind sensors. As long as the pump provides a sufficiently low pressure (below 260 Torr), any variation in pumping characteristics will not be noticed by the impactor. It will be critical to provide a stable, accurate pressure regulator for the clean side inlet flows, since it is the combination of the orifice size, upstream pressure and temperature

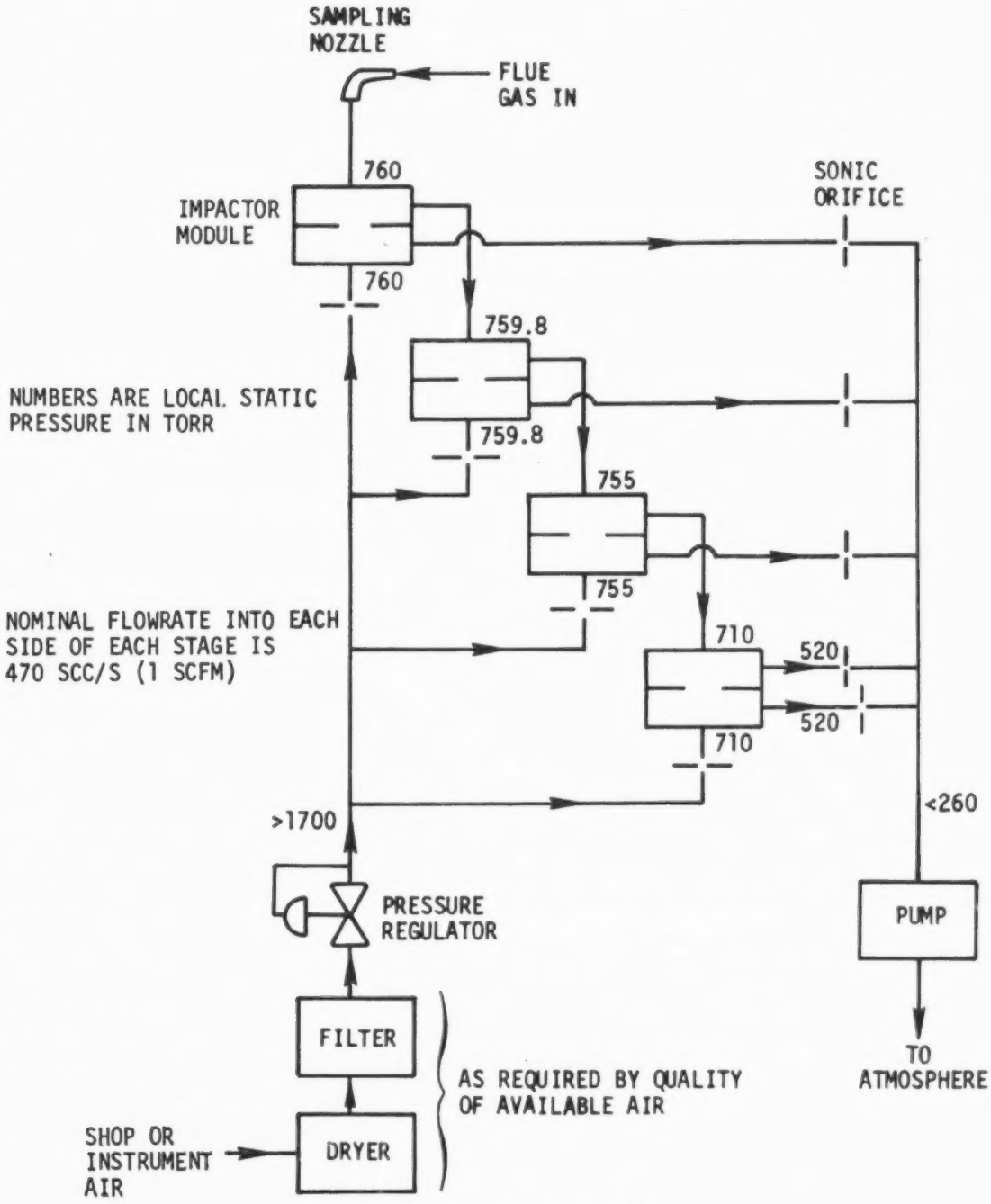

Figure 36. Flow system schematic and pressure hierarchy for staged continuous flow impactor

which provides the correct flowrate of clean air to each state. Monitoring of the output streams will be performed between the clean side outlet and respective sonic orifices, and between the final aerosol side outlet and its orifice. The optical monitoring technique, discussed in the following paragraph, will have no effect on the pressure or flow distribution.

A sketch of the entire installed system is shown in Figure 37. Key features are as follows:

- The heart of the system (impactor modules, metering orifices, optics) is contained in the first 75 cm (29 inches) of the sampling probe. It will be essential that this section be maintained at stream temperature. The obvious way to accomplish this is by maintaining a minimum 75 cm insertion depth. The more complex method for lesser insertions would be use of a servo-controlled heating mantle.
- The pressure regulator need not be in situ, nor would it require temperature control.
- Use of a pump such as a Gast Model 2565 would eliminate a need for any conditioning of the stream ahead of the pump.
- A laser is an integral part of the optical monitoring system. It would be mounted ex situ with appropriate safety measures.
- The electronic readout for the optical subsystem may be located wherever desired.
- Since the flowrate through the device will be held constant, a pitot probe (not shown) will be required to perform a preliminary velocity measurement at the selected sampling point (or points) in order to select an appropriate sampling nozzle I.D. A pitot probe could be made an integral part of the assembly.
- Preliminary design efforts have led to the conclusion that the probe O.D. will be compatible with insertion through a four inch Schedule 40 pipe nipple (10.3 cm I.D.).

A sketch of an impactor module is shown in Figure 38. The major difference between this unit and the laboratory model is of course the smaller overall size and smaller plenums. The arrangement of the exhaust tubing came about

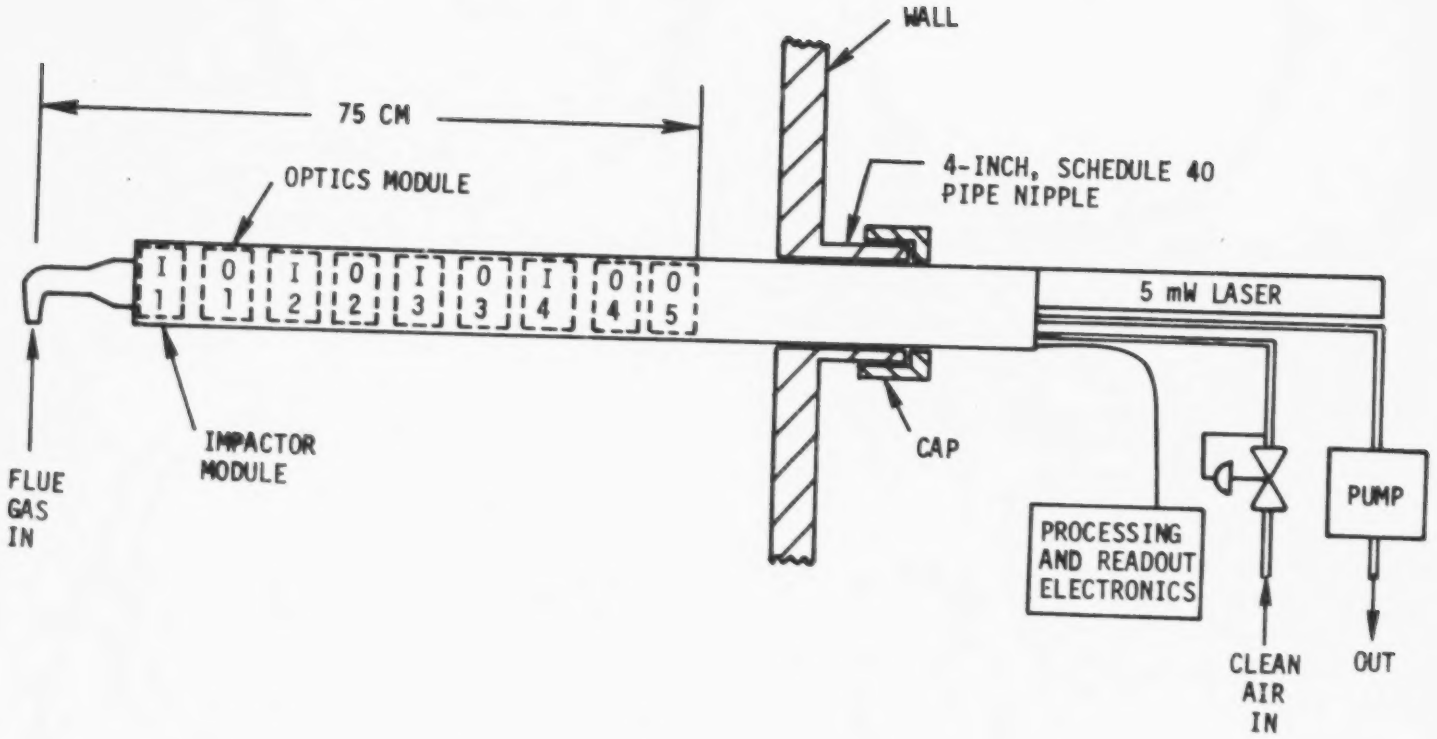

Figure 37. Staged continuous flow impactor installation

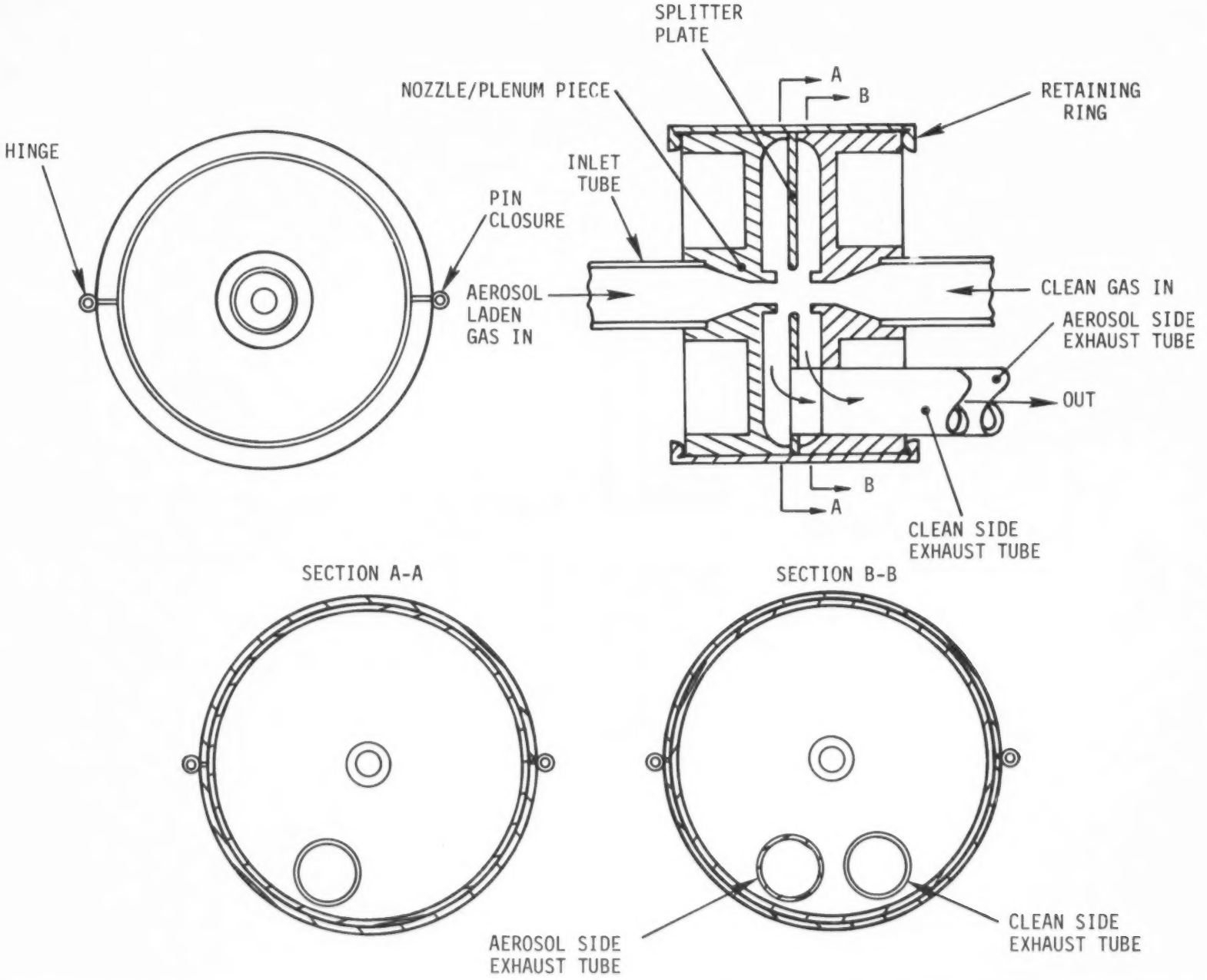
SPLITTER PLATE
NOZZLE/PLENUM PIECE
A
B
RETAINING RING
HINGE
INLET TUBE
PIN CLOSURE
AEROSOL LADEN GAS IN
CLEAN GAS IN
AEROSOL SIDE EXHAUST TUBE
OUT
B
A
CLEAN SIDE EXHAUST TUBE
SECTION A-A
SECTION B-B
AEROSOL SIDE EXHAUST TUBE
CLEAN SIDE EXHAUST TUBE

primarily from packaging requirements to stay within the four inch envelope. The non-symmetry is presently considered to be a necessary evil imposed by the packaging constraints. An installation sketch of the first two modules is shown in Figure 39. In this sketch, a slightly different treatment of the clean gas inlet is shown. The purpose of this alternate approach is to provide maximum space for optics components between the impactor stages. The aerosol side interstage tube is kept as short and straight as possible to minimize interstage losses. The first stage needs to be as large in diameter as possible due to the relatively low jet velocity. Other stages can then be made smaller to allow for passage of tubing, light, etc., without adversely affecting performance. Other notable features are:

- Components requiring critical alignment (nozzle and splitter plate) are all axysymmetric. Alignment is assured through close, concentric fits easily achieved by machining on a lathe.
- Exhaust is accomplished very near to the splitter plate surface on both sides. This is an important modification to the laboratory design to insure the absence of pressure gradients normal to the splitter plate which could cause disruption of the jet interface and resultant gas transfer across the interface. The design also minimizes recirculation regions within the module, which helps to minimize interstage particle losses.
- The second, third, and fourth modules may be made identical except for the nozzle and splitter plate orifice diameter, which helps to keep production costs down.
- Inlet and outlet sonic orifices will be located as close as possible to the respective modules to insure that the proper orifice temperature is maintained. Since the critical portion of the probe will be fully inserted into the flow, proper temperature will be maintained automatically by the flue gas inself with no additional controls and no diagnostics required.
- The direct coupling between the sampling nozzle and the first stage minimizes aerosol losses.

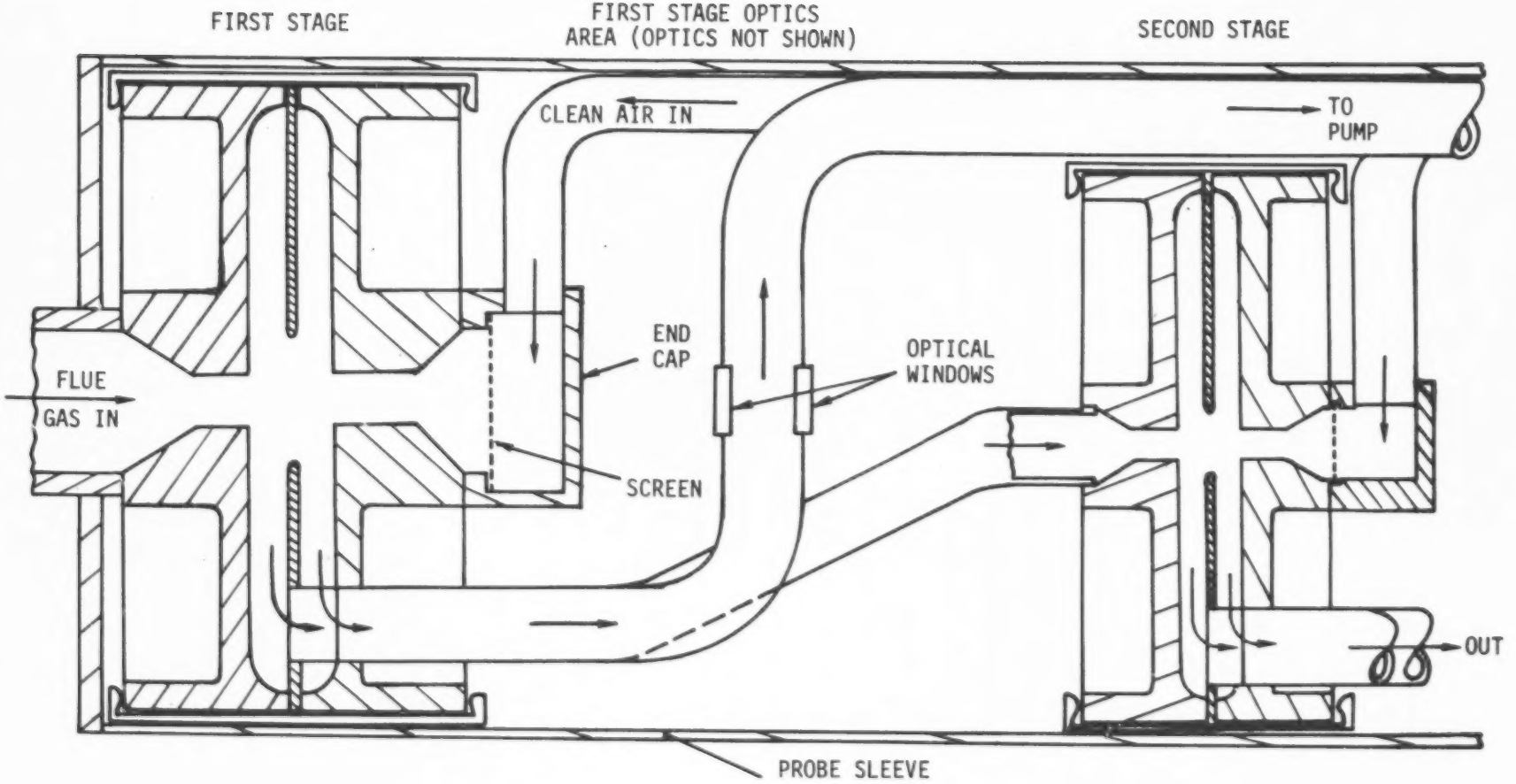

Figure 39. Staged continuous flow impactor assembly - first two stages

8.1.2 Optical Monitor Components

During laboratory testing, a Royco particle counter was used to monitor the impactor output streams. The particle counter accelerates the aerosol laden flow through a nozzle to produce a high speed, small diameter jet. The jet then passes through an optical viewing volume which has a slightly larger diameter, and the particles are detected using a light scattering technique. Particle size is obtained through pulse height analysis of the scattered light pulse.

Optical monitoring is the most obvious technique to consider for the staged continuous flow impactor. Use of optical techniques for a commercial device such as that shown in Figure 37 implies the following constraints:

- Optical components must be inexpensive, reliable, and not require adjustments in the field.
- With the exception of the light source selected, the components must be capable of withstanding stream temperatures.
- Each optical module must be able to be packaged in a small space.

The approach eventually selected from among several considered is single particle imaging with modified pulse height analysis. Detailed background, including supporting calculations, is presented in Appendix B. A sketch of an optical subassembly is shown in Figure 40. The basic technique used is near-forward scattering of the incident light beam. Due to the constraints mentioned above, the proposed technique differs in several particulars from standard optical counters. The main features of the system shown in Figure 40 are as follows:

- The optical path lengths involved are compatible with the required envelope, although some folding will be needed.
- Components are available to withstand the normal range of stream temperature.
- For each stage, the output electronics will only count particles above a specified size by requiring a minimum detector output per pulse.

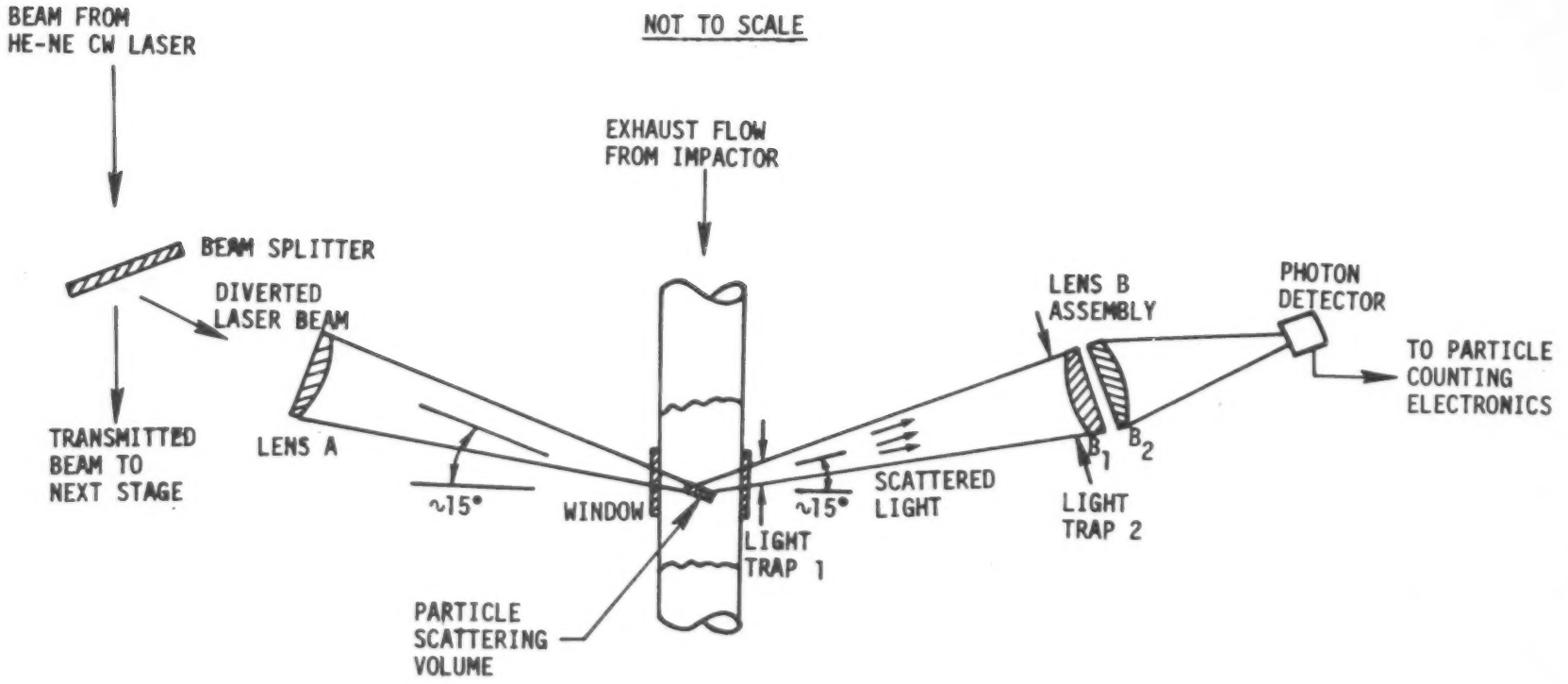

CW LASER: 0.5 MW HE-NE (0.63μ)
LENS A: $(f/D)_A = 4$ D_A = 1/4-INCH
LENS B:
LENS B_1: $(f/D)_{B_1} = 4$ D_{B_1} = 1/2-INCH
LENS B_2: $(f/D)_{B_2} = 2$ D_{B_2} = 1/2-INCH
DETECTOR: PIN PHOTODIODE.

Figure 40. Schematic diagram of optical concept.

- The viewing volume for each stage will be made as large as possible while avoiding the presence of more than one particle above the minimum size in the viewing volume.
- Minimum time response requirements dictate that the viewing volume cross-sectional area will be smaller than the stream cross-sectional area.
- Calculations in Appendix B show a good probability of being able to resolve (count) particles down to 0.2μ diameter. This will need to be confirmed experimentally.

The major difference between the proposed optical technique and normal particle counters is that the impactor optics will be working on size fractionated streams. This allows important simplifications. In a standard particle counter, an observed particle is assigned to a size range by producing a signal large enough to trigger one channel but too small to trigger the next larger one. In the continuous impactor, the upper cutoff is accomplished mechanically in the separation process, so the optics need only establish the lower threshold. The monitoring subsystem can also ignore undesired small particles in each stage, which helps to optimize system accuracy.

Limitations on input power (size, cost, and safety aspects of the laser) and size of the collector optics (space constraints) limit the minimum response time for detection. This means that the optics will only be looking at a portion of each output stream, thus requiring uniform particle distribution within the stream to insure accurate measurements. It is important to maintain the flowrate as high as possible to avoid particle losses to the walls through settling and diffusion so accuracy would suffer if the flowrate were cut down in order to reduce the area. As each individual flow leaves its respective impactor stage ahead of the optics, it will undergo approximately a four to one area contraction to provide a uniform flow past the optics. The fact that size fractionation will have occurred prior to the contraction will help to insure a uniform particle distribution due to the relatively narrow size range and substantial mixing which will occur at the stage outlet.

The major effort to this point in the optics area has been to analytically determine feasibility (Appendix B) and select appropriate hardware components. The next step will be to demonstrate adequacy of the approach and package the components in an acceptable manner. At this point, we feel confident that an optical system to monitor five separate streams in an in situ probe can be manufactured at reasonable cost, and have good accuracy and reliability.

8.1.3 Application

The primary use of the device is expected to be determination of total particulate mass emission rate and size distribution. The most likely specific applications will be control device efficiency testing (inlet and outlet measurements) and continuous regulatory monitoring. These two applications would likely involve instruments with different cutoff ranges. nominal ranges are shown in Table 3. The control device evaluation instrument will concentrate primarily on the smaller sizes to provide maximum information on fine particle emissions, while the regulatory instrument will cover a broader range to both provide information on fine particles and cover the higher size ranges to more accurately determine the total particulate mass emission rate. The use of a modular design will maximize this type of flexibility without significantly impacting cost. Basic readout will be the same for either device — counts per channel over a prescribed sampling period.

The primary advantage of this device over a standard impactor for control device evaluation is elimination of the normally large differential between inlet and outlet sampling times. The continuous impactor is not concerned about overloading a stage, which is the normal inlet problem, nor will it need to sample for long periods of time at an outlet due to the low outlet grain loading.

8.2 ADDITIONAL CONFIGURATIONS

A number of applications different from the mass monitor described above have been postulated. Two will be described briefly here — a staged impactor to collect samples in an inert environment, and a single stage impactor to selectively remove large particles from a stream which will then go into another device, such as a standard impactor.

Table 3. NOMINAL SIZE RANGES FOR STAGED CONTINUOUS FLOW IMPACTOR APPLICATIONS

OUTPUT STREAM	NOMINAL PARTICLE SIZE RANGE, MICRONS	
	FINE PARTICLE MONITOR	TOTAL PARTICULATE MASS MONITOR
1	>3.2	>10
2	1.6-3.2	5-10
3	0.8-1.6	3-5
4	0.4-0.8	1-3
5	0.2-0.4	.2-1

8.2.1 Inert Atmosphere Collection

It is often desirable in process stream evaluation work to collect a particulate sample and immediately quench any chemical reactions which may be occurring, so that subsequent analysis will reveal the particle composition at the sampling point. In standard inertial separation devices, the collected particles are continually exposed to the flue gas during the sampling period. The continuous flow impactor offers a unique capability to rapidly transfer particles from the flue gas to an inert gas (nitrogen is the easiest). This will help to radially quench any reactions. Particle collection can then take place on a filter element within the probe. A prototype holder is shown in Figure 41. The filter element used would be selected for compatibility with the stream temperature and subsequent analytical techniques. The filter holder would be used in place of the optics modules shown in Figure 37, which would make the device essentially a high capacity staged impactor in which the particles are collected in an inert (quenching) atmosphere.

8.2.2 Single Stage Preconditioner

Several standard types of impactors and trains employ a cyclone at the inlet to remove particles to avoid overloading the subsequent device. The characteristics of the continuous flow impactor make it an ideal device to perform this same function without the cyclone's cup capacity and orientation limitations. For this application, only a single stage would be needed, which would cut down the clean air and pumping requirements. The cutoff would be selected in accordance with the characteristics of the downstream device.

8.3 COST ESTIMATES

Rough estimates of hardware costs based on a production run of ten units are presented in Table 4 for the three configurations considered: a four stage impactor with five sets of optical monitors, a four stage impactor with five filters, and a single stage preconditioning impactor. It is emphasized that these are very rough estimates. The hardware design was carried far enough to show that an in situ device is feasible, and that the probe diameter will be allow for insertion through a four

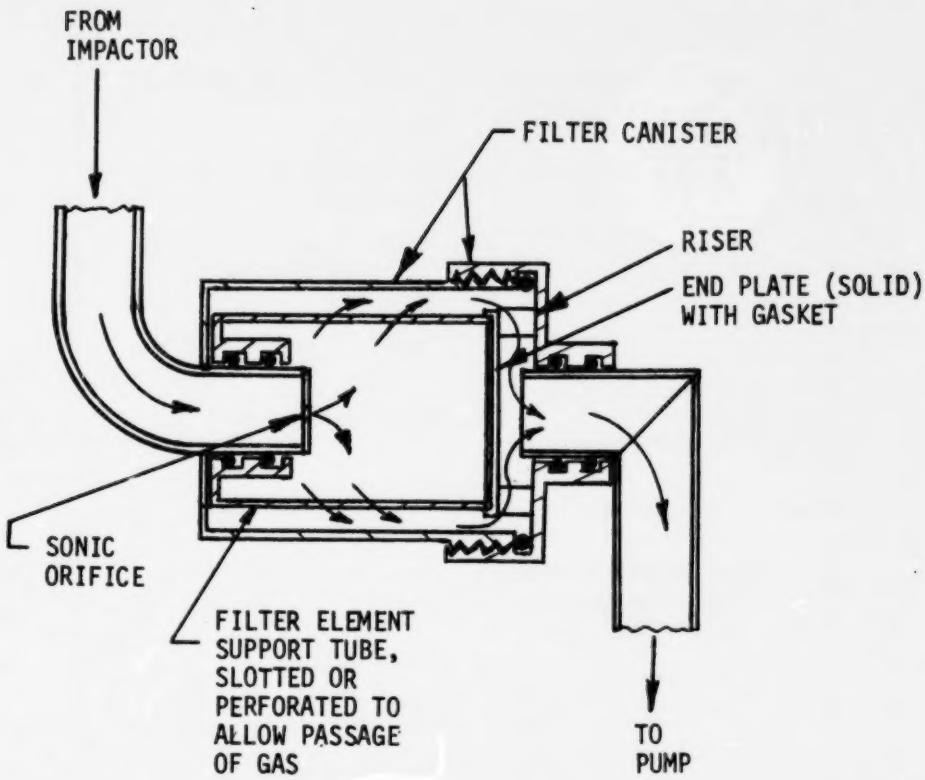

Filter element (Millipore filter, glass filter, etc.) forms a cylindrical surface on the inside of the filter element support tube. Filter element is recovered by unscrewing canister lid and removing end plate. Sonic orifice must be located ahead of filter to avoid flowrate change as filter loads up.

Figure 41. Filter holder subassembly

Table 4. CONTINUOUS FLOW IMPACTOR PRODUCTION COST ESTIMATES

Configuration	Subsystem	Estimated Cost
4 Stage Impactor With 5 Channels of Optical Monitoring	Impactor Modules	1600
	Optics	2000
	Processing & Readout Electronics	300
	Probe Body, Including Alignment & Support Hardware	1000
	Pump, Regulator, and Air Cleaning Components	800
	Sampling Nozzles (6)	150
	Total:	$ 5850
4 Stage Impactor With 5 Filters for Collection in an Inert Gas	Impactor Modules	1600
	Filter Assemblies	400
	Probe Body	700
	Pump, Regulator, and Air Cleaning Components	800
	Sampling Nozzles (6)	150
	Total:	$ 3650
Single Stage Pre-conditioning Impactor	Impactor Module	500
	Pump, Regulator, and Air Cleaning Components	400
	Sampling Nozzles (6)	150
	Total:	$ 1050

Estimated cost is estimated production cost for a production run of ten systems of the particular configuration.

inch pipe nipple. Optical design was primarily concerned with being sure that the small particles (around .2 μ) could be detected, and that there were readily available components which would be inexpensive, able to tolerate high temperatures, and be compatible with the selected probe size. More accurate cost estimates cannot be made until actual production drawings are made.

SECTION 9

DISCUSSION OF RESULTS

All of the primary task objectives were accomplished. Test hardware was fabricated after an initial literature search indicated feasibility of the concept. Reasonable jet stability was demonstrated prior to particle separation testing. Testing with the larger splitter plate orifice showed good correlation between the calculated and measured 50% cut points, while use of the smaller orifice shifted the 50% cut point to larger particle sizes. A reasonably good separation efficiency capability was demonstrated during the final laboratory test phase, after some initial problems had been diagnosed and overcome. Preliminary design work showed that it will be reasonable to integrate multi-stage hardware into a probe capable of being inserted through a standard four inch pipe nipple, with an optical monitoring subsystem on each of five output streams. Important questions to be answered during further development deal with instrument accuracy, cost, reliability, and handling characteristics. Basic proof of principle, including demonstration of a field acceptable hardware concept, has been accomplished.

Luna's work was very helpful in providing a basic understanding of the stability of impinging gas jets. Because the projected use for the continuous flow impactor, process stream sampling, our hardware configuration differed significantly from Luna's. It was one of these differences -- lack of active control over the individual inlet flowrates, which was the source of the major flow instability observed early in the test program. This instability was the single largest surprise received during testing, although the probability of its occurrence is obvious in retrospect.

The first phase of particle separation testing resulted in relatively poor sharpness of cutoff, including carryover of a very substantial amount of the small particle population. The problem was diagnosed after completion of the intial test effort and corrected as part of the additional test work. The separation achieved in the final configuration was excellent except for

some small particle carryover resulting from unsteadiness in the gas feed and exhaust lines.

The final subtask was a brief study to insure that the instrument could be packaged for in situ monitoring, and to investigate the use of optical techniques to monitor the output streams. Based primarily on laboratory test data, the current opinion is that packaging impactor modules and optics in a probe to fit a standard four inch pipe nipple will not present a problem, nor will it have a notably adverse affect on accuracy. Loss of accuracy during an extraction process would likely be greater than that which will occur due to compromises required to obtain an in situ instrument.

The next step in the instrument development process should be fabrication, laboratory test, and field test of a multistage version of the impactor. For this effort, it would be most reasonable to use particle collection in filters as the operating mode. This testing should be followed by a demonstration of the optical subsystem, which could be done mainly with available in-house components. The simplicity of the continuous flow impactor components and assembly, its coordination of many of the attractive features of traditional impactors and optical particle counters while avoiding their primary drawbacks, and its potential usefulness as a diagnostic and monitoring tool all strongly recommend that the effort begun during this task should be continued.

SECTION 10
REFERENCES

1. Luna, R. E., "A Study of Impinging Axisymmetric Jets and Their Application to Size Classification of Small Particles," Ph.D. dissertation, Princeton University, 1965, University Microfilms, Inc., Ann Arbor, Michigan

2. Witze, P.O. and Dwyer, H. A., "The Turbulent Radial Jet," Journal of Fluid Mechanics, Vol. 75, Part 3, June 1976

3. Marple, V. A., and Liu, B. Y. H., "Characteristics of Laminar Jet Impactors," Journal of Environmental Science and Technology 8: 648-654, July 1974

4. Marple, V. A., and Willeke, K., "Inertial Impactor: Theory, Design and Use," Fine Particles: Aerosol Generation, Measurement, Sampling, and Analysis, Academic Press, Inc., 1976

5. Smith, R. H., and Wang, C. T., "Contracting Cones Giving Uniform Throat Speeds," Journal of the Aeronautical Sciences, pp 356-360, October, 1944

6. Ranz, W. E., and Wong, J. B., "Impaction of Dust and Smoke Particles," I & E Chem. 44: 1371, 1952

7. Davies, C. N. Ed., Aerosol Science, Academic Press, New York, 1966

SECTION 11
GLOSSARY

SYMBOL	USAGE
A_p	geometric cross-section of particle, cm^2
C	Cunningham slip correction factor
D	lens diameter, cm
D_p	particle diameter, cm
$f(\theta)$	scattering function, sr^{-1}
f	focal length of lens, cm
I_o	laser beam illumination intensity, W/cm^2
$J(\theta)$	light intensity scattered at angle θ, W/sr
m	refractive index of particle
N	number of photons incident on particle
N_{scatt}	number of photons scattered onto detector by particle
P	laser beam power, W
P_{scatt}	power of light scattered onto detector by particle, W
r_{jet}	impactor nozzle radius, cm
t	thickness of diffraction cylinder at test section center, μM
V	particle velocity, cm/sec
V_o	mean jet velocity, cm/sec
α	particle size parameter
ε	energy per photon, ergs/photon
θ	scattering angle, radians
λ	wavelength of light incident on particle, μM

SYMBOL	USAGE
μ	gas viscosity, g/cm-sec
ρ_p	particle density, g/cm^3
τ	transit time of particle through illuminated scattering volume, sec
Ω	solid angle of scattered light subtended by light trap lens, sr

APPENDIX A
STABILITY DATA

The purpose of this appendix is to present strip chart traces taken during the stability test phase. The traces display three different differential pressures:

1. Differential pressure across the splitter plate - this indicates the difference in static pressure across the splitter plate, and is an indication of how accurately the pressure fields on either side of the interface are matched. Ideally, this differential pressure will be zero.

2. & 3. Right and left nozzle differential pressures - for each nozzle, this will be the difference between the total and the static pressure at the nozzle exit - the same differential pressure as would be measured by a very small pitot-static probe located at the nozzle exit. The nozzle flowrate is proportional to the square root of the nozzle differential pressure. The right and left nozzle differential pressures should be equal for proper operation.

Segments 1 through 5 were obtained from the setup shown in Figure 11b in the text (the modified stability test configuration) while Segments 6 through 9 were obtained from the setup shown in Figure 11a (the initial stability test configuration). The traces were lined over with a felt tip pen, as the original traces were too weak to reproduce properly. Notation added to the traces shows the applicable pressure scales, the time rate of motion of the chart paper, and identifies which parameter is being measured. Segments 1 through 5 form a continuous trace except for the identified interuption between segments 4 and 5. Segments 6 through 9 also form a continuous trace.

Segment 1 shows the differential pressure across the splitter plate. Two things are worthy of note. First, the effect of the drift of the nitrogen regulator on this differential pressure is quite apparent. The effect was lessened during particle separation testing by using a group of interconnected nitrogen bottles rather than the single one used when this trace was taken. Second, the measured differential pressure (0 - 0.01 Torr) was small compared with the measured nozzle differential pressures (.16 - .17 Torr) which is desirable.

Segments 2 through 5 alternately show the right and left nozzles. The observed variations were due to random unsteadiness in the flow. The magnitude of the variations was about $\pm$ 3% of the measured differential pressure, which means that the actual nozzle flowrate variations were about $\pm$ 1.5%. This qualifies as stable operation.

Unstable operation is shown in segments 6 through 9. In this case, the flowrate through the right nozzle was about a factor of 2.5 higher than the flowrate through the left nozzle. For the trace shown, the differential in flowrates stayed constant. During other runs using the initial configuration, the right and left nozzle flowrates were observed to vary in a random manner over a period of several minutes - first one would be higher, then the other. The improvement in performance of the configuration in Figure 11b in the main text over that of the configuration in Figure 11a is made dramatically clear through a comparison of Segments 2 through 5 (stable operation) with segments 6 through 9 (unstable ooeration).

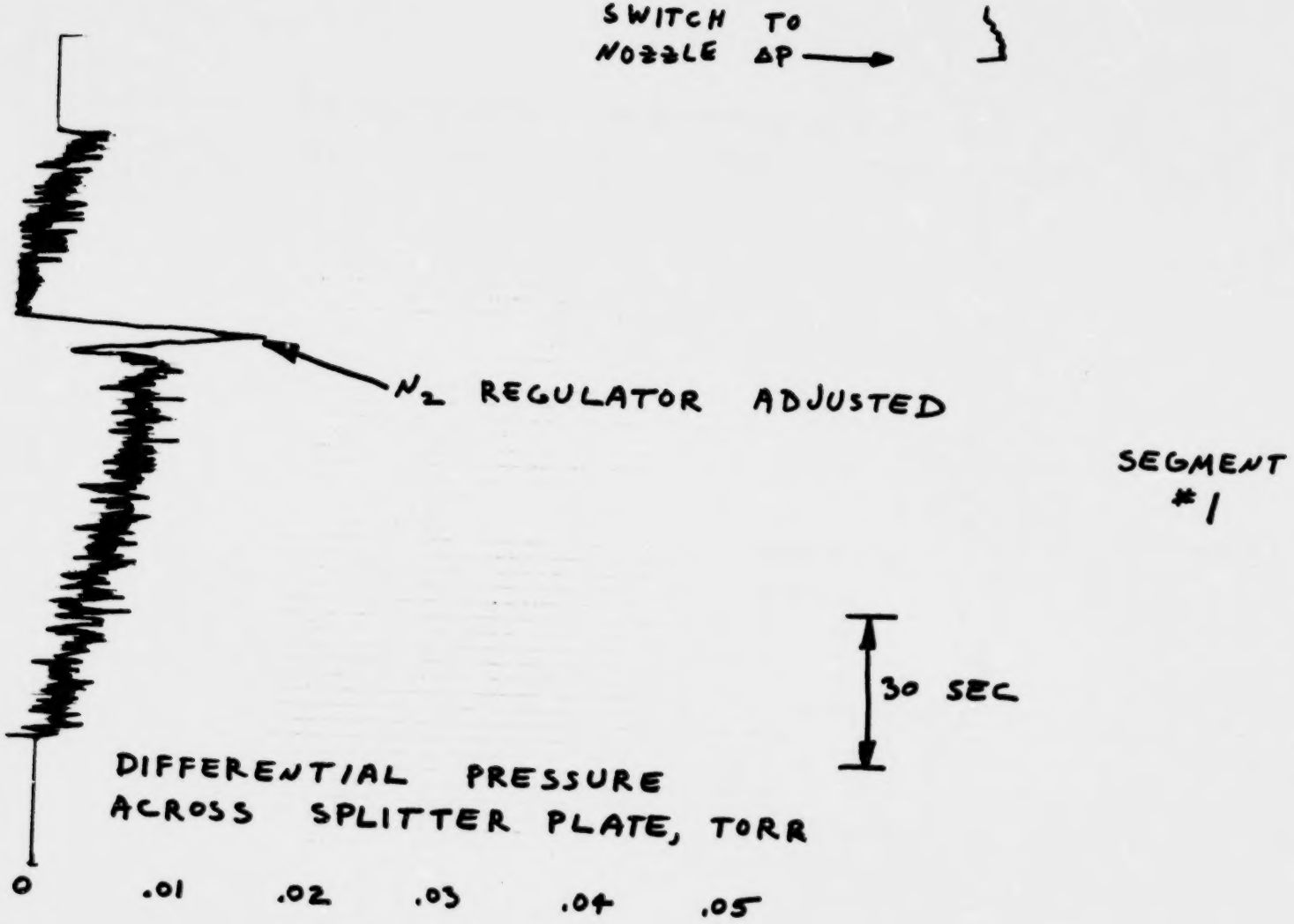
SWITCH TO
NOZZLE ΔP
N_2 REGULATOR ADJUSTED
SEGMENT
#1
30 SEC
DIFFERENTIAL PRESSURE
ACROSS SPLITTER PLATE, TORR
0
.01
.02
.03
.04
.05

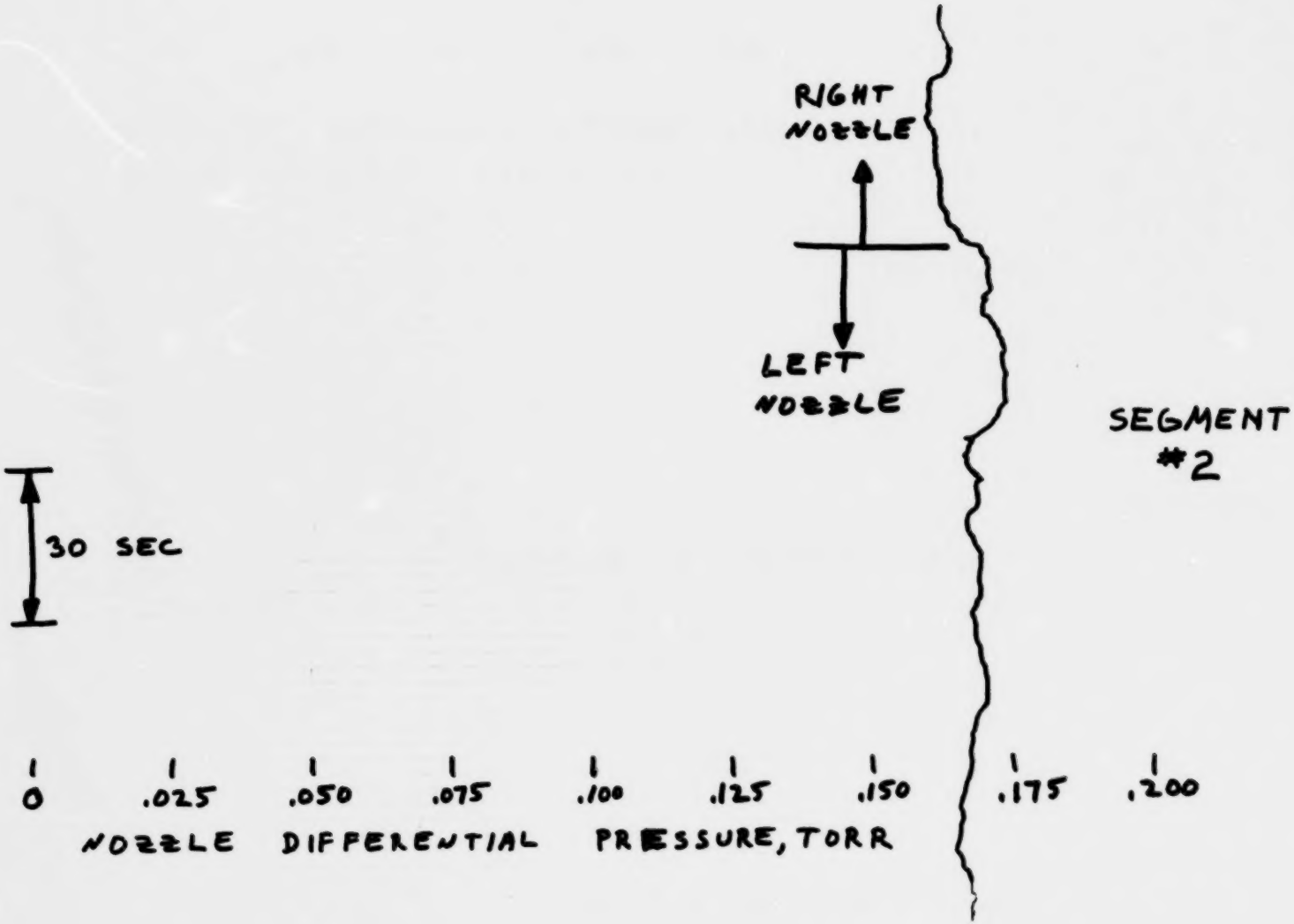
RIGHT NOZZLE
LEFT NOZZLE
SEGMENT #2
30 SEC
0
.025
.050
.075
.100
.125
.150
.175
.200
NOZZLE DIFFERENTIAL PRESSURE, TORR

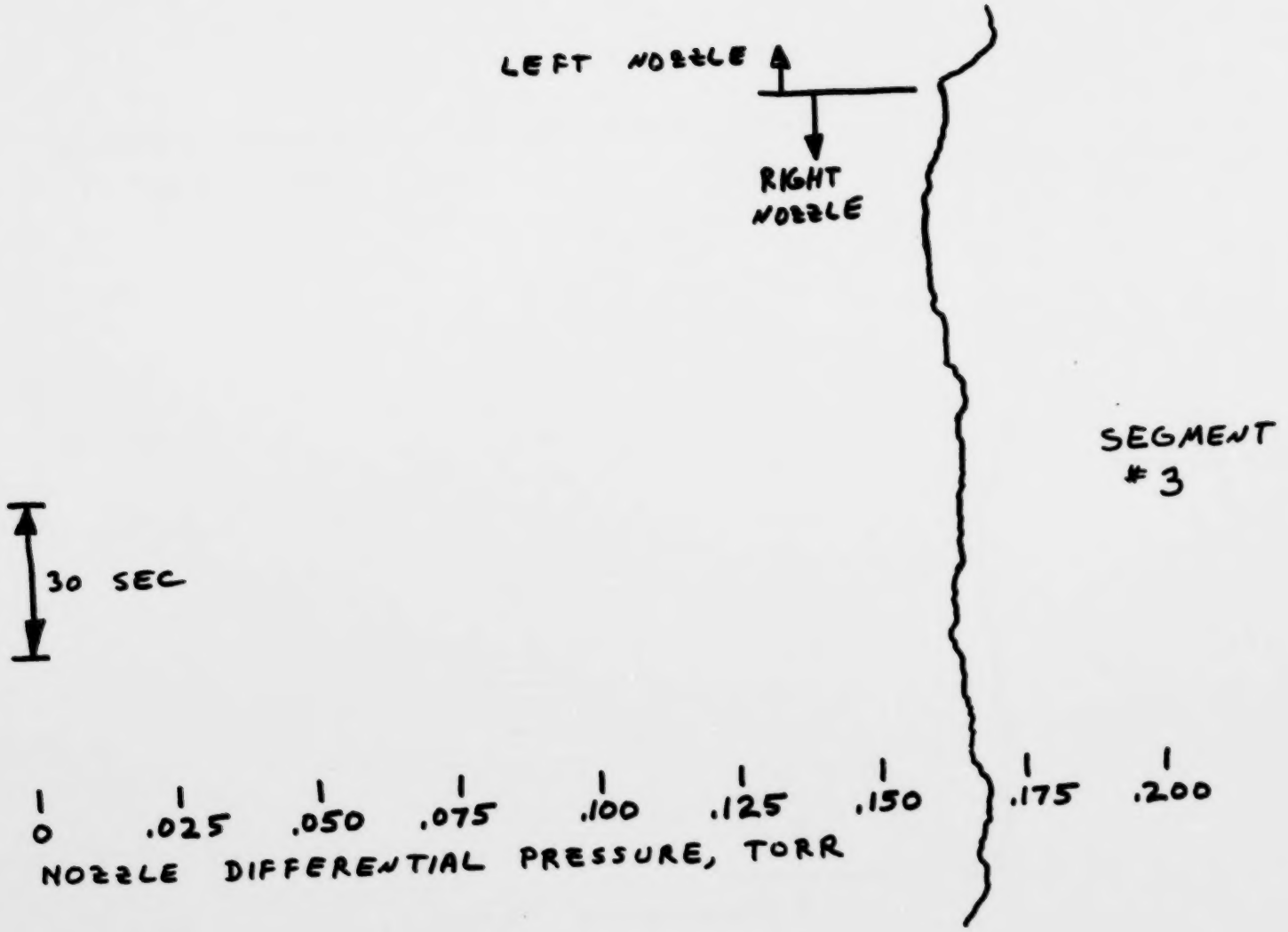
LEFT NOZZLE
RIGHT NOZZLE
SEGMENT #3
30 SEC
0
.025
.050
.075
.100
.125
.150
.175
.200
NOZZLE DIFFERENTIAL PRESSURE, TORR

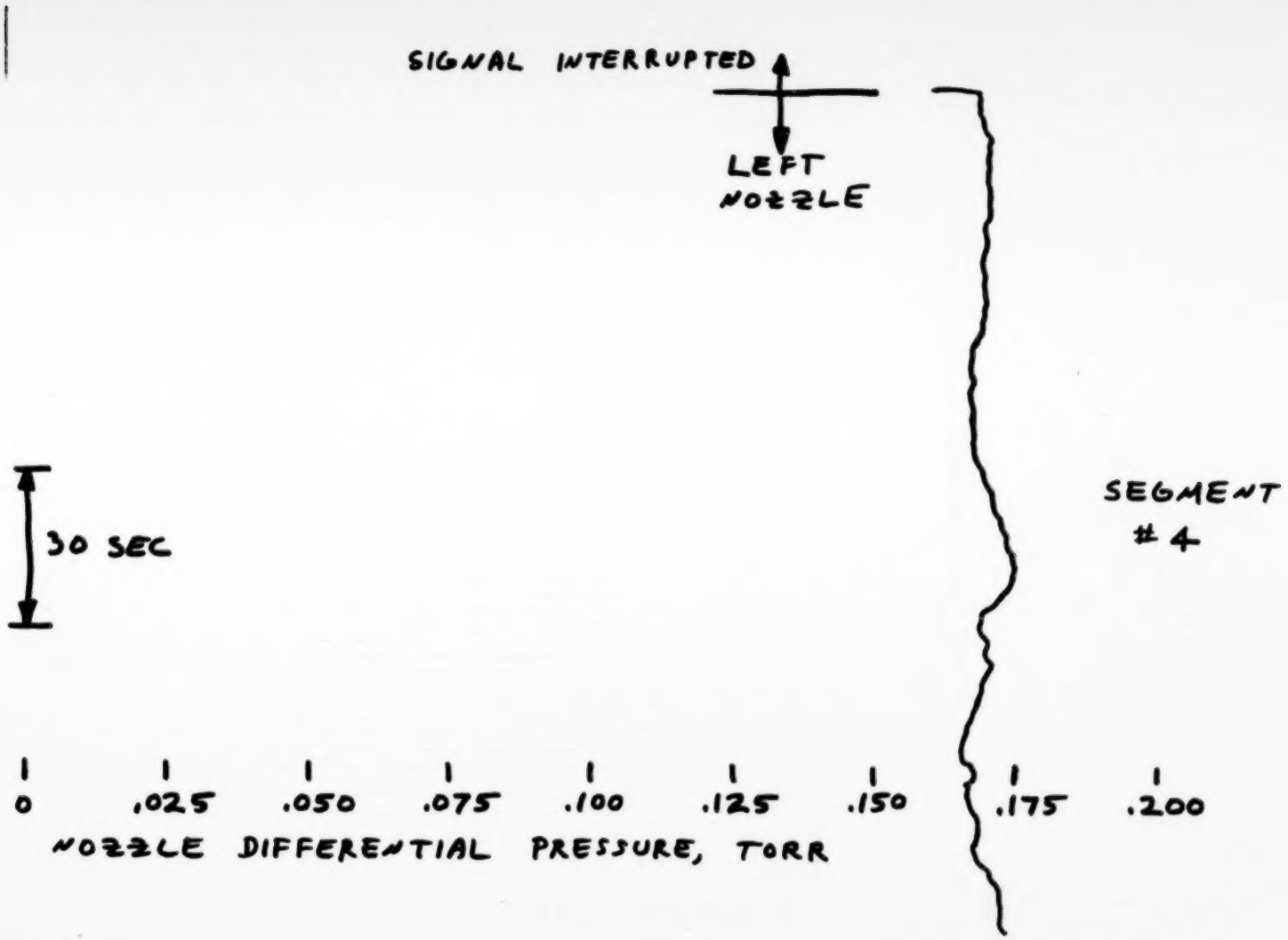
SIGNAL INTERRUPTED
LEFT NOZZLE
30 SEC
SEGMENT #4
0
.025
.050
.075
.100
.125
.150
.175
.200
NOZZLE DIFFERENTIAL PRESSURE, TORR

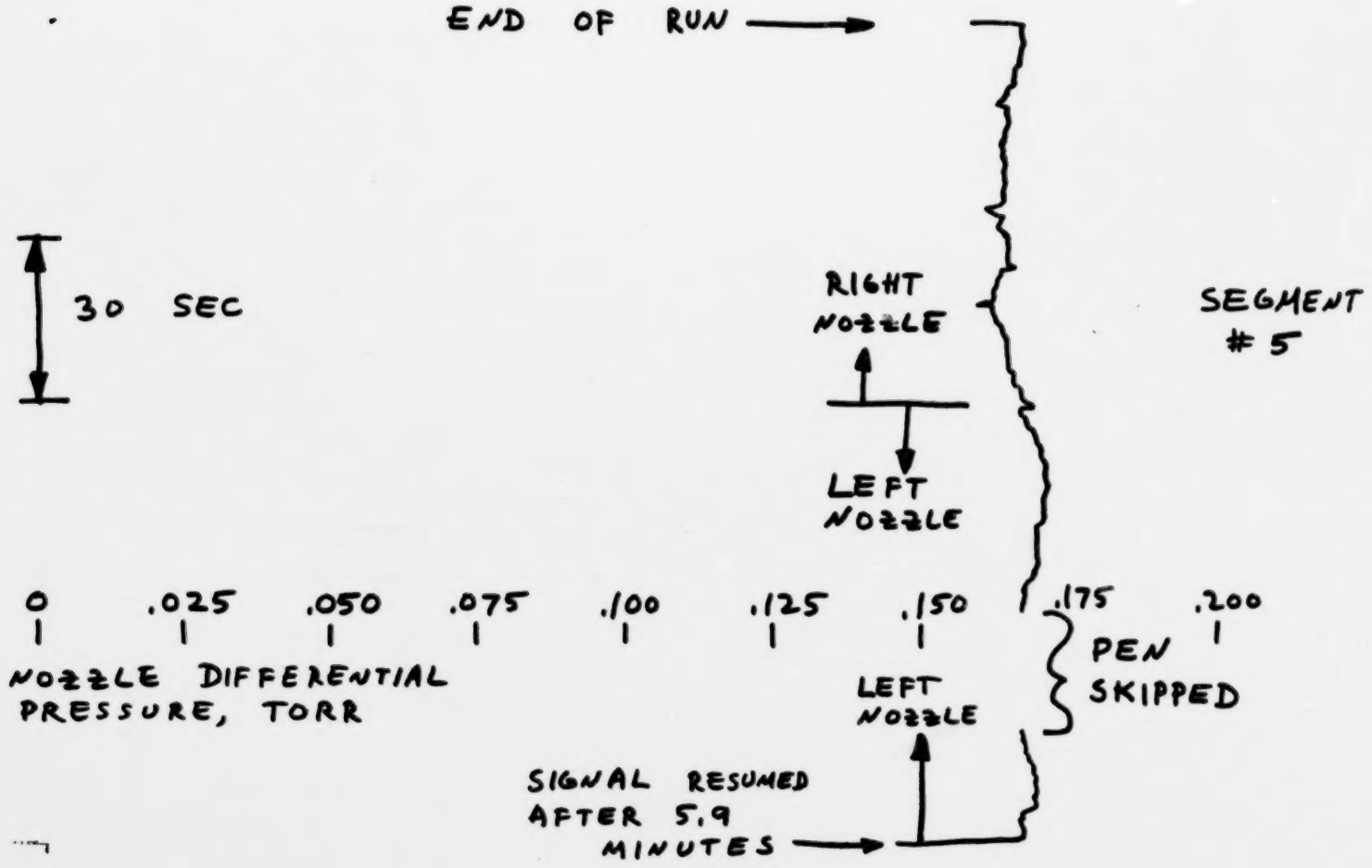
END OF RUN
30 SEC
RIGHT NOZZLE
LEFT NOZZLE
SEGMENT # 5
0
.025
.050
.075
.100
.125
.150
.175
.200
NOZZLE DIFFERENTIAL PRESSURE, TORR
PEN SKIPPED
LEFT NOZZLE
SIGNAL RESUMED AFTER 5.9 MINUTES

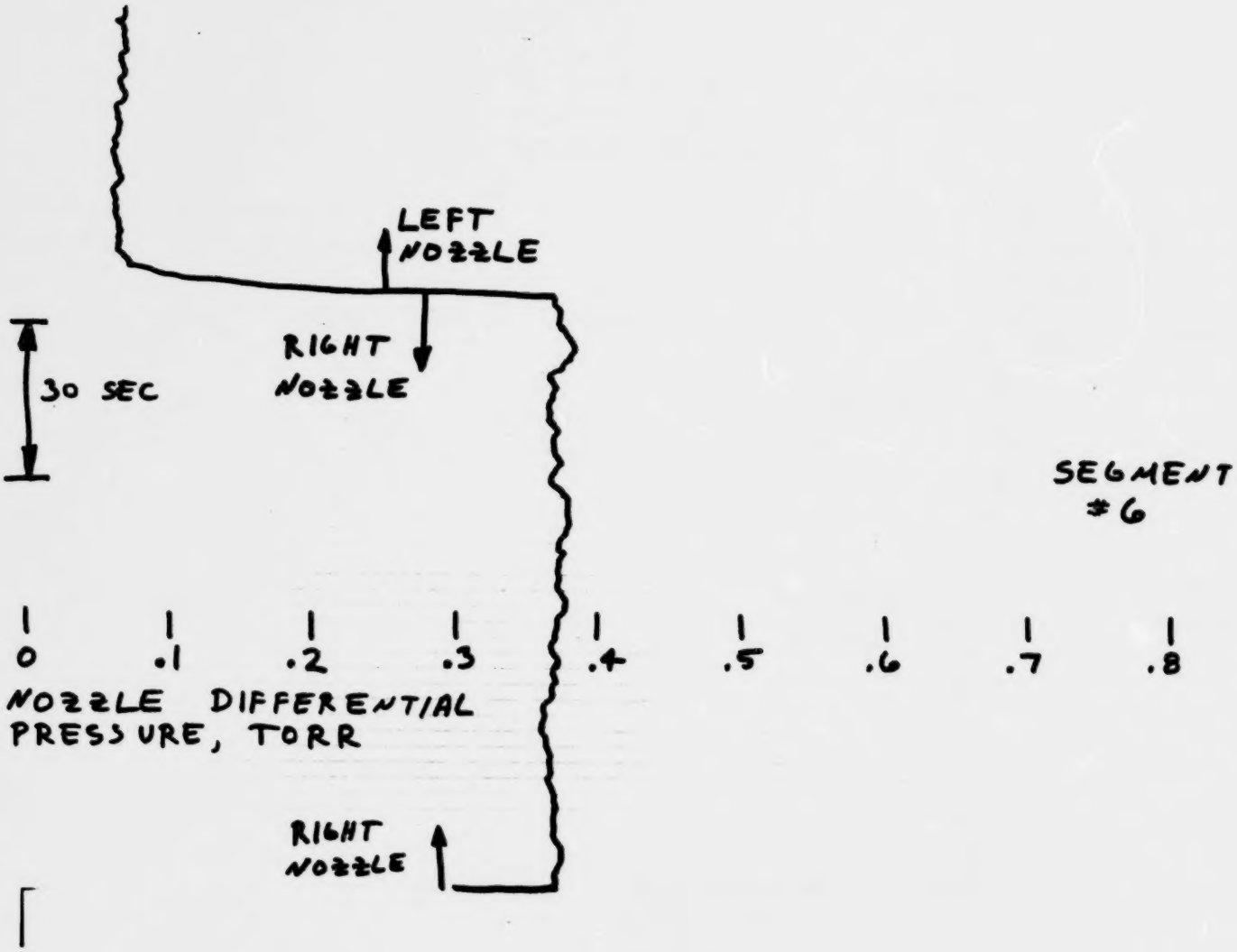
LEFT NOZZLE
RIGHT NOZZLE
30 SEC
SEGMENT #6
0
.1
.2
.3
.4
.5
.6
.7
.8
NOZZLE DIFFERENTIAL PRESSURE, TORR
RIGHT NOZZLE

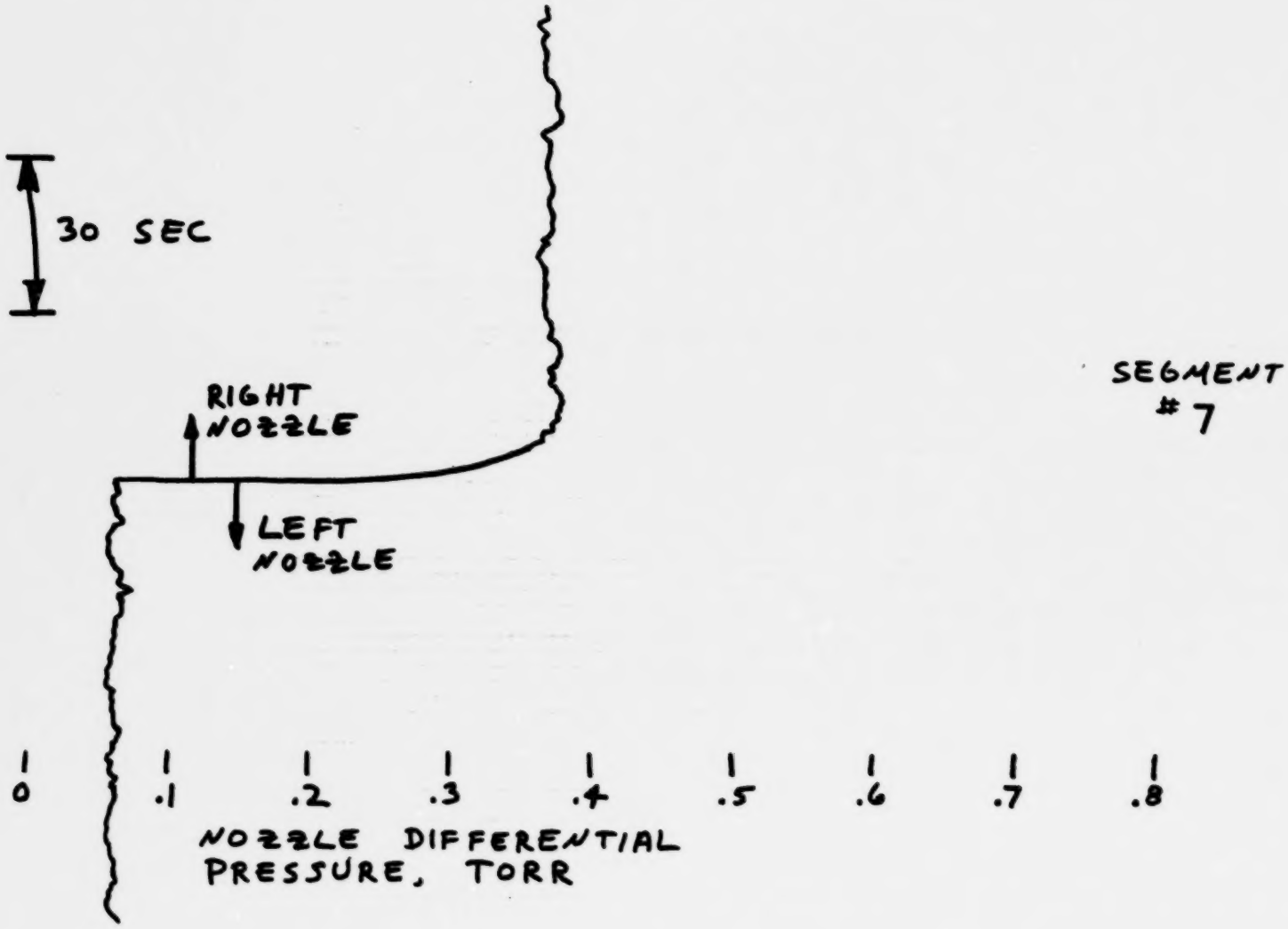
30 SEC
RIGHT NOZZLE
LEFT NOZZLE
SEGMENT #7
0
.1
.2
.3
.4
.5
.6
.7
.8
NOZZLE DIFFERENTIAL PRESSURE, TORR

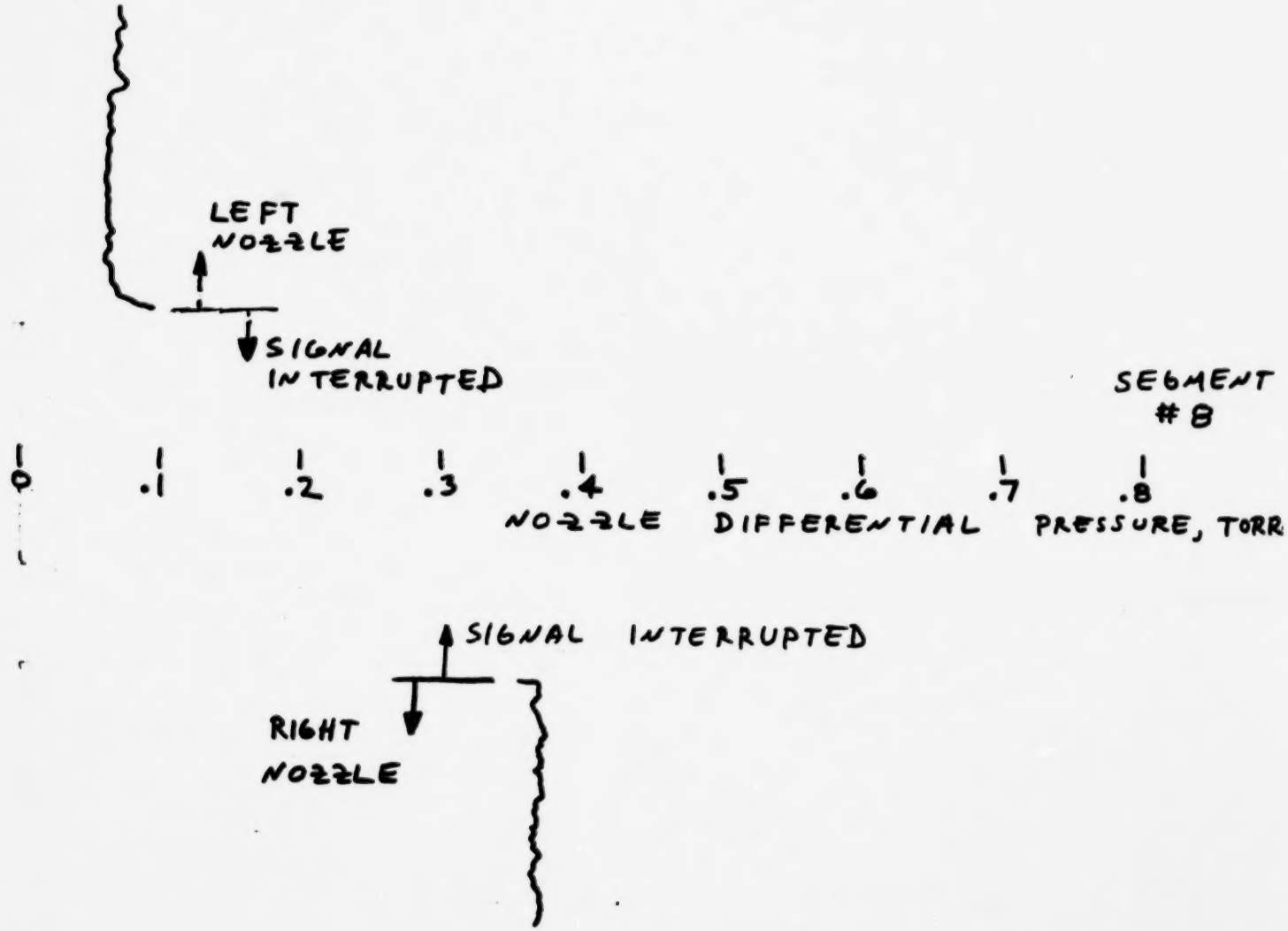
LEFT
NOZZLE
SIGNAL
INTERRUPTED
SEGMENT
#8
0
.1
.2
.3
.4
.5
.6
.7
.8
NOZZLE DIFFERENTIAL PRESSURE, TORR
SIGNAL INTERRUPTED
RIGHT
NOZZLE

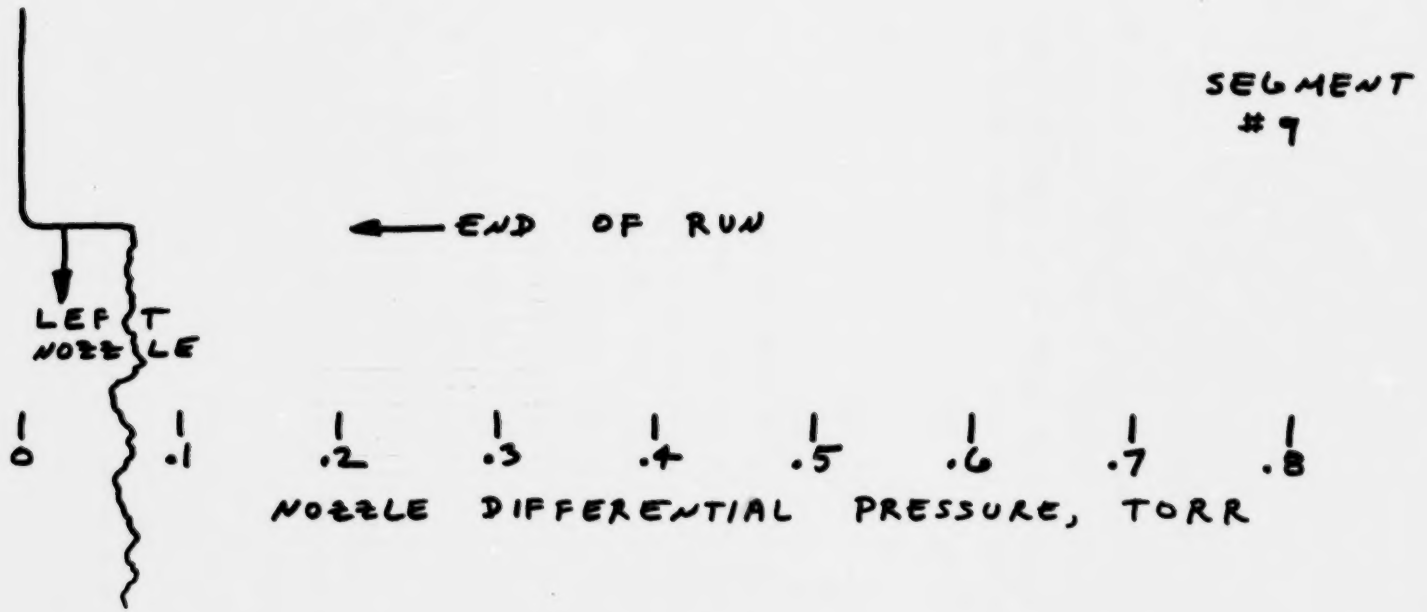
SEGMENT
#9
END OF RUN
LEFT
NOZZLE
LE
0
.1
.2
.3
.4
.5
.6
.7
.8
NOZZLE DIFFERENTIAL PRESSURE, TORR

APPENDIX B

OPTICAL MONITORING OF CONTINUOUS FLOW IMPACTOR OUTPUT STREAMS

B.1. INTRODUCTION

The purpose of this Appendix is to document analyses performed on an aerosol detection device utilizing forward scattering of light from a standard, low power laser. Table B-1 summarizes the requirements and performance of the system concept shown schematically in Figure B-1 (Figure 31 in text).

With a 5mW He-Ne cw laser, the system is designed to produce count rates of individually resolved particles up to about 10^6 particles/sec (0.2 μsec response time) corresponding to a flow velocity of 15 m/sec and particle concentrations of 7×10^3 per cubic millimeter. Beam splitters are used with a single laser source and 5 identical sets of optics to monitor the particle flow in the center of 5 output streams in the impactor system. The most sensitive monitoring channel would produce readily detectable signals with particles down to 0.2-0.5μ diameter, using a photodiode detector.

All optical components are standard, commercial items. The cost of the optical elements only (including the laser source, but without external hardware or particle counting electronics) is estimated to be about $1420 for 5 channels. The mechanical design and physical size will be consistent with mounting the optical system within the probe shown in Figure 29 in the main text.

B.2. LIGHT SCATTERING FROM PARTICLES

The relationships governing the light scattered from small particles depend on the ratio of the particle size to the incident light wavelength. The particle size parameter,

$$\alpha = \frac{\pi d}{\lambda} \quad , \qquad \text{(B-1)}$$

Table B-1. REQUIREMENTS AND ESTIMATED PERFORMANCE OF LIGHT SCATTERING SYSTEM CONCEPT

Requirements	Performance
• Count aerosol particle flow at impactor exhuasts • Detect particle sizes down to 0.2-0.5μ size.	• Concept utilizes forward scattering of 5 mW He-Ne laser beam; 0.2-0.5μ diameter particles estimated to produce S/N ∿ 12. Individual particles resolved in center of flow. All particles larger than stage threshold size are counted.
• Optics size compatible with preliminary impactor design (package within ∿ 10 cm O.D.)	• 3 lens system concept with D ≲ 0.5", L ∿ 6"; single laser with beam splitter for 5 impactor outlets. Power supplies for detectors and laser mounted external to probe.
• Capability for remote readout	• Photodiode responds to individual particles above set threshold size; remote indication of particle count is straightforward.

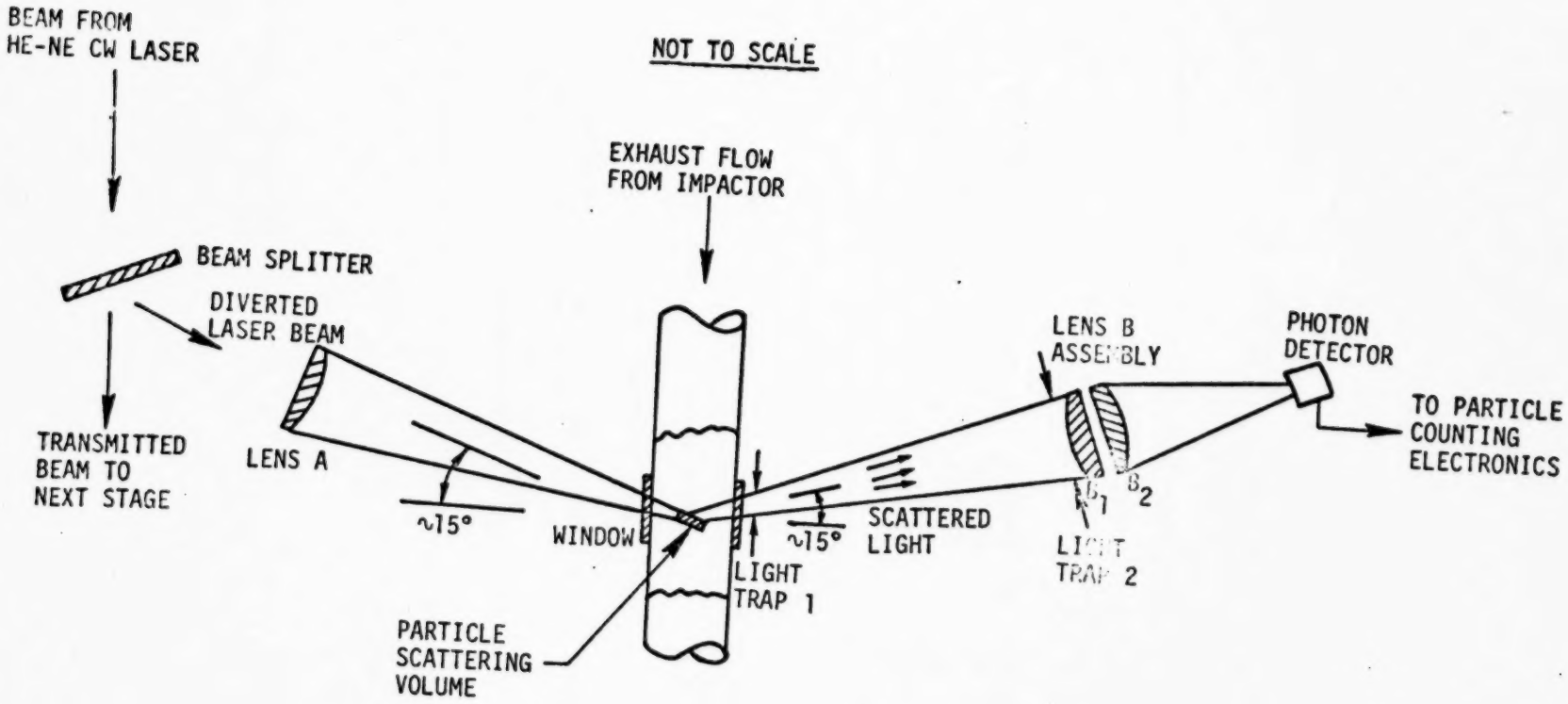

CW LASER: 0.5 MW HE-NE (0.63μ)
LENS A: $(f/D)_A = 4$ D_A = 1/4-INCH
LENS B:
LENS B_1: $(f/D)_{B_1} = 4$ D_{B_1} = 1/2-INCH
LENS B_2: $(f/D)_{B_2} = 2$ D_{B_2} = 1/2-INCH
DETECTOR: PIN PHOTODIODE.

Figure B-1. Schematic diagram of optical concept.

describes the appropriate scattering regime, where d is the particle diameter, and λ the wavelength of the illuminating light. For the smallest size particles considered here (d = 0.2μ), and a He-Ne laser (λ = 0.63), α = 0.99. The scattering is strongly dependent on the index of refraction of the particles and is outside the pure Rayleigh regime (for which α < 0.3) and in the so-called intermediate or Mie Rayleigh-Gauss regime (cf., Reference 7). Analytical formulations for the intermediate regime require very detailed calculations, and since the Rayleigh results are conservative and we are not far from the Rayleigh regime, we shall use estimates based on Rayleigh scattering functions.

Considering a beam of illumination density, I_o(W/cm^2) incident upon a single spherical particle, the intensity (W/sr) scattered at an angle θ is given by

$$J(\theta) = I_o f(\theta)\, A_p \quad , \quad (W/sr) \qquad (B\text{-}2)$$

where $f(\theta)$ is the scattering function (sr^{-1}) from scattering theory, and A_p is the geometric cross-section of the particle (cm^2). The illumination density is determined from the light source intensity and the optics geometry.

For Rayleigh scattering, we have

$$f(\theta) = \frac{\alpha^2}{2\pi}\left(\frac{m^2-1}{m^2+2}\right)^2 (1 + \cos^2\theta) \quad , \quad (sr^{-1}) \qquad (B\text{-}3)$$

where m is the refractive index, taken here to be 1.5 for graphite/carbon particles. Thus, for 0.2 particles, we have* $f(0°) = 0.0138$ sr^{-1} and equation (B-2) can then be written as

$$J(0°) = 1.08\text{x}10^{-10}\, I_o\, d_p{}^2 \quad , \quad (W/sr) \qquad (B\text{-}4)$$

where d_p is the particle diameter in μm.** From Equation (B-4), we see that the intensity of scattered light is proportional to the illumination density at the scattering volume and to the square of the particle diameter.

*Graphical data in Reference 7 (Figure 7, p.321) shows that $f(0°) \sim 0.019$ sr^{-1} for α = 1.0, d = 0.17μ, and m = 1.5.

**The optical system of Figure 1 actually detects scattering at angles somewhat different from 0°, but differing only by a small amount.

We shall now discuss the requirements for an optical system to provide laser illumination onto the particles in the impactor exhaust stream.

B.3 OPTICAL SUBSYSTEM REQUIREMENTS

Assuming an optical system as shown in Figure B-1, we can formulate a general expression for the power (or number of photons) scattered per particle in the scattering volume. Since our scattering angles are set to be small, we shall assume the scattering function is 0.0138 sr^{-1} throughout.

The instantaneous power scattered into the detector is

$$P_{scatt} \simeq J(0°)\ \Omega \quad , \quad (W) \tag{B-5}$$

where $J(0°)$ is given by Equation (B-4) and Ω is the solid angle of scattered light subtended by the lens B. Neglecting off-axis effects, Equation (B-5) may be written in terms of the f-number of lens B as

$$P_{scatt} \simeq J(0°)\ \frac{\pi}{4(f/D)_B^2} \quad . \quad (W) \tag{B-6}$$

The illumination density, I_o, at the scattering volume is determined by the size to which the diverted laser beam can be focused. This is limited by diffraction; the thickness (diameter) of the diffraction "cylinder" at the test section center is

$$t = 1.22\ \lambda(f/D)_A \simeq 3\mu \quad . \tag{B-7}$$

Thus, for a laser beam power of P_1 in the first stage, we have

$$I_o = \frac{P_1}{\frac{\pi}{4}\ t^2} \quad . \quad (W/cm^2) \tag{B-8}$$

The exit optics should be set to image a small region about the scattering volume onto the detector; no critical requirement exists, however.

From Equations (B-6), (B-8), and (B-2), we obtain the power scattered by a single particle as

$$P_{scatt}/P_1 = f(0°) \left(\frac{d_p}{t}\right)^2 \frac{\pi}{4(f/D)_B^2} \tag{B-9}$$

For the optics of Figure B-1, with $(f/D)_B = 4$, then

$$\frac{P_{scatt}}{P_1} = 0.75 \times 10^{-4} \mu_p^2 \quad , \qquad \text{(B-10)}$$

where μ_p is the particle diameter in microns.

Along with detector threshold levels, Equation (B-10) defines the limit of particle size detectability for a given diverted laser beam power. For 0.2 particles, we would have $p_{scatt}/P_o = 3x10^{-6}$; for 0.5μ particles we would have $8.3x10^{-6}$.

B.4 PERFORMANCE ESTIMATES

For reliable detection of the scattered light, we use the following criteria for various detectors

Table B-2. PHOTONS REQUIRED FOR RELIABLE DETECTION

Detector	Scattered Photons/Particle Required for Reliable Detection
PIN photodiode	10^3 - 10^4
Avalanche photodiode	10^3
Photomultiplier	10^2

For cost and simplicity, we would prefer to use PIN photodiodes to detect particles down to 0.2μ diameter

Equation (B-10) can also be written as the ratio of the scattered photons to incident photons, viz.,

$$\frac{N_{scatt}}{N} = 0.75 \times 10^{-4} \mu_p^2 \quad . \qquad \text{(B-11)}$$

The number of incident photons is the product of the photon rate (from the laser beam) and the transit time, τ, of a particle through the illuminated scattering volume; this is

$$N_1 = P_1 \tau/\varepsilon \quad . \tag{B-12}$$

where $\varepsilon = hc/\lambda$ is the energy per photon which for He-Ne 0.63μ light is 0.314×10^{-11} ergs/photon. The transit time is

$$\tau = \frac{t \cos 15^\circ}{V} \quad , \text{ (sec)} \tag{B-13}$$

where V is the particle flow velocity defined by the impactor stage design. From Reference 1, we take V = 14 m/sec so that $\tau \sim 0.2$ μsec. Hence,

$$N_1 = 0.68 \times 10^{12} P_1 \quad , \tag{B-14}$$

Figure B-2 is a plot of the calculations for photons scattered per particle vs. the beam power of the final stage, for various diameter particles. As can be seen, a 5 mW laser source, with 50% diverted to the final stage (P_1 = 2.5 mW) would allow counting (with 0.2 μsec response) of 0.5μ particles with high certainty, and 0.2μ particles with lower confidence. An experimental determination of the size detectability of our optics concept is discussed in Section B.6.

B.5 MECHANICAL DESIGN AND COST

The components of the optical system shown in Figure B-1 are small and can be installed in a small space. No detailed layout has been made here, but installation in the required 10 cm diameter tube should present no major problems. Small plane mirrors can be used in the optical path to "fold back" the beam to utilize the available space to full advantage.

Depending on the environment, some attention should be given to preventing buildup of dirt, etc., on the optics. The most desirable system would be basically airtight; a minimum approach would at least allow access for cleaning.

It is envisioned that the power supplies for the laser and photodiode, the laser head, and particle counting electronics (not discussed here) would all be located outside the probe.

Approximate costs for the components are given in Table B-3. A more detailed cost analysis was not performed since the mechanical design was not laid out in detail.

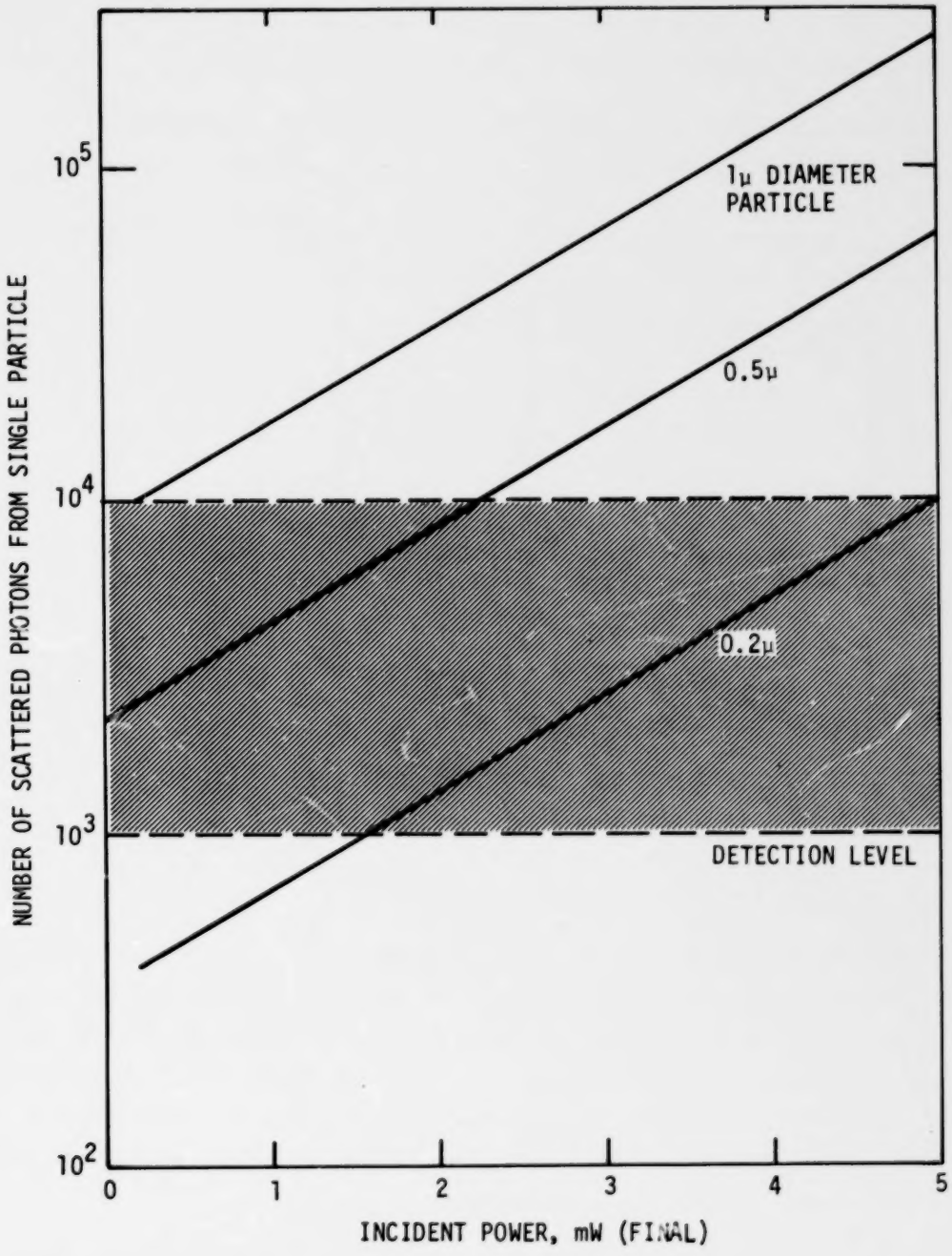

Figure B-2. Calculated photons scattered vs. incident power for impactor stage.

No trade-off analyses have been attempted here. It is likely that some performance gain could be obtained by optimizing the geometry and sizes of the system components. The configuration shown in Figure B-1 should be considered a preliminary design.

Table B-3. ESTIMATED COSTS FOR PRIMARY OPTICAL COMPONENTS OF FIGURE B-1.

Item No.	Description (Refer to Figure B-1)	Approx. Cost (Each)	Number Required	Total Component Cost
1	5 mW He-Ne laser with power supply	$650	1	$650
2	beam splitter	70	5	350
3	lens A	30	5	150
4	window	5	10	50
5	light trap 1	5	5	25
6	light trap 2	5	5	25
7	lens B_1	10	5	50
8	lens B_2	10	5	50
9	photodiode	15	5	65
10	photodiode power supply (batteries)	5	1	5
			Total	$1420

B.6 RECOMMENDED SENSITIVITY EXPERIMENTS

Since there is some latitude in the parameters used for the performance predictions, especially in values used for the scattering function, laboratory experiments should be performed to determine the threshold sensitivity for particle detection for the system concept of Figure B-1. The procedure would use the TSI vibrating orifice monodisperse aerosol generator used for separation testing, to produce a known flow rate and, hence, concentration of particles of precise diameter.

In the laboratory, a buildup of the optical equivalent of the Figure B-1 system would be set up to observe the flow of monodisperse particles through an approrpiate test section at the aerosol outlet. Prior determination of

the illuminated region would be made by observing the exposed pattern on photosensitive material placed in the test section and subjected to laser radiation.

With a calibrated, steady flow of known diameter particles, a series of tests would be performed for various laser beam powers. For high power, particles will be easy to detect. As the energy is lowered, illumination levels will eventually become so low that the particles will not be detectable; that level is the threshold detectability for that particular size of particles observed. From the laboratory threshold data, final design parameters could be determined for a prototype system.